

SUTER CONSULTANTS INC *Consulting Engineers*

38 Auriga Drive, Suite 200, Nepean, Ontario Canada K2E 8A5
TEL: (613) 224-4426 FAX: (613) 224-6055

**STRUCTURAL EVALUATION
OF ISOBLOC
CONCRETE BLOCK MASONRY**

**REPORT FOR
LES PRODUITS ISOBLOC INC.
526, Ch. du Parc Industriel
Bromptonville, Quebec
JOB 1H0**

PROJECT 94119

December 1, 1995

Table of Contents

1	INTRODUCTION	1
2	DESCRIPTION OF ISOBLOC UNITS AND WALL SYSTEM	1
2.1	General	1
2.2	Unit Dimensions	2
2.3	Unit Compressive Strength	2
2.4	Polystyrene Core Strength and Stiffness	2
3	DESIGN IMPLICATIONS OF STRUCTURAL TEST RESULTS	3
3.1	General	3
3.2	Axial Load	4
3.2.1	Concentric Compression	4
3.2.2	Modulus of Elasticity	4
3.2.3	Eccentric Compression	4
3.2.4	Slenderness Effects	5
3.2.5	Creep Effects	6
3.3	Vertical Bending	7
3.3.1	Key Wall Characteristics	7
3.3.2	Development of Interaction Diagrams	8
3.3.3	Slenderness Effects	9
3.3.4	M-P Interaction Diagram	9
3.3.5	Design Examples	10
3.3.5.1	Example 1: Commercial Building 1	10
3.3.5.2	Example 2: Commercial Building 2	11
3.3.5.3	Example 3: Industrial Building	12
3.3.5.4	Example 4: Two-Storey Building	13
3.3.5.5	Conclusions from Example Results	14
3.4	Horizontal Bending	14
3.4.1	Key Wall Characteristics	14
3.4.2	Maximum Spacing between Lateral Supports	15
3.4.3	Lateral Support for Isobloc Masonry Walls	15
3.5	Concentrated Loading from Joist Hanger	16

3.6	Shear Load	17
3.7	Design for Movements	17
3.8	Tie-Down of Roofs	17
3.9	Summary of Design Approach	18
4.	DESIGN IN ACCORDANCE WITH NBC PART 9	18
5.	DESIGN IN ACCORDANCE WITH NBC PART 4	20
6.	DESIGN DETAILS	21
	APPENDIX A: ISOBLOC TESTS PHASE I	
	APPENDIX B: ISOBLOC TESTS PHASE II	
	APPENDIX C: SUPPLEMENTARY ISOBLOC TESTS	
	APPENDIX D: SPECIAL TESTS ON EXPANDED POLYSTYRENE INSULATED CONCRETE MASONRY WALLS TYPE ISOBLOC	

STRUCTURAL EVALUATION OF ISOBLOC CONCRETE BLOCK MASONRY

1. INTRODUCTION

This structural evaluation of Isobloc concrete block masonry is based on the following test program reports:

1. "Isobloc Tests Phase I", dated February 8, 1995. Work conducted by Suter Consultants Inc. See Appendix A.
2. "Isobloc Tests Phase II", dated June 27, 1995. Work conducted by Suter Consultants Inc. See Appendix B.
3. "Supplementary Isobloc Tests", dated September 1, 1995. Work conducted by Suter Consultants Inc. See Appendix C.
4. "Special Tests on Expanded Polystyrene Insulated Concrete Masonry Walls Type Isobloc", dated January 1987. Report prepared by L.I.E. Controle - Montreal. See Appendix D.

The 1995 test programs were in general agreement with the technical requirements specified by the Canadian Construction Materials Centre (CCMC) for approval of Isobloc as a National Building Code of Canada (NBC) Part 4 and Part 9 building material. This report presents and discusses all the 1995 and relevant prior test findings in the light of design implications for both NBC Part 4 and Part 9 Isobloc applications. Reference throughout will be made to the 1990 edition of the NBC.

2. DESCRIPTION OF ISOBLOC UNITS AND WALL SYSTEM

2.1 General

The Isobloc masonry unit consists of two outer concrete blocks or shells dovetailed to an expanded polystyrene core as shown in Fig.1. The outer shells are the structural components of the masonry unit. The concrete shells and the polystyrene core are connected by means of three dovetails per shell which are moulded in the manufacturing plant as the two components are fabricated. The concrete blocks or shells are joined to the polystyrene core by means of a hydraulic press to form an Isobloc unit.

Units of a standard width of 240 mm are available as stretcher units, half units, and left and right corner units. Isobloc wall construction consists of laying up the units by means of mortar in much the same way as standard concrete block units. Care in workmanship must be taken in filling joints with just the right amount of mortar in order to achieve firstly, continuity of the interlocking insulation cores and secondly, good bond between the concrete shells in the outer and inner wythes of a wall.

2.2 Unit Dimensions

As part of Phase II work (Appendix A), five randomly selected stretcher units were used to check dimensions. From the detailed measurements given in Table 1 it can be seen that the average height, width and length were 189.6, 240.2 and 390.8 mm respectively and that the average thickness of a shell was 59.8mm. Based on these measurements and the fact that some variability in dimensions must be expected for random samples taken at another time, it is useful to refer to stretcher unit dimensions simply as 190 x 240 x 390 mm with a 60 mm shell thickness. As shown in Fig. 2, these dimensions lead to a net area per unit of 41 500 mm² and an equivalent shell thickness of 53.2 mm. The equivalent shell thickness makes allowance for the concrete area lost due to the dovetail slots.

2.3 Unit Compressive Strength

The Isobloc unit compressive strengths shown in Table 2 indicate average compressive strengths of 22.9 MPa and 18.5 MPa from two separate sources. Note that the strengths are based on slightly different net areas of 41 500 mm² for the SCI tests and 47 000 mm² for the LIE tests. It is likely that the LIE net area did not account for the presence of the dovetails as shown in Fig. 2; assuming that is so and the true LIE net area should also be 41 500 mm², the LIE average stress would be 21.0 MPa. At any rate, both average strengths satisfy the minimum 15 MPa compressive strength requirement of CSA CAN3-A165.1 for exterior block.

2.4 Polystyrene Core Strength and Stiffness

The strength and stiffness of the polystyrene core connecting the two concrete shells was assessed as discussed in the report of Appendix C. The following key conclusions are relevant:

1. The polystyrene core/concrete shell sandwich is relatively strong and stiff in compression; also recovery rates upon unloading are high. This indicates that an Isobloc block can be expected to respond well under wind pressure conditions.
2. While the polystyrene core/concrete shell sandwich is relatively weak and soft in tension, strength and stiffness are judged as adequate under normal wind suction conditions and under the NBC Part 9 conditions that will be recommended in this report. For high wind suction conditions in combination with NBC Part 4 designs, ties across the polystyrene core are recommended.

3. DESIGN IMPLICATIONS OF STRUCTURAL TEST RESULTS

3.1 General

A summary of the structural properties tests reported by Suter Consultants Inc. (SCI) and L.I.E. Controle-Montreal (LIE) has been presented in Table 3.

The SCI Phase I test program was carried out to establish the behaviour and capacity of firstly, four assemblages subjected to concentric and eccentric compression and secondly, two full height single storey walls subjected to lateral loading under vertical bending. A key variable in both the assemblage and wall tests was the absence or presence of standard Z ties between the two block shells. The presence of Z ties would establish to what extent such connectors could provide a measure of composite action between the concrete shells.

The SCI Phase II test program comprised the following specimens and types of tests:

- (1) Five blocks (190 x 240 x 390 mm) to determine their average compressive strength and variability. The results have been dealt with already in this report's Section 2.3.
- (2) Six 3-unit high assemblages for eccentric compressive strength testing to determine average strength, variability and deformational behaviour. Three assemblages each were tested for top and bottom eccentricities of $t/6$ and $t/3$.
- (3) Two 5-unit high assemblages for creep testing under eccentric compression. One assemblage each was tested for top and bottom eccentricities of $t/6$ and $t/3$ to determine their strength and deformational behaviour.
- (4) Two 1 m high x 2 m wide walls for flexural load testing in the *strong direction* to determine their horizontal bending capacity and their deformational behaviour.
- (5) Two 1.2 m wide x 2.8 m high walls reinforced with wood studs for flexural load testing in the *weak direction* to determine their vertical bending capacity and deformational behaviour. Note that the two walls were tested under simulated wind pressure and wind suction.
- (6) One joist hanger concentrated load test to determine Isobloc wall behaviour and capacity under concentrated loading.

The relevant structural tests reported on by LIE dealt with the compressive strength of Isobloc units (results of these tests have been dealt with already in Section 2.3), the strength of a storey high (8 ft) wall subjected to concentric compression, and the shear capacity of three full size (8 x 8 ft) walls under in-plane racking loads.

The design implications of all of the structural tests reported on by SCI and LIE will next be discussed.

3.2 Axial Load

3.2.1 Concentric Compression

The concentric compression strengths of the two 3-course high assemblages were 700 kN and 650 kN respectively (Phase I report, Section 5.2.2). These strengths were obtained for a block strength of 22.9 MPa and type S mortar with a strength of 12.1 MPa. Based on a net area of 41 500 mm², the average concentric compressive strength is 16.3 MPa.

From CSA CAN3-S304-M84 "Masonry Design for Buildings" (simply referred to as S304 henceforth), Table 2, the ultimate masonry compressive strength, f'_m , for a 20 MPa hollow block and type S mortar is 13.0 MPa. Interpolating Table 2 values for the given 22.9 MPa Isobloc units gives an $f'_m = 14.3$ MPa. In comparing this 14.3 MPa value with the test strength of 16.3 MPa shows that the CSA value is conservatively lower. This indicates that the Table 2 values of S304 apply to Isobloc masonry.

3.2.2 Modulus of Elasticity

Four assemblage tests from the Phase I work yielded modulus of elasticity results as follows: 12 500 MPa and 6600 MPa for the concentrically loaded assemblages, and 12 000 and 10 700 MPa for the eccentrically loaded prisms with the load centered on the one shell (Phase I report, Figs. 3 and 5). The average of the four values is 10 500 MPa.

From S304-M84, Table 4, the modulus of elasticity, E_m , is to be taken as 1000 f'_m . For the test strength of $f'_m = 16.3$ MPa, E_m therefore would be 16 300 MPa which is significantly higher than the average 10 500 MPa value obtained in tests. In fact dividing 10 500 by 16.3 gives a multiplier of 644 rather than 1000.

This discrepancy between the 1984 CSA Standard and test evidence is not surprising. It has been recognized in the industry for some time that firstly, CSA E_m values tend to be too high and secondly, E_m values fall in a wide scatter region. The first issue has been recently addressed in the 1995 edition of S304.1 where the multiplier has been reduced to 850 from 1000. A review of the literature indicates that the multiplier can readily vary between about 400 and 1300 (interpreted from Fig. 5.18 of "Masonry Structures" by R.G. Drysdale, A.A. Hamid and L.R. Baker, Prentice Hall, 1994) for concrete masonry. The test value of 644 falls safely within this wide scatter band thus indicating that the modulus of elasticity of Isobloc masonry is much the same as of standard concrete block masonry.

For design purposes, it is recommended to use $E_m = 650 f'_m$.

3.2.3 Eccentric Compression

A total of 8 eccentric compression tests were carried out on 3-course high assem-

blages as follows: 3 tests at $e/t = 0.167$ (Phase II report, Section 5.3.2), 3 tests at $e/t = 0.333$ (Phase II report, Section 5.3.2), and 2 tests at $e/t = 0.375$ (Phase I report, Section 5.2.2). Note that e refers to the eccentricity from the centroid of the Isobloc unit and $t = 240$ mm.

The following average ultimate capacities were obtained:

1. $e/t=0.167$: $P_u = 666$ kN. This represents 99% of the 675 kN concentric capacity.
2. $e/t=0.333$: $P_u = 395$ kN. This represents 58% of the 675 kN concentric capacity.
3. $e/t=0.375$: $P_u = 360$ kN. This represents 53% of the 675 kN concentric capacity.

The results indicate that when the eccentricity is small, i.e. $e/t = 0.167$, there is no significant effect on the overall Isobloc capacity. With increasing eccentricity more and more load is being resisted by the more highly loaded wythe until at an eccentricity of $e/t=0.375$ virtually all the load is taken up by the one wythe. Since at $e/t = 0.375$ the load in fact is centered on the one wythe (see Fig. 1 of the Phase I report), the Isobloc behaviour is as expected.

S304-M84, Clause 5.6.5.4 states “where a cavity wall is loaded on both wythes, the load shall be distributed to each wythe according to the eccentricity of the load from the centroidal axis of the wall”. Although the Isobloc wall is not a cavity wall from a building science point of view, it can be seen that in a structural sense it acts like a cavity wall in a predictable way.

3.2.4 Slenderness Effects

The effect of slenderness on concentric axial load capacity can be assessed by reviewing Phase I results for three assemblages (two 3-course high assemblages and one 7-course high assemblage) and one wall result reported by LIE (Appendix D) as follows:

1. 3-course assemblages:
 - $h/t = 2.5$ for $t = 240$ mm
 - $h/t = 5.65$ for $t = 2 t_s = 106.4$ mm where $t_s =$ shell thickness
 - average $P_u = 675$ kN
2. 7-course assemblage:
 - $h/t = 5.8$ for $t = 240$ mm
 - $h/t = 13.15$ for $t = 2 t_s = 106.4$ mm
 - $P_u = 585$ kN
2. 12-course high wall:
 - $h/t = 10.0$ for $t = 240$ mm
 - $h/t = 22.5$ for $t = 2 t_s = 106.4$ mm
 - $P_u = 360$ kN (failure load adjusted to 390 mm wide wall)

From S304-M84, Table 7, the slenderness coefficient, C_s , for concentric loading is seen to vary between 1.0 for $h/t = 5$ to 0.40 for $h/t = 30$ as an upper limit on

wall slenderness. Applying the Table 7 values to the 3-course assemblage, the load capacity would remain unaltered at 675 kN since $C_s = 1.00$ up to $h/t = 7$. Applying the Table 7 values to the 7-course assemblage, the load capacity was found to be 578 kN ($C_s = 0.856$ for $h/t = 13.15$). Since the actual test capacity was 585 kN, the slenderness effects as given in Table 7 reflect well the Isobloc wall behaviour with only an error of 1.2 %.

Similarly for the 12-course high wall, Table 7 of the S304-M84 predicted the wall capacity to be 405 kN ($C_s = 0.6$ for $h/t = 22.5$). Since the actual test capacity was 360 kN, the slenderness effects as given in Table 7 reflect reasonably well the Isobloc wall behaviour with only an error of 12.5 %.

Also, by employing the limiting formula of the CAN3-S304 (Clause 5.6.1.1) for the slenderness ratio (h/t) as $10(3 - e_1/e_2)$, the height of a load bearing Isobloc masonry wall should not exceed 3.2 m based on an effective thickness of 106.4 mm and e_1/e_2 equal to zero. Note also that height limitations would vary according to a project's particular design details which can introduce single or double curvature bending. Until more experience has been gained with the Isobloc wall system or additional testing has been carried out, it is recommended not to rely on any double curvature bending effects and hence not to use e_1/e_2 less than zero in the above h/t equation.

Summarizing, the Isobloc slenderness behaviour can be reasonably well predicted by employing the S304 C_s values for an Isobloc wall thickness equal to the sum of the two wythes' thicknesses. This behaviour can be explained by considering the lateral support effect of the polystyrene core on the relatively slender concrete masonry wythes especially of taller walls. To delay premature buckling of these wythes only a small lateral stabilizing force is needed and while the polystyrene is a low stiffness material it nevertheless furnishes an adequate lateral support for the Isobloc walls to reach relatively high compression capacities under slender wall conditions.

For design purposes within the Isobloc limitations later set out in this report, high compressive capacities at high slenderness ratios will not be required. For designs according to NBC Part 4 beyond these limitations, caution is required in interpolating capacities for larger slenderness values than those tested. Higher Isobloc walls could also be achieved by providing lateral supports at intermediate points of the wall height. This could be achieved, for example, by shortening the spacing between the intersecting walls and employing the connection between the load bearing Isobloc wall and the intersecting walls to provide additional lateral stability to the Isobloc wall. A good tying mechanism between both wythes of the Isobloc wall and the intersecting wall is required to achieve good lateral support.

3.2.5 Creep Effects

Two 5-unit high assemblages were loaded eccentrically for creep behaviour over a 24-hour period (Phase II report, Section 5.3.3). The total applied eccentric load

was based on the masonry allowable compressive stress for a 20 MPa block per S304-M84 (i.e. $0.25 f'_m = 0.25 \times 13 = 3.25$ MPa) plus 25% according to the CCMC Technical Requirements. The total applied load was then taken as $3.25 \times 1.25 \times$ net area of $46\,800 \text{ mm}^2 = 190\,125 \text{ N}$ or 190.1 kN. Note firstly, that the larger net area was used which did not account for the dovetail slots as shown in Fig. 2 and secondly, that the applied load amounted to about 28% of the concentric compression capacity; such a load represents a relatively high load level for creep testing.

One assemblage was tested at a relatively small eccentricity of $e/t=0.167$ and the other at a large eccentricity of $e/t=0.333$.

For the case of $e/t=0.167$, both wythes shared the load just as they had done under the short-term eccentric load test, the creep deformations were negligible and the deformation recovery rates upon unloading were high (65% and 86% at 24 hours after unloading for the more highly and less highly loaded wythes respectively).

For the case of $e/t=0.333$, the more highly loaded shell was stressed to more than 50% of the ultimate masonry strength. As expected, this produced relatively high strains both upon initial loading and creep loading; in spite of reaching a final strain of about 0.0018, the assemblage did not fail and exhibited good recovery rates of 66% and 96% at 24 hours after unloading for the highly and less highly loaded wythes respectively.

Spreading deformations between the two wythes of each of the two assemblages were small and little influenced by the duration of loading. In summary, the creep behaviour of the Isobloc assemblages was found to be satisfactory.

3.3 Vertical Bending

3.3.1 Key Wall Characteristics

The Isobloc walls tested under bending in the vertical (weak) direction indicated the following key wall characteristics:

- There was little composite action between the two wythes of the Isobloc wall.
- Cracking load capacities of the walls were small and appeared to be slightly increased by the presence of wood studs. The cracking load moments were 325N.m for both the Phase I and Phase II test walls.
- The wall tested with studs in tension simulating the wind pressure case sustained an ultimate load of 7500 N (ultimate moment = 4875 N.m) while the wall tested with studs in compression simulating the wind suction case sustained an ultimate load of 1750N (ultimate moment = 1138 N.m).
- After reaching the cracking load for plain Isobloc walls, the wall stiffness decreased markedly and large deflections took place.

- Load/deflection behaviour of the walls with studs on the tension or compression side simulating wind pressure and suction cases, respectively, indicated a stiffer response than that observed with walls without wood studs.

3.3.2 Development of Interaction Diagrams

Clause 5.7.3 of CAN3 S304 states that the allowable resistance of a section can be determined from a moment-axial load M-P interaction diagram determined as follows and illustrated in Fig. 3. The upper portion of the diagram is constructed by joining point P_o with $(P_o e_k/2, P_o/2)$ where $P_o = f_m A_m$, f_m is the allowable compressive stress, A_m is the net masonry area and e_k is the kern eccentricity. The lower part of the diagram is constructed by joining $(P_o e_k/2, P_o/2)$ with M_o where M_o is the pure moment capacity of the section.

Throughout the development of interaction diagrams for vertical bending in combination with axial loads, the assumption was made that Isobloc walls would be reinforced with wood studs as tested during Phase II work. This was done because if such reinforcement is not provided, the vertical bending capacity is too low to be of much design use for storey high walls. Also, in arriving at allowable pure moment capacities of walls under wind pressure and wind suction, different safety criteria were considered because of the very different load-deflection behaviour of the walls as follows: For the wind pressure case, the effect of the wood studs was very significant and led to a stiff load-deflection response almost up to ultimate failure (Phase II report, Fig. 13); to arrive at an allowable moment capacity it was therefore decided to take the ultimate capacity and divide it by 2.5. For the wind suction case, the presence of the studs ensured firstly, stiff behaviour up to twice the cracking load or 1000 N and secondly, continued safety, albeit at a lowered stiffness, beyond 1000 N up to an ultimate load of 1750 N or 3.5 times the cracking load; for an allowable moment capacity it was decided to use 500 N because of the continued stiffness to twice that value and a reasonable level of safety beyond the cracking load. Applying these criteria, the following allowable or service load pure moment capacities were calculated: 1.92 kN/m² (40 psf) for the wind pressure case and 0.32 kN/m² (6.7 psf) for the wind suction case.

Typically, for solid sections $e_k = t/6$ and for hollow sections, the value is larger. In the case of the Isobloc wall, test results indicated that there is no composite action between the two wythes. Therefore, it is reasonable to analyse the Isobloc wall as a *cavity wall* where each of its wythes behaves independently in the vertical direction while being adequately connected laterally by the insulation core. In this case, the kern eccentricity shall be determined for each wythe as $t_s/6$ where t_s is the thickness of a single wythe or concrete shell.

Clauses 5.6.5.3 and 5.6.5.4 of CAN3-S304 state that when a cavity wall is loaded on both wythes, the load shall be distributed to each wythe according to the eccentricity of the load from the centroidal axis of the wall and for each individual wythe the eccentricity shall be measured from the centroid of the loaded wythe. Recogniz-

ing the fact that the insulation core will cause both wythes to bend together, two cases will be addressed. In the first case, both wythes will be analysed as acting together in resisting the *lateral bending* with no composite action being considered. In the second case, each wythe will be analysed and designed independently under the actual applied *vertical load, lateral bending and end moments*. As illustrated schematically in Fig. 3, two interaction diagrams will be developed and each of the previous cases will be considered.

3.3.3 Slenderness Effects

Clause 5.7.3 of CAN3 S304 states that the effect of slenderness on wall capacity can be taken into consideration in design using the moment magnification method. Therefore, a wall section should be designed for the unfactored applied axial load and magnified moment equal to the unfactored maximum applied moment times the moment magnification factor, δ , where

$$\delta = 1/(1 - P/P_{cr})$$

where

P = unfactored applied axial load

$$P_{cr} = \text{buckling load} = \frac{\pi^2 E_m I_{eff}}{4h^2}$$

in which

E_m = modulus of elasticity

$$I_{eff} = (I_1 + I_2)/4 \text{ for } 0 \leq e_1/e_2 \leq 1$$

where

I_1 and I_2 are the cracked or uncracked moments of inertia of the sections (depending on e_1 and e_2) at ends 1 and 2.

It must be noted here that the composite action between the two wythes must not be considered when calculating the effective moment of inertia for the whole section of the wall. Also, in case of designing each wythe independently, the effective moment of inertia should be based on only the inertia of a single wythe and two moment magnification factors could be developed for each wythe. Each magnification factor will be used to magnify the primary moment due to end moments and lateral load moment.

3.3.4 M-P Interaction Diagram

As illustrated in Fig. 3, the M-P interaction diagram can be constructed by identifying 3 main points A, B, and C as follows:

Point A

Point A can be defined as the axial capacity of the wall section where $P_o = f_m A_m$, in which f_m is the allowable compressive stress and A_m is the net area of the wall section.

$$P_o = 3.25 \times 1000 \times 53.2 \times 2 \times 1 / 1000 = 345.8 \text{ kN/m}$$

Point B

Point B can be defined as $(P_o e_k / 2, P_o / 2)$ where $P_o = f_m A_m$ and e_k is the kern eccentricity $((t_s)_{equiv.} / 6)$

$$P_o e_k / 2 = 345.8 \times (60 / 6) / 2 \times (1 / 1000) = 1.729 \text{ kN.m}$$

Point C

Point C can be defined by M_{os} and M_{op} , the pure moment capacities of the section, simulating wind suction or wind pressure cases, respectively.

Wind Suction Case:

$$M_{os} = \frac{PL}{4} \text{ (P is the lateral load recorded at the 1st crack)}$$

$$P = 0.5 \text{ kN (see Phase I \& Phase II Reports)}$$

$$P = 0.5 \times 1 / 1.2 = 0.42 \text{ kN/m}$$

$$M_{os} = 0.42 \times 2.6 / 4 = 0.273 \text{ kN.m/m}$$

Wind Pressure Case:

$$M_{op} = \frac{PL}{4} \text{ (P is the ultimate lateral load divided by 2.5)}$$

$$P = 7.5 / 2.5 = 3.0 \text{ kN (see Phase I \& Phase II Reports)}$$

$$P = 3.0 \times 1 / 1.2 = 2.5 \text{ kN/m}$$

$$M_{op} = 2.5 \times 2.6 / 4 = 1.625 \text{ kN.m/m}$$

In a similar fashion, the sub-interaction diagram for the design of a single wythe can be constructed as illustrated in Fig. 3.

3.3.5 Design Examples

In the following examples, the Isobloc wall will be designed in two steps. First, each single wythe will be designed independently and its capacity will be checked against the sub-interaction diagram illustrated in Fig. 3. Second, both wythes will be designed together by combining their capacities linearly, then their combined capacity will be checked against the main interaction diagram illustrated in Fig. 3. Also, it was assumed that the effective moment of inertia of the wall cross-section is the sum of the uncracked moments of inertia of each wythe calculated independently while no composite action is present. The combined moment of inertia was used to determine the buckling load and the moment magnification factors due to the fact that the inner insulation core is well tied to both wythes and will cause them to buckle together.

3.3.5.1 Example 1: Commercial Building 1

A 3.0 m high wall in a commercial building carries an axial compressive load of 30 kN/m and resists a wind pressure of 0.8 kN/m^2 and a wind suction of 0.5 kN/m^2 as shown in Fig. 4. Using 20 MPa compressive strength block and type S mortar, f'_m

equals 13 MPa and f_m equals 3.25 MPa ($0.25 f'_m$). By using the effective moment of inertia of the two wythes, P_{cr} is equal to 76 kN/m and, therefore, the moment magnification factor $\delta = 1/(1 - P/P_{cr}) = 1/(1 - \frac{15}{76}) = 1.246$.

For moment due to wind pressure, $\rho \frac{h^2}{8}/2 = 0.8 \frac{3^2}{8}/2 = 0.45$ kN.m/m. For a single wythe, the combined design loads of $P = 30/2 = 15$ kN/m and $M = 0.45 \times 1.246 = 0.561$ kN.m/m are inside the sub-interaction diagram in Fig. 5 and, therefore, the wythe design is satisfactory. Also, the combined design loads of $P = 30$ kN/m and $M = (0.45 \times 1.246) \times 2 = 1.121$ kN.m/m are inside the main interaction diagram in Fig. 5 and therefore, the wall design is satisfactory.

Similarly, for the wind suction case, for moment due to wind suction, $\rho \frac{h^2}{8}/2 = 0.5 \frac{3^2}{8}/2 = 0.28$ kN.m/m. For a single wythe, the combined design loads of $P = 30/2 = 15$ kN/m and $M = 0.28 \times 1.246 = 0.349$ kN.m/m are outside the sub-interaction diagram in Fig. 5 and, therefore, the wythe design is unsatisfactory. Also, the combined design loads of $P = 30$ kN/m and $M = (0.28 \times 1.246) \times 2 = 0.698$ kN.m/m are outside the main interaction diagram in Fig. 5 and therefore, the wall design is unsatisfactory.

Since the previous design is unsatisfactory due to the single wythe's capacity and the overall wall's capacity under suction load, the same wall design could be adequate in areas with lower *hourly wind pressure values (1/30)*. To demonstrate this, assume that the same building is subjected to a wind pressure of 0.5 kN/m^2 and a wind suction of 0.3 kN/m^2 . Following the same procedures illustrated above, one can find that the wythe design as well as the overall wall design are satisfactory as illustrated in Fig. 6.

3.3.5.2 Example 2: Commercial Building 2

This building is similar to that of Example No. 1 except that only one shell is loaded with 30 kN/m and resists a wind pressure of 0.8 kN/m^2 and a wind suction of 0.5 kN/m^2 as shown in Fig. 7. Using 20 MPa compressive strength block and type S mortar, the value of f'_m equals 13 MPa and f_m equals 3.25 MPa ($0.25 f'_m$). By using the effective moment of inertia of the two wythes, P_{cr} is equal to 76 kN/m and therefore, the moment magnification factor for the interior wythe $\delta = 1/(1 - P/P_{cr}) = 1/(1 - \frac{30}{76}) = 1.652$ and for the exterior wythe equals to 1.0.

For moment due to wind pressure, $\rho \frac{h^2}{8}/2 = 0.8 \frac{3^2}{8}/2 = 0.45$ kN.m/m. The combined design loads of $P = 30$ kN/m and $M = 0.45 \times 1.652 = 0.743$ kN.m/m are inside the sub-interaction diagram in Fig. 8 and, therefore, the interior wythe design is satisfactory. The combined design loads of zero axial load and $M = 0.45$ kN.m/m acting on the exterior wythe are inside the sub-interaction diagram in Fig. 8 and therefore, the wythe design is satisfactory. Also, the combined design loads of $P = 30$ kN/m and $M = (0.45 \times 1.652) + 0.45 = 1.193$ kN.m/m are inside the main interaction diagram in Fig. 8 and therefore, the wall design is satisfactory.

Similarly, for the wind suction case, for moment due to wind suction on the interior wythe, $\rho \frac{h^2}{8} / 2 = 0.5 \frac{3^2}{8} / 2 = 0.28 \text{ kN.m/m}$. The combined design loads of $P = 30 \text{ kN/m}$ and $M = 0.28 \times 1.652 = 0.463 \text{ kN.m/m}$ are outside the sub-interaction diagram in Fig. 8 and therefore, the wythe design is unsatisfactory. The combined design loads of zero axial load and $M = 0.28 \text{ kN.m/m}$ acting on the exterior wythe are outside the sub-interaction diagram in Fig. 8 and therefore, the wythe design is unsatisfactory. Also, the combined design loads of $P = 30 \text{ kN/m}$ and $M = (0.28 \times 1.652) + 0.28 = 0.743 \text{ kN.m/m}$ are outside the main interaction diagram in Fig. 8 and therefore, the wall design is unsatisfactory.

Since the previous design is unsatisfactory due to the single wythe's capacity and the overall wall's capacity under suction load, the same wall design could be adequate in areas with lower *hourly wind pressure values (1/30)*. To demonstrate this, assume that the same building is subjected to a wind pressure of 0.5 kN/m^2 and a wind suction of 0.3 kN/m^2 . Following the same procedures illustrated above, one can find that the wythe design as well as the overall wall design are satisfactory as illustrated in Fig. 9.

3.3.5.3 Example 3: Industrial Building

The 5.2 m high isolated masonry wall carries an axial compressive load of 30 kN/m and resists a wind pressure of 1.0 kN/m^2 and a wind suction of 0.67 kN/m^2 as shown in Fig. 10. While the height of the wall is more than the height limit imposed by the slenderness ratio reported in the CAN3-S304 (Clause 5.6.1.1), this example illustrates the inadequacy of a slender Isobloc wall in resisting lateral loading. Using 20 MPa compressive strength block and type S mortar, the value of f'_m equals 13 MPa and f_m equals 3.25 MPa ($0.25 f'_m$). By using the effective moment of inertia of the two wythes, P_{cr} is equal to 25.3 kN/m and, therefore, the moment magnification factor $\delta = 1/(1 - P/P_{cr}) = 1/(1 - \frac{15}{25.3}) = 2.456$.

For moment due to wind, $\rho \frac{h^2}{8} / 2 = 1.0 \frac{5.2^2}{8} / 2 = 1.69 \text{ kN.m/m}$. The combined design loads of $P = 15 \text{ kN/m}$ and $M = 1.69 \times 2.456 = 4.151 \text{ kN.m/m}$ are outside the sub-interaction diagram in Fig. 11 and therefore, the wall design is unsatisfactory. Also, the combined design loads of $P = 30 \text{ kN/m}$ and $M = (1.69 \times 2.456) \times 2 = 8.301 \text{ kN.m/m}$ are outside the main interaction diagram in Fig. 11 and therefore, the wall design is unsatisfactory.

Similarly, for the wind suction case, for moment due to wind suction, $\rho \frac{h^2}{8} / 2 = 0.67 \frac{5.2^2}{8} / 2 = 1.132 \text{ kN.m/m}$. The combined design loads of $P = 15 \text{ kN/m}$ and $M = 1.132 \times 2.456 = 2.78 \text{ kN.m/m}$ are outside the sub-interaction diagram in Fig. 11 and therefore, the wall design is unsatisfactory. Also, the combined design loads of $P = 30 \text{ kN/m}$ and $M = (1.132 \times 2.456) \times 2 = 5.56 \text{ kN.m/m}$ are outside the main interaction diagram in Fig. 11 and therefore, the wall design is unsatisfactory.

Since the previous design is unsatisfactory due to the single wythe and the over-

all wall capacities under both pressure and suction load, the same wall design was checked against lower lateral pressure simulating areas with lower *hourly wind pressure values (1/30)* where the same building is subjected to a wind pressure of 0.5 kN/m^2 and a wind suction of 0.3 kN/m^2 . Following the same design procedures, the results illustrated in Fig. 12 indicate that the wall design is inadequate even with a reduced wind pressure.

The lateral capacity of a slender Isobloc wall to resist the applied lateral loading could also be increased by reducing the effective height of the wall by providing intermediate supports or by tying the wall back to a transversal supporting element (such as an intersecting wall, buttress or column) that will add to the wall lateral stability.

3.3.5.4 Example 4: Two-Storey Building

A two-storey building carries an axial compressive load from the roof of 30 kN/m , an axial compressive load from the 1st floor of 40 kN/m on the interior wythe, and resists a wind pressure of 0.8 kN/m^2 and a wind suction of 0.5 kN/m^2 as shown in Fig. 13. Using 20 MPa compressive strength block and type S mortar, the value of f'_m equals 13 MPa and f_m equals 3.25 MPa ($0.25 f'_m$).

The 2nd storey wall can be designed as illustrated before in Example No. 1. For the 1st storey wall, firstly, each wythe will be designed independently to satisfy the sub-interaction diagram, and, secondly, both wythes will be designed together to satisfy the main interaction diagram.

For the interior wythe, by using the effective moment of inertia of the two wythes, P_{cr} is equal to 76 kN/m and therefore, the moment magnification factor δ for the interior wythe = $1/(1 - P/P_{cr}) = 1/(1 - \frac{45}{76}) = 2.45$.

For moment due to wind pressure, $\rho \frac{h^2}{8}/2 = 0.8 \frac{3^2}{8}/2 = 0.45 \text{ kN.m/m}$. The combined design loads of $P = 45 \text{ kN/m}$ and $M = 0.45 \times 2.45 = 1.103 \text{ kN.m/m}$ are outside the sub-interaction diagram in Fig. 14 and therefore, the wythe design is unsatisfactory.

Similarly, for the wind suction case, for moment due to wind suction, $\rho \frac{h^2}{8}/2 = 0.5 \frac{3^2}{8}/2 = 0.28 \text{ kN.m/m}$. The combined design loads of $P = 45 \text{ kN/m}$ and $M = 0.28 \times 2.45 = 0.686 \text{ kN.m/m}$ are outside the sub-interaction diagram in Fig. 14 and therefore, the wythe design is unsatisfactory.

For the exterior wythe, again by using the effective moment of inertia of the two wythes, P_{cr} is equal to 76 kN/m and therefore, the moment magnification factor δ for the interior wythe = $1/(1 - P/P_{cr}) = 1/(1 - \frac{15}{76}) = 1.246$.

For moment due to wind pressure, $\rho \frac{h^2}{8}/2 = 0.8 \frac{3^2}{8}/2 = 0.45 \text{ kN.m/m}$. The combined design loads of $P = 15 \text{ kN/m}$ and $M = 0.45 \times 1.246 = 0.565 \text{ kN.m/m}$ are inside the sub-interaction diagram in Fig. 14 and therefore, the wythe design is satisfactory.

Similarly, for the wind suction case, for moment due to wind suction, $\rho \frac{h^2}{8} / 2 = 0.8 \frac{3^2}{8} / 2 = 0.28 \text{ kN.m/m}$. The combined design loads of $P = 15 \text{ kN/m}$ and $M = 0.28 \times 1.246 = 0.349 \text{ kN.m/m}$ are outside the sub-interaction diagram in Fig. 14 and therefore, the wythe design is unsatisfactory.

For the overall wall and wind pressure case, by combining the moment magnification effect for both wythes, the combined design loads of $P = 60 \text{ kN/m}$ and $M = 0.45 \times 2.45 + 0.45 \times 1.246 = 1.663 \text{ kN.m/m}$ are on the main interaction diagram in Fig. 14 and therefore, the wall design is satisfactory.

For the overall wall and wind suction case, by combining the moment magnification effect for both wythes, the combined design loads of $P = 60 \text{ kN/m}$ and $M = 0.28 \times 2.45 + 0.28 \times 1.246 = 1.035 \text{ kN.m/m}$ are outside the main interaction diagram in Fig. 14 and therefore, the wall design is unsatisfactory.

While the previous design is unsatisfactory due to the single wythe and overall wall deficiencies under both wind pressure and suction loading, the same wall design could be adequate in areas with lower *hourly wind pressure values (1/30)*. To demonstrate this, assume that the same building is subjected to a wind pressure of 0.5 kN/m^2 and a wind suction of 0.3 kN/m^2 . Following the same procedures illustrated above, one can find that the wythe design as well as the overall wall design are satisfactory as illustrated in Fig. 15.

3.3.5.5 Conclusions from Example Results

The results obtained in the examples indicate that Isobloc walls can be satisfactorily designed as vertical bending elements as long as the lateral loads are relatively small and the axial loads are relatively high. Note that the interaction diagrams and all of the examples assume that the Isobloc walls are built with wood studs attached to the interior wythe according to the Phase II test program details.

3.4 Horizontal Bending

3.4.1 Key Wall Characteristics

The Isobloc walls tested under bending in the horizontal (strong) direction indicated the following key wall characteristics:

- A slight composite action exists between the two wythes of the Isobloc wall.
- Cracking load capacities of the walls were relatively high (4750 N and 6000 N). Corresponding cracking moments were 2138 N.m and 2700 N.m.
- Crack widths at the cracking load were determined as less than 0.1 mm.
- Ultimate flexural capacities of the walls were equal to 6380 N and 7850 N with an average value of 7115 N. Corresponding ultimate moments were 2871 N.m and 3533 N.m.

- At a selected deflection of 0.4 mm, the horizontal bending stiffness is three times greater than the vertical bending stiffness.

3.4.2 Maximum Spacing between Lateral Supports

The maximum allowable horizontal spacing that a wall can span between two vertical supports can be determined as follows:

Calculate the equivalent distributed wind pressure, ρ_e , from

$$M = \frac{P_s L}{4} = \frac{\rho_e L^2}{8}$$

Therefore,

$$\rho_e = \frac{2P_s}{L} = \frac{2P_{ult}/2.5}{L} = \frac{P_{ult}/1.25}{L}$$

in which M is the bending moment capacity of the vertical wall section, P_s is the service load, and P_{ult} is the ultimate load at failure.

Note that in arriving at an allowable service load, the average ultimate test load was divided by 2.5. The 2.5 value was selected based on the Phase II results (Phase II report, Section 5.4) which indicated cracking capacities of about 75% of ultimate capacities and a relatively smooth and stiff deflection response up to ultimate failure.

From the last equation the maximum allowable horizontal spacing between vertical lateral supports can be calculated as

$$L = \frac{P_{ult}/1.25}{\rho}$$

where ρ is the wind pressure or suction at selected locations.

For a location of high wind pressure of 1.44 kN/m^2 or 30 psf (hourly wind pressure of about 0.94 kPa for 1/30 year wind), the maximum allowable horizontal spacing between vertical lateral supports can be determined as $L = 7115 / (1.25 \times 1.44) = 3.96 \text{ m}$. This value for the maximum spacing of lateral supports agrees well with the 3.8 m value listed in Table 12 of the Commentary on Part 9 of the NBC 1990. Designs at wider spacings are possible for lower hourly wind pressures.

3.4.3 Lateral Support for Isobloc Masonry Walls

The main requirements of the lateral support for Isobloc walls are:

- to provide adequate load capacity;
- to furnish enough rigidity so that the wall bends in the horizontal (strong) direction;
- to tie in well with the supported wall.

The lateral support could be, but is not limited to, one of the following: a transverse masonry wall including an Isobloc wall, a reinforced concrete masonry column, a

steel column (HSS), a reinforced brick masonry column, or a reinforced concrete column.

At wall returns of Isobloc wall construction, it is obviously advantageous to rely on the Isobloc wall at right angles to provide lateral support. Elsewhere, the compact shape of HSS sections properly tied into the Isobloc wall may prove economical. Table 4 lists sample HSS dimensions versus various wall heights; these sections were determined for a wind pressure of 1.44 kN/m^2 (30 psf) and a maximum spacing between lateral supports of 2.4 m and 3.8 m. The designer must ensure that any selected cross-section provides adequate strength and stiffness to sustain the applied local wind pressure.

3.5 Concentrated Loading from Joist Hanger

The Phase II floor test (Phase II report, Section 5.6) subjected 6 joist hangers and the Isobloc walls which supported them to concentrated loading. The loading was applied to a maximum load of 22 kN over a floor area of 7.2 m^2 . The maximum floor loading of 3.06 kN/m^2 was approximately 1.6 times the 1.9 kN/m^2 live loading normally used in the design for residential areas. The joist hangers were screwed to the Isobloc concrete shell by means of two screws (Tapcon pre-drilled screws, 3/16 in. diameter, 1 in. length) as shown in Fig. 18 of the Phase II report; this screwed down connection was necessary to prevent a premature rotational bending failure of the joist hanger under the particular test setup where there was no continuity of the Isobloc wall above the test floor level. The bearing stress under the joist hanger at maximum floor loading amounted to about 0.83 MPa. Such a bearing stress is very small and as expected produced no local bearing distress in the Isobloc unit or the wall. The walls did experience local cracking as discussed in connection with Fig. 20 of the Phase II report. Where in practice no Isobloc wall continuity exists above the floor or roof level and the floor or roof is connected to the walls with joist hangers in a similar way as tested, local cracking must be expected; the design must then incorporate measures such as surface coatings or finishes to control moisture penetration of the wall.

Additional joist hanger assemblage tests were carried out to determine if the screwed connection could be omitted when mortar joints from Isobloc masonry courses above the joist hanger level would provide a certain clamp-down capacity (Appendix C). The tests of 6 joist hangers on three assemblages determined firstly, an average ultimate load capacity per hanger of 10.38 kN and secondly, that the clamp-down capacity of even a single mortar joint above the joist hanger is sufficient to prevent a premature rotational bending failure of the joist hanger. The average ultimate load produced a bearing stress of about 2.4 MPa which again is small and caused no bearing distress in the Isobloc shell. In summary, the test results indicate that no screws are required to tie down a joist hanger as long as at least a single course of masonry is present above the joist hanger level.

3.6 Shear Load

The behaviour of Isobloc walls under lateral in-plane shear load can be assessed by reviewing three wall results reported by LIE (Appendix D). The wall specimens were 2397 mm (7' 10 3/8") in height by 2394 mm (7' 10 1/4") in length with a thickness of 240 mm (9 5/8"); the mortar was type M with a compressive strength of 29.3 MPa at 26 days. Under monotonic lateral in-plane loading, diagonally stepped fissures appeared in the mortar joints at a load of 106.8 kN (24 000 lb) in wall No.1, at a load of 89.0 kN (20 000 lb) in wall No. 2 and at a load of 120.1 kN (27 000 lb) in wall No. 3; the average diagonal cracking load therefore was equal to 105.3 kN (23 667 lb).

Also, the maximum loads applied to reach failure were 133.4 kN (30 000 lb) for walls No. 1 and 3, and 120.1 (27 000 lb) for wall No. 2; the average shear failure load therefore was equal to 129.0 kN (29 000 lb).

By employing a net area of 249 000 mm² for the 6-block horizontal wall cross-section, shear stresses of 0.42 MPa and 0.52 MPa were determined corresponding to the diagonal cracking load and the ultimate failure load respectively. By comparing these shear stresses with the allowable shear stress of $v_m = 0.23$ MPa (according to S304-M84, Table 4, type M or S mortar), safety factors against diagonal cracking and ultimate failure amount to 1.8 and 2.3 respectively. Because these safety factors are judged to be slightly low, it is recommended to use an allowable shear stress of 0.20 MPa for Isobloc walls constructed with type M or S mortar. Applying a similar reduction to the S304-M84 allowable shear stress for type N mortar, it is recommended to use 0.14 MPa for Isobloc walls constructed with type N mortar.

3.7 Design for Movements

Isobloc walls must be expected to move due to the effects of temperature, short term and long term loading, moisture and shrinkage. The test results discussed in the previous report sections dealing with short term axial loading, short term eccentric loading, creep loading, slenderness effects and bending all indicate that Isobloc masonry behaves in a predictable way and in much the same fashion as normal concrete masonry; while no tests have been carried out on thermal movements, Isobloc's overall similar behaviour to concrete masonry indicates that thermal behaviour would also be similar to that of concrete masonry.

Based on these considerations and the modulus of elasticity value of $E_m = 650 f'_m$, it is recommended that design for movements be carried out according to the general requirements of NBC Part 4 with due regard to CAN3-S304 and the Commentary D in the Supplement to the NBC.

3.8 Tie-Down of Roofs

Roof uplift forces create tensile forces on walls which in the case of unreinforced masonry such as Isobloc masonry must be resisted by members especially designed

and detailed for this purpose. Because Isobloc masonry does not lend itself to reinforcing and grouting internally, it is easiest to employ vertical wood furring strips, wood studs or metal studs attached to the roof members and to the Isobloc wall. It is vital that these tie-down strips or studs are continuous vertically and extend down far enough to anchor the roof uplift forces effectively. A schematic design detail for the tie-down of roofs is given in Fig. 19 as part of this report's Section 6.

3.9 Summary of Design Approach

The Isobloc test results and wall examples indicate that Isobloc walls subjected to relatively light lateral loads in combination with relatively high axial loads acting concentrically or at small eccentricities of $e/t \leq 0.167$, can be satisfactorily designed as vertical bending elements. For all other cases, Isobloc walls can best be designed as horizontal bending elements spanning between vertical lateral supports. The design can be carried out in accordance with the NBC's Part 9 or Part 4 as discussed in the following two sections of this report.

4. DESIGN IN ACCORDANCE WITH NBC PART 9

For buildings conforming to Clause 2.1.3 of NBC-1990, the design and construction provisions in Clause 9.15 and 9.20 of Part 9 for concrete block construction can be applied using the additional requirements given below. Alternative design in accordance with Part 4 and CAN3-S304 can be carried out as discussed in Section 5.

1. Footings for Isobloc buildings shall consist of concrete in compliance with Section 9.15.3. To reduce the potential for differential settlements caused by cracking in footings, it is recommended to reinforce footings longitudinally by a minimum of 2-15 mm reinforcing bars in a continuous fashion. Foundation walls for Isobloc buildings shall consist of concrete or unit masonry in compliance with Section 9.15.4. Isobloc units must NOT be used below grade in any form such as foundation or basement walls.
2. In velocity- or acceleration-related seismic zones greater than 4, loadbearing masonry elements made of Isobloc must NOT be used. (Clause 9.20.1.3 Sentence 1). This restriction should be reviewed in the future in the light of Isobloc wall performance in more moderate earthquake regions or in the light of additional test information.
3. In velocity- or acceleration-related seismic zones of 4, loadbearing masonry elements made of Isobloc must NOT be constructed more than 1 storey in building height (Clause 9.20.1.3 Sentence 1). Until more experience has been gained about the performance of Isobloc buildings subjected to earthquakes

or additional test information becomes available, the height limit for one storey shall be 3.2 m (10.5 ft).

4. In velocity- or acceleration-related seismic zones of 2 and 3, loadbearing masonry elements made of Isobloc must NOT be constructed more than 1 storey in building height (Clause 9.20.1.3 Sentence 2). Again, a 3.2 m (10.5 ft) limit for the one storey shall apply.
5. In velocity- or acceleration-related seismic zones of 0 and 1, loadbearing masonry elements made of Isobloc must NOT be constructed more than 2 storeys in building height (Clause 9.20.1.3 Sentence 2) except for end gable walls extending above the second storey wall. Each individual storey height including the height of gable walls shall not exceed 3.2 m (10.5 ft).
6. Chases and recesses in Isobloc walls shall not be permitted except as non-conforming chases or recesses in compliance with Clause 9.20.7.4.
7. Except as specified in point 11, beams and columns shall NOT be supported on Isobloc walls but shall be independently supported on pilasters (Clause 9.20.8.4 Sentence 1).
8. Except for the joint hanger dealt with in this report, Isobloc walls shall NOT have any supporting member attached to it such as a shelf angle or the flange of a beam (Clause 9.20.8.5).
9. Isobloc walls must always span HORIZONTALLY and shall be supported at right angles to the wall by intersecting masonry walls or buttresses. (Clause 9.20.10.1). The maximum spacing of such supports shall be 4m for hourly wind pressures not exceeding 0.94 kPa for 1/30 year wind.
10. Roof systems of wood-frame construction shall be tied to exterior walls by nailing the wall's interior furring strips directly to the roofing system. Furring strips must be continuous or adequate splicing shall be provided (Clause 9.20.11.4 Sentence 2). In lieu of wood furring strips, wood studs, metal studs or metal straps of adequate capacity can be used to prevent roof uplift.
11. For the support of masonry over openings, Clause 9.20.5.2 shall apply with the additional requirement that detailing shall be provided to achieve equal loading of the two Isobloc wythes. Also, where roof tie-down requirements are affected by openings, the designer shall provide detailing to prevent roof uplift.

The NBC Part 9 requirements given in this report incorporate conservative assumptions which the author deems appropriate at this time. As the Isobloc wall

system becomes more extensively used and a performance record is established, these requirements should be reviewed and possibly liberalized in a few years.

5. DESIGN IN ACCORDANCE WITH NBC PART 4

The following points highlight the key characteristics of the Isobloc wall system that must be considered when buildings are designed in accordance with Part 4 involving use of CAN3-S304.

1. From the experimental findings it is evident that there is no significant composite action between the two concrete wythes of the Isobloc wall. Therefore, composite action shall not be assumed in design calculations.
2. As wood strapping of the interior of Isobloc walls improves significantly the walls' vertical bending capacities, this technique could be used in areas of relatively low wind pressure and suction as well as in regions of relatively low seismic activity. It is the responsibility of the designer to ensure that this system is adequate to resist the applied lateral loads.
3. In designing an Isobloc wall, the wall can be considered as a cavity wall with two wythes acting independently in the vertical direction and tied together in the horizontal direction in such a way that both wythes share the applied lateral loads. For most combinations of vertical and lateral loads, Isobloc wall design will be based on the wall spanning horizontally between stiff lateral supports spanning vertically.
4. Where the load from the floor is transmitted to the Isobloc wall interior wythe by means of joist hangers, the design of the wall must consider the effect of the load eccentricity and the magnification of the bending moment based on the slenderness of the wall.
5. The maximum spacing of vertical supports required according to Clause 9.20.10.1 could be increased in areas subject to relatively low lateral loads.
6. For the design of openings in Isobloc walls, detailing shall be provided firstly, to ensure equal loading of Isobloc wythes from structural members spanning the opening and secondly, to achieve roof tie-down safety. Also, the wall needs to be checked for its structural capacity in both the horizontal and vertical directions.
7. The limiting formula of the CAN3-S304 (Clause 5.6.1.1) for the slenderness ratio (h/t) as $10(3 - e_1/e_2)$ can be used for Isobloc wall design except that e_1/e_2 must NOT be taken as less than zero.

6. DESIGN DETAILS

Figs. 16 to 21 present sample design details. The following comments apply to these schematic illustrations:

1. Figs. 16 and 17 deal with foundation details between concrete foundation walls and the startup of Isobloc walls. The use of either a ledge (Fig. 16) or joists embedded in slots at the top of the foundation wall (Fig. 17) provides satisfactory support conditions for the first floor level. In the case of Fig. 17, the Isobloc wall can readily span over the slots left in the concrete foundation wall.
2. Fig. 18 deals with joists supported on joist hangers as tested during the Phase II test program. The provision of ties between the two Isobloc wythes at every joist hanger location will control cracking associated with the relatively large eccentric loading of the Isobloc wall. Any such cracking will be further minimized by axial loads present in the wall and by the effect of load spreading in mortared construction.
3. Fig. 19 illustrates a roof detail between roof joists/rafters or trusses and an Isobloc wall. The capping on top of the wall ensures reasonably concentric loading while the strapping nailed or screwed to the roof joists prevents roof uplift. Since the Isobloc wall cannot be relied upon to resist vertical tensile forces, it is important that the tie-down furring strips be continuous far enough downward and be anchored effectively to resist all roof uplift forces. By using splices, the furring strips can be readily extended down to the foundation wall if required or else anchored to the floor diaphragm. Note that lighter furring strips than those shown on Fig. 19 can be employed for NBC Part 9 buildings.
4. Fig. 20 provides schematic connection details between a horizontally spanning Isobloc wall and a lateral support. The type of connection used between the wall and the lateral support will vary depending on whether the lateral support is a reinforced masonry column, HSS section, or reinforced concrete column. At each connection, it is recommended to tie in both wythes of the Isobloc wall for increased strength and stiffness; this can be achieved by a separate tie as shown in Fig. 20a or by a single continuous tie as shown in Fig. 20b.
5. Fig. 21 illustrates a schematic opening detail of a horizontally spanning Isobloc wall. As the structural capacity of the Isobloc wall is affected by the size and location of openings, the designer must check the adequacy of the horizontal bending capacity of various wall regions.

It is to be noted that the details presented in Figs. 16 to 21 are schematic in nature only and it is the responsibility of the designer to provide the exact details which will ensure the safety and serviceability for a particular project.



Dr. G.T. Suter, P.Eng.



Table1 Measured Dimensions of Isobloc Units (mm)

Unit No.	Height	Width	Length	Shell Thickness
1	189	240	390	60
2	190	240	391	61
3	189	241	391	59
4	190	240	391	60
5	190	240	391	59
Average	189.6	240.2	390.8	59.8
Use	190	240	390	60

Table 2 Compressive Strength of Isobloc Units

Source	Sample	Compressive Strength (MPa)
SCI	1	23.7
	2	23.9
	3	20.7
	4	24.0
	5	22.1
	Average	<u>22.9</u>
	COV (%)	6.0
LIE	1	19.1
	2	16.5
	3	19.9
	Average	<u>18.5</u>
Note: SCI = Suter Consultants Inc., Phase II report, Table 2, based on 41 500 mm ² net area		
LIE = L.I.E. Controle - Montreal, Report No. 2.1, based on 47 000 mm ² net area		
COV = coefficient of variation		

Table 3 Summary of Structural Properties Tests

Type of Test	Test Report Source	Report Location
Assemblage under concentric compression	SCI	Appendix A
Assemblage under eccentric compression	SCI	Appendix A & B
Assemblage under eccentric compressive creep loading	SCI	Appendix B
Wall under concentric compression	LIE	Appendix D
Wall under eccentric concentrated load (joist hanger tests)	SCI	Appendix B
Wall under flexural loading spanning vertically	SCI	Appendix A & B
Wall under flexural loading spanning horizontally	SCI	Appendix B
Wall under in-plane shear loading (racking test)	LIE	Appendix D

**Table 4 Selected HSS sections for lateral support
versus wall height**

Spacing Between Lateral Supports (m)	Wall Height (m)	Column Cross-Section
2.4	3.0	HSS 4 x 4 x 0.250
2.4	4.0	HSS 4 x 4 x 0.375
2.4	5.0	HSS 6 x 6 x 0.250
2.4	6.0	HSS 6 x 6 x 0.375
3.8	3.0	HSS 5 x 5 x 0.250
3.8	4.0	HSS 5 x 5 x 0.375
3.8	5.0	HSS 7 x 7 x 0.250
3.8	6.0	HSS 7 x 7 x 0.375

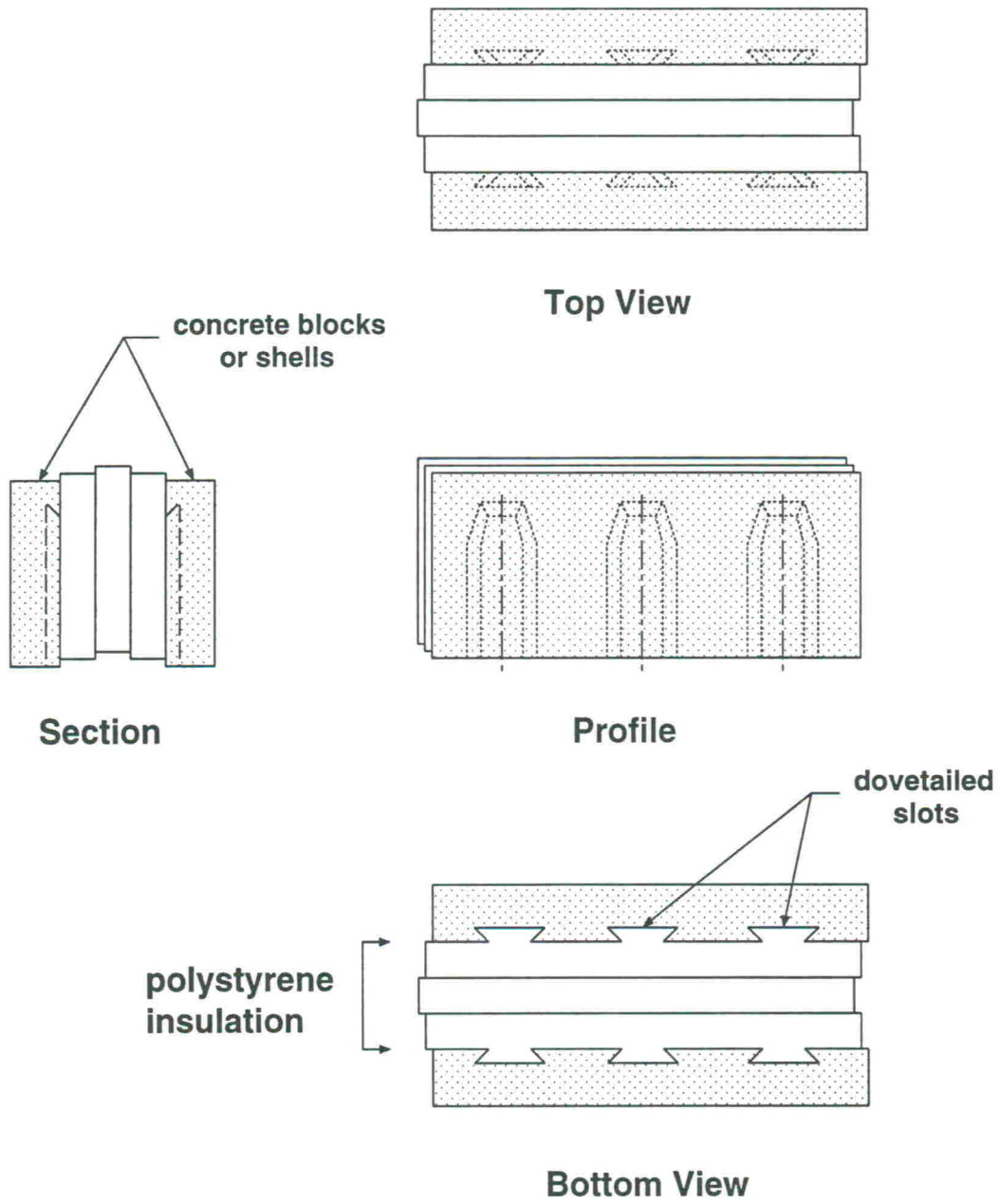
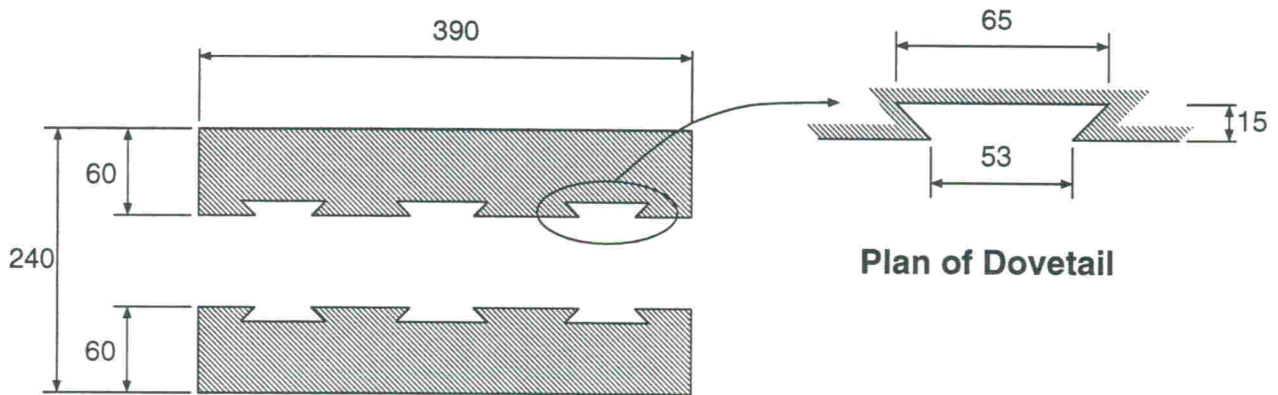


Fig. 1 Isobloc unit



Plan of Shells

Plan of Dovetail

$$\text{Net area} = 390 \times 60 \times 2 - 59 \times 15 \times 6 \text{ dovetails}$$

$$= 41\,490 \text{ mm}$$

$$= 41\,500 \text{ mm for calculations}$$

$$\text{Equivalent shell thickness} = \frac{41\,500}{390 \times 2} = 53.2 \text{ mm}$$

Fig. 2 Net area of Isobloc unit

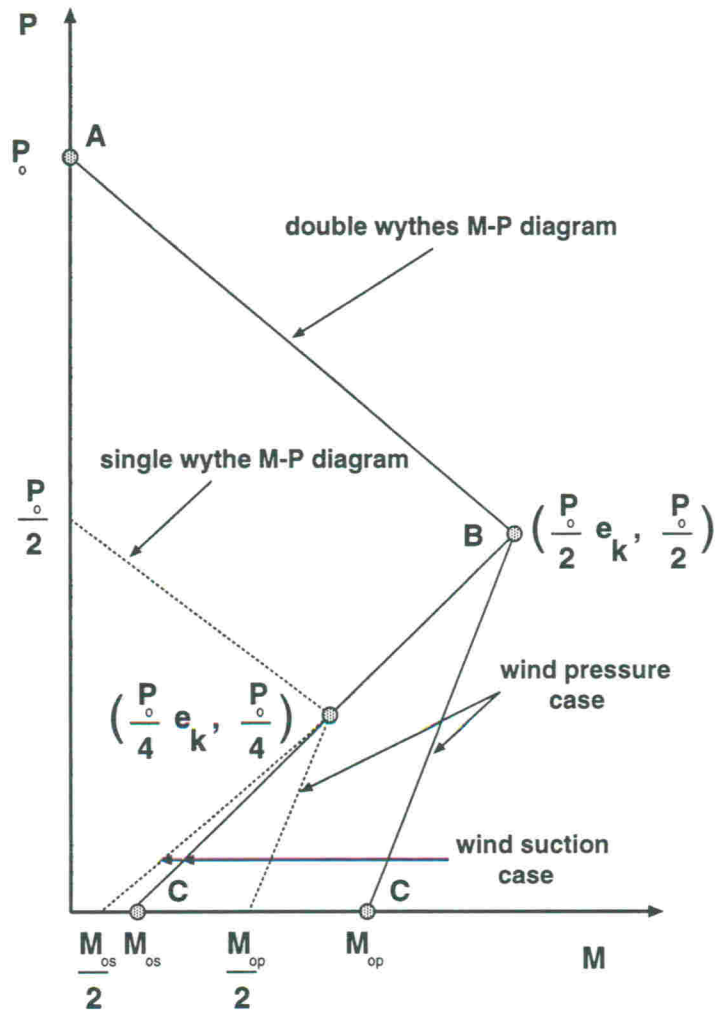


Fig. 3 Illustration of the interaction diagrams for Isobloc walls having 38 x 64 mm wood studs attached to one wythe

Notation:

P_0 = Axial load

M_{op} = Pure moment simulating the wind pressure case with the wood studs in tension

M_{os} = Pure moment simulating the wind suction case with the wood studs in compression

e_k = Kern eccentricity

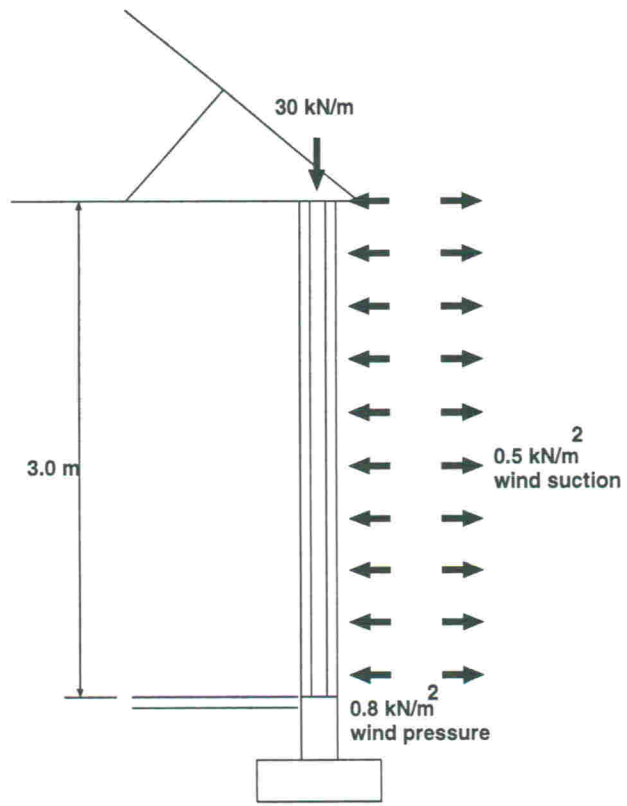


Fig. 4 3m high wall in a commercial building of Example 1

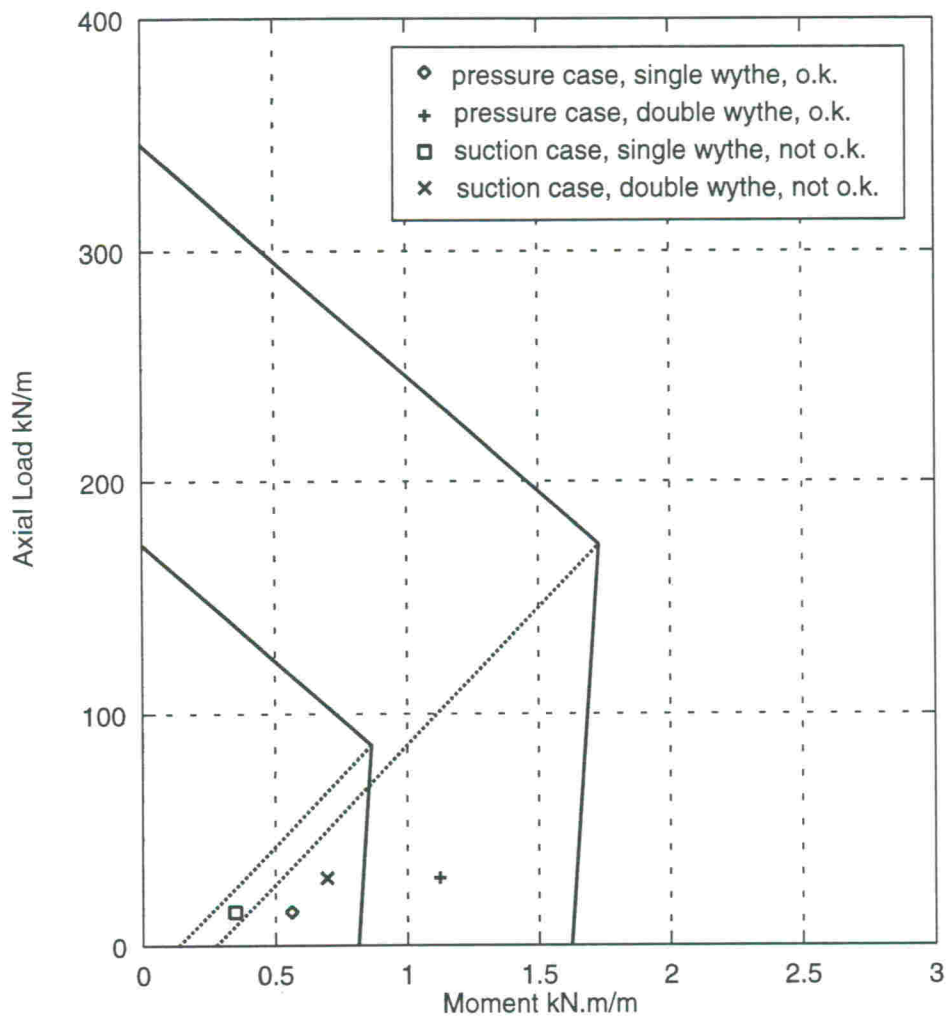


Fig. 5 M-P interaction diagram, example 1

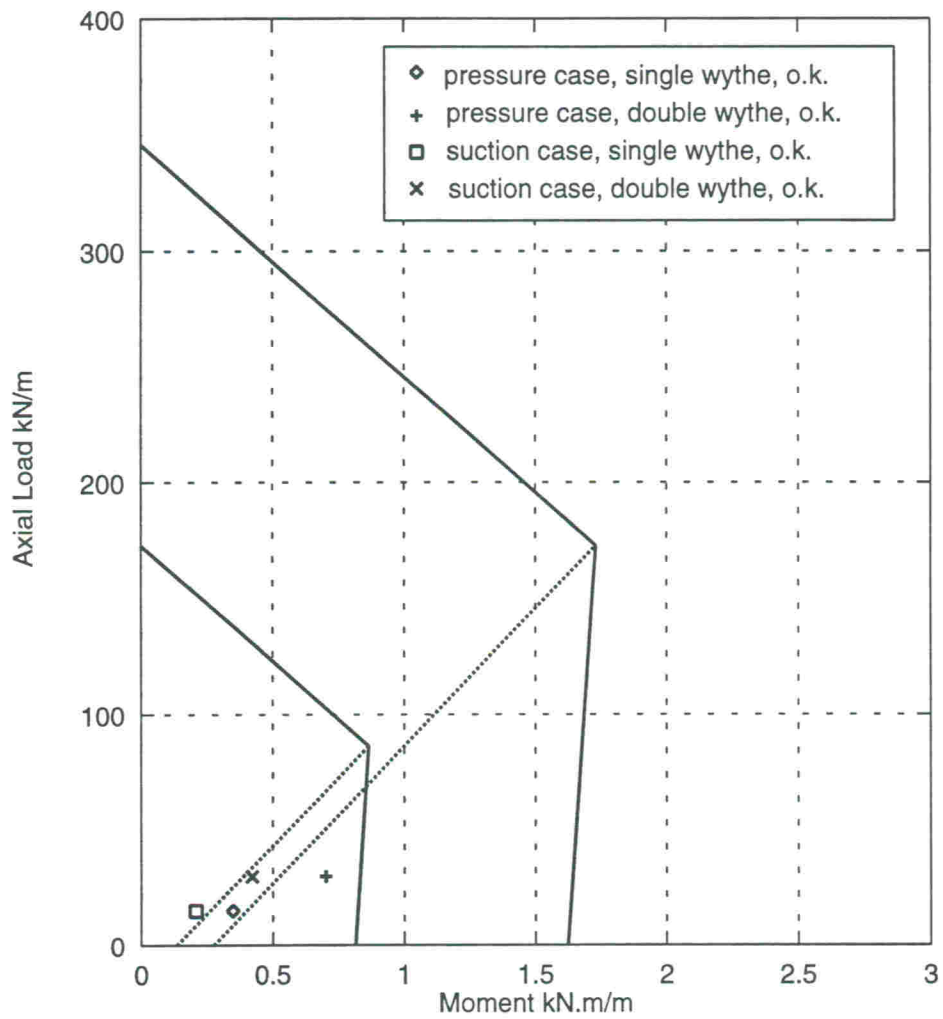


Fig. 6 M-P interaction diagram, example 1 with reduced wind pressure and reduced wind suction

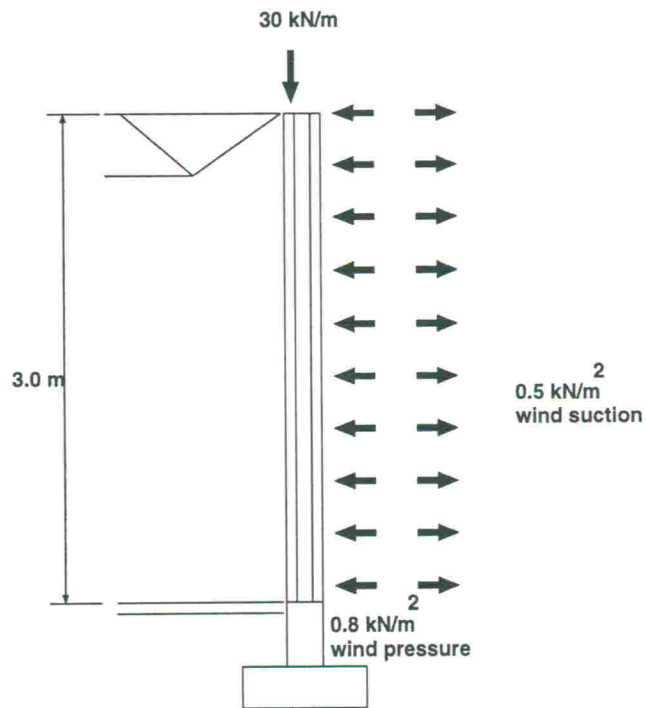


Fig. 7 3m high wall in a commercial building of Example 2

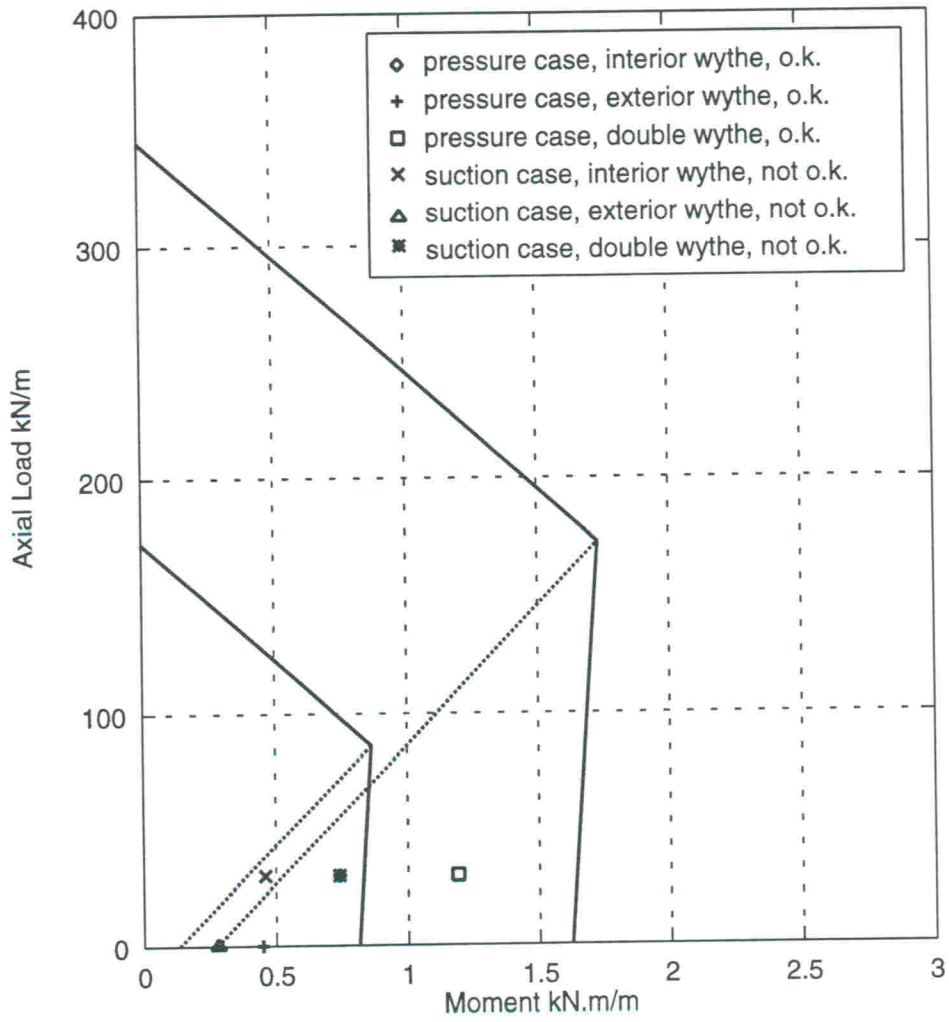


Fig. 8 M-P interaction diagram, example 2

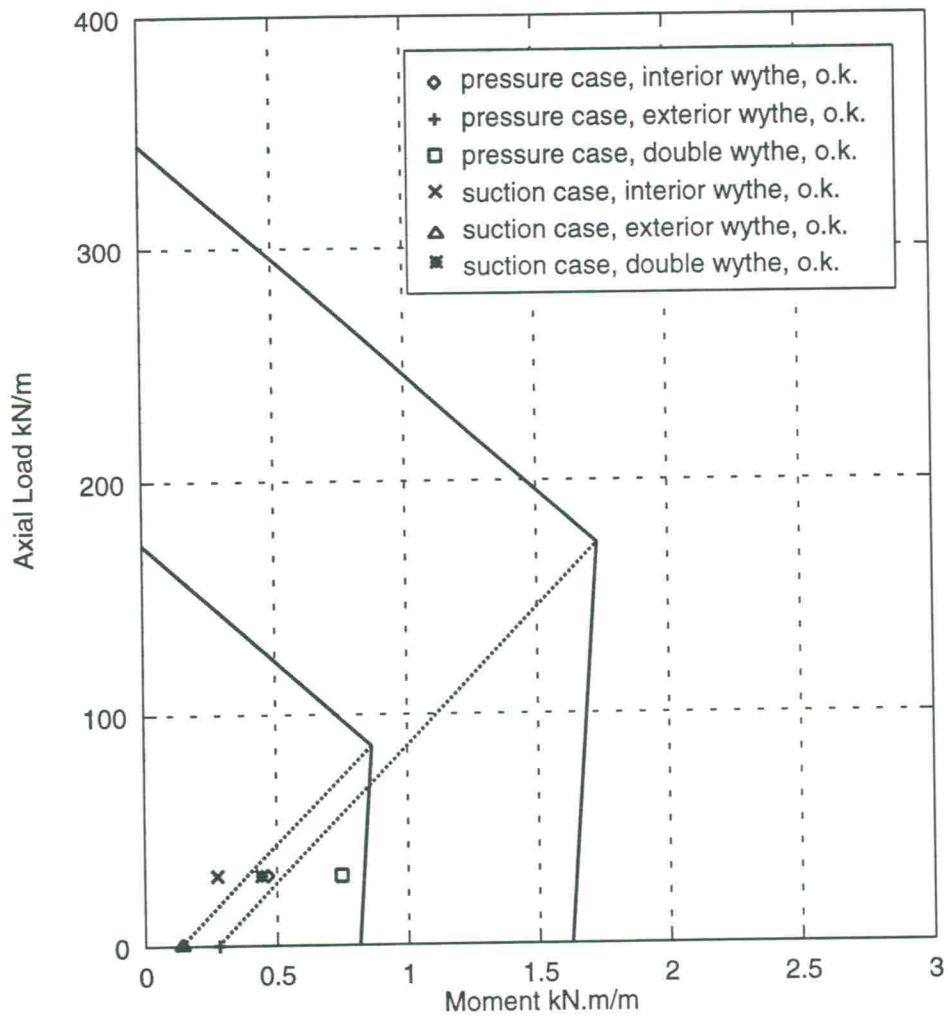


Fig. 9 M-P interaction diagram, example 2 with reduced wind pressure and reduced wind suction

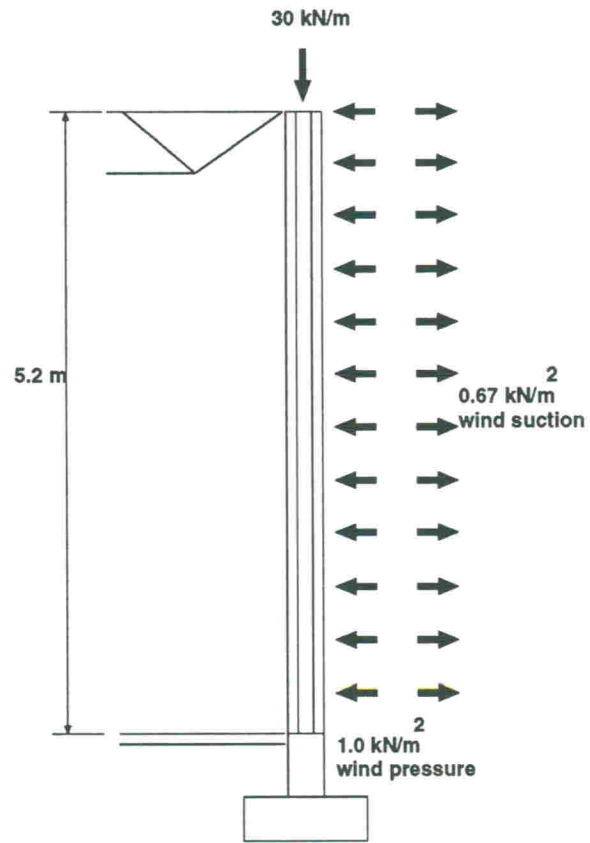


Fig. 10 5.2m high wall in an industrial building of Example 3

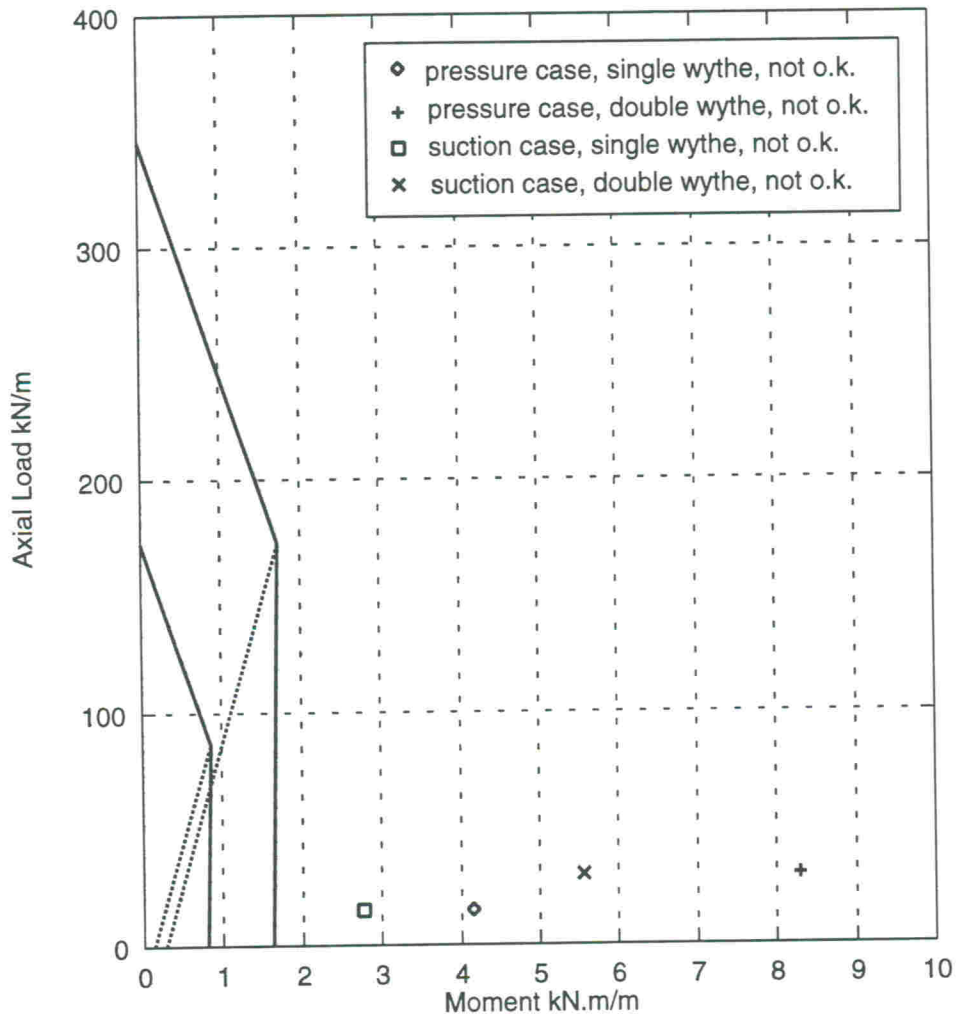


Fig. 11 M-P interaction diagram, example 3

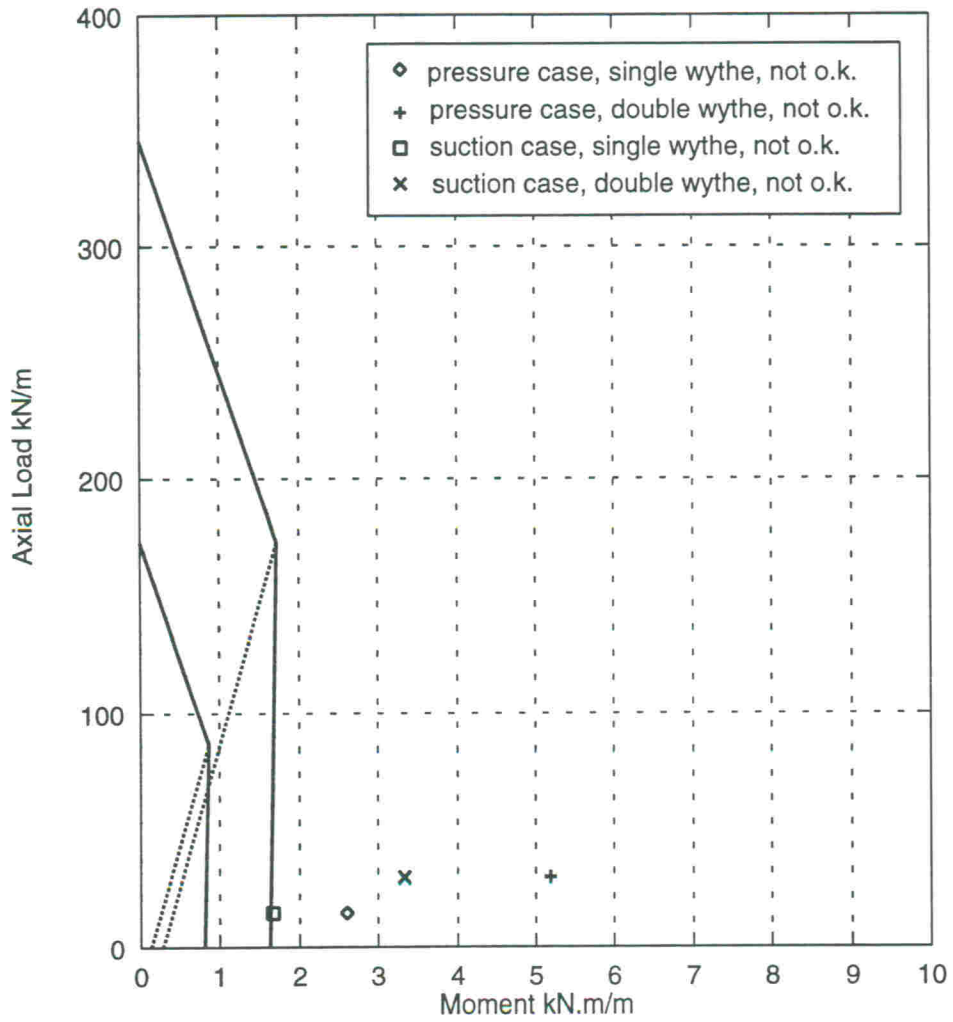


Fig. 12 M-P interaction diagram, example 3 with reduced wind pressure and reduced wind suction

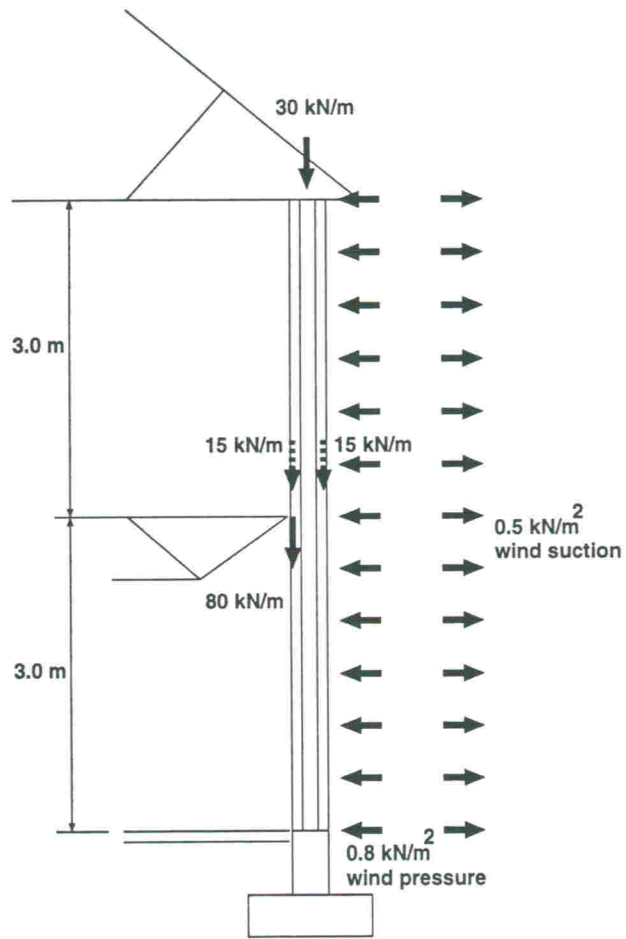


Fig. 13 Two-storey high wall in building of Example 4

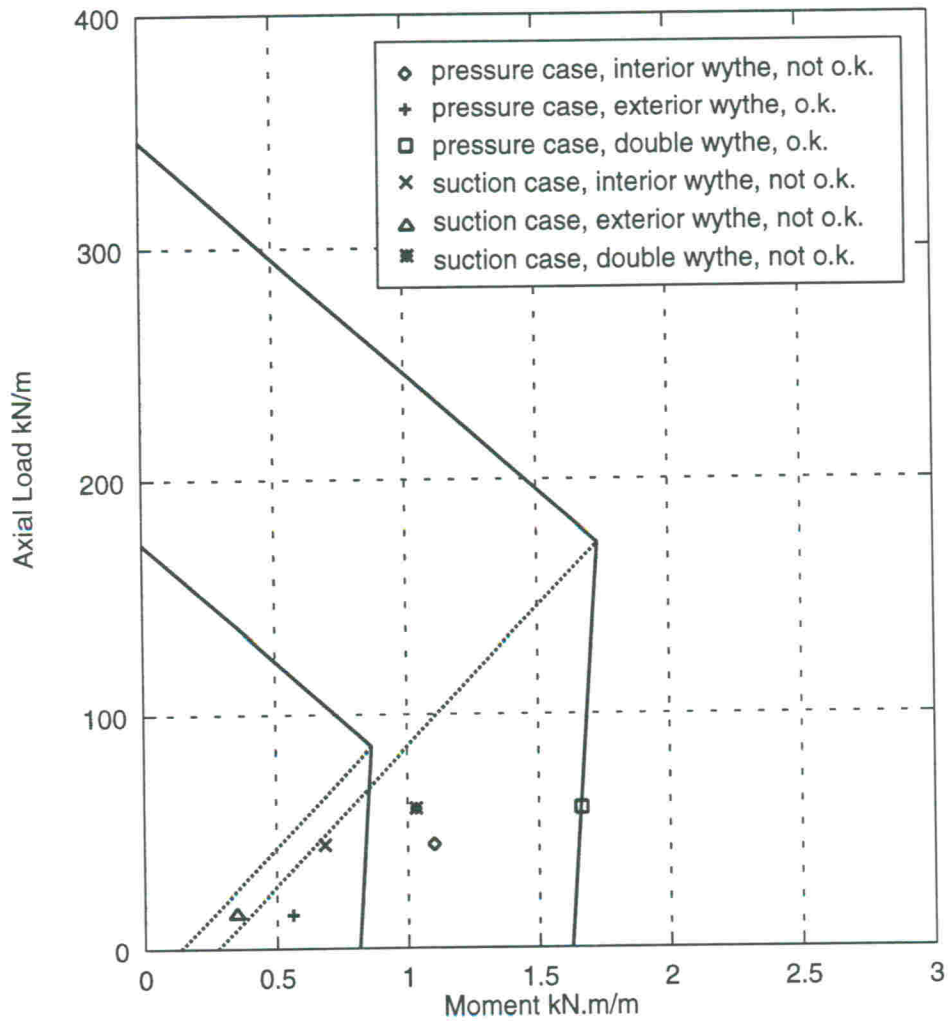


Fig. 14 M-P interaction diagram, example 4

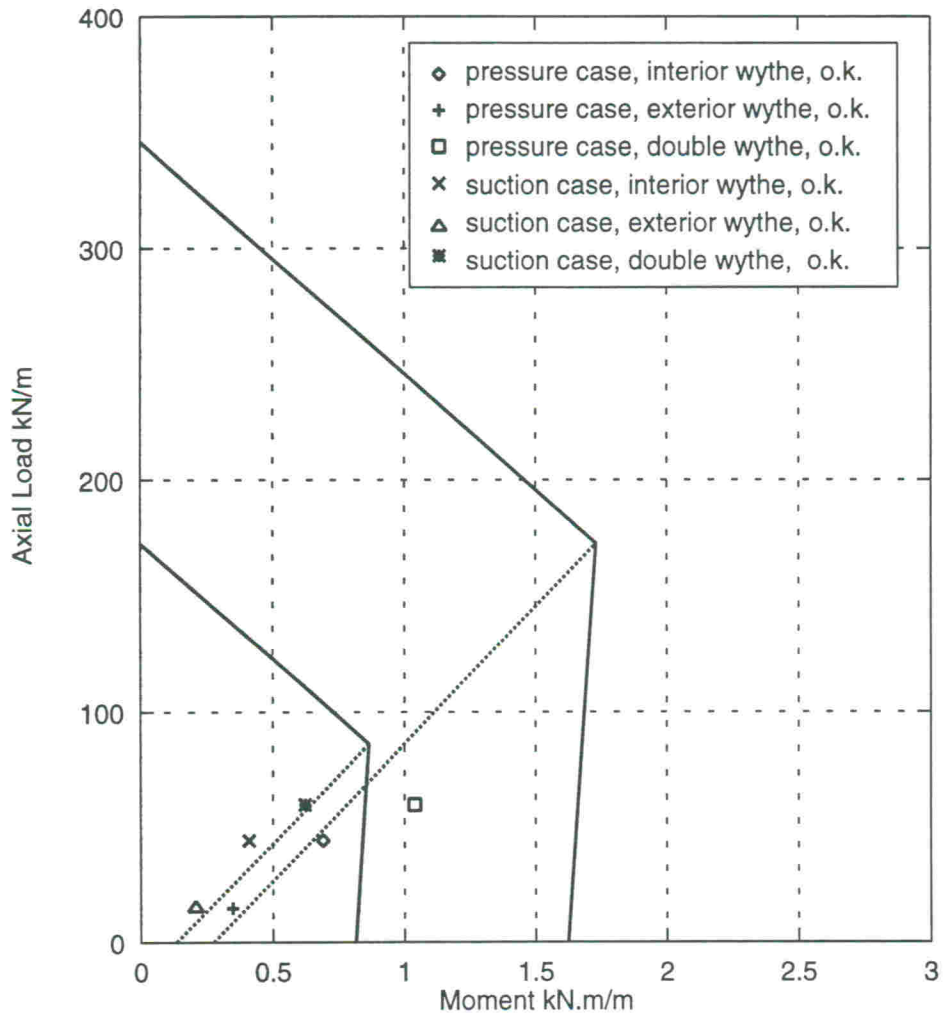


Fig. 15 M-P interaction diagram, example 4 with reduced wind pressure and reduced wind suction

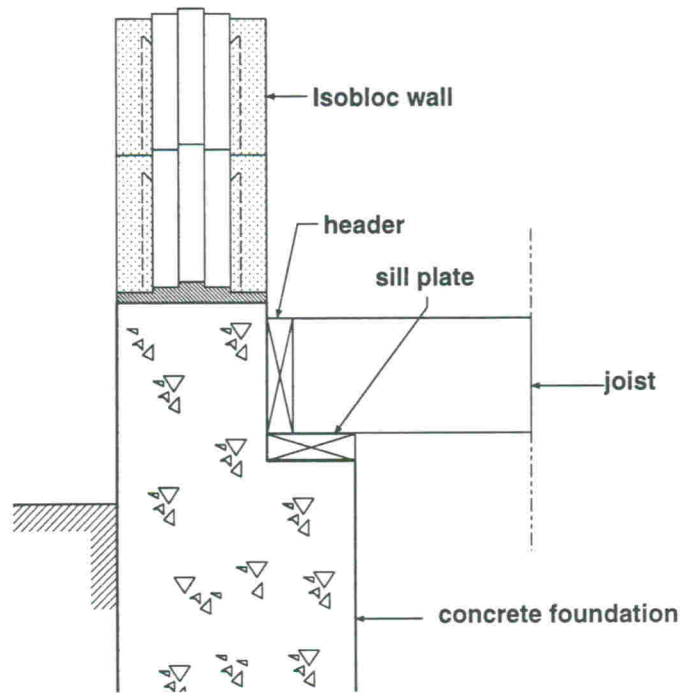


Fig. 16 Floor joists supported on ledge formed in the foundation wall

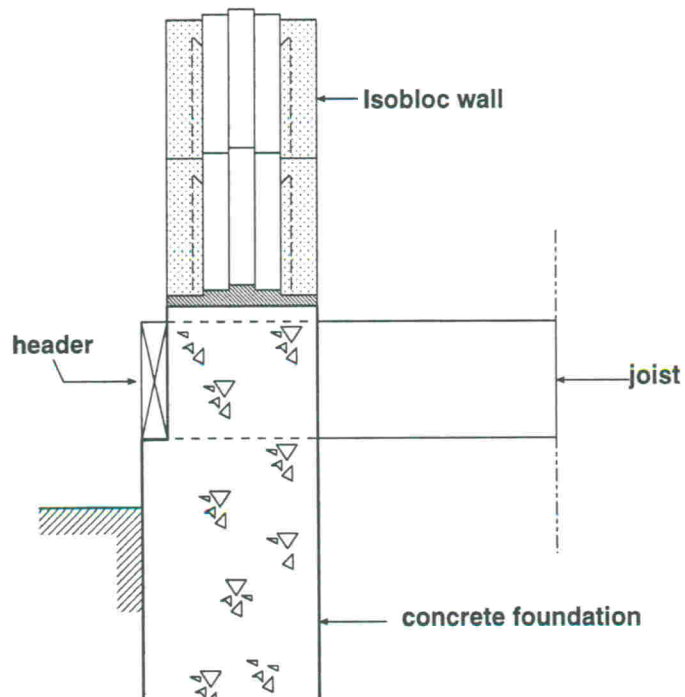


Fig. 17 Floor joists embedded in the top of the foundation wall

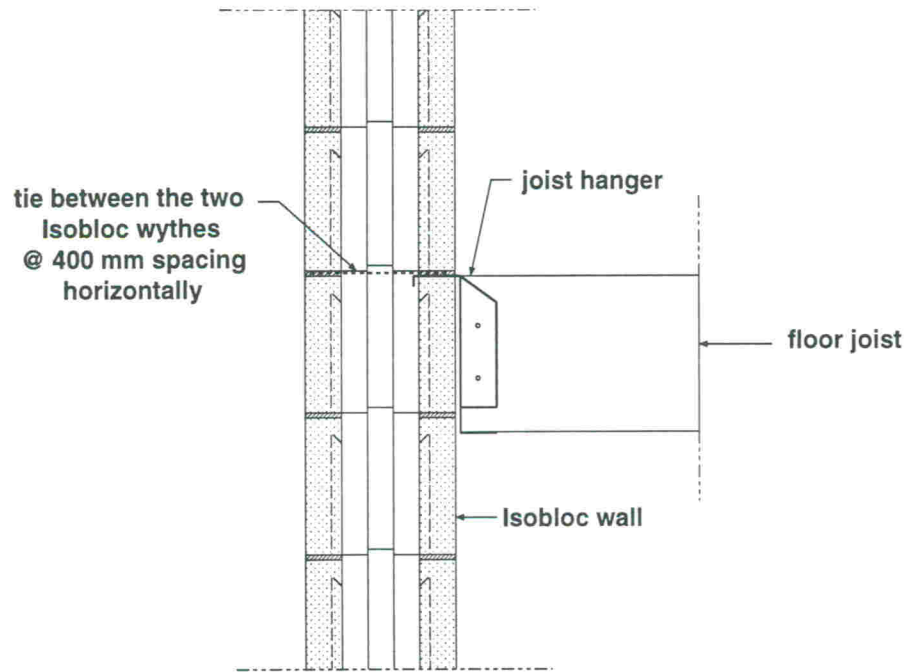


Fig. 18 Floor joists supported on joist hangers

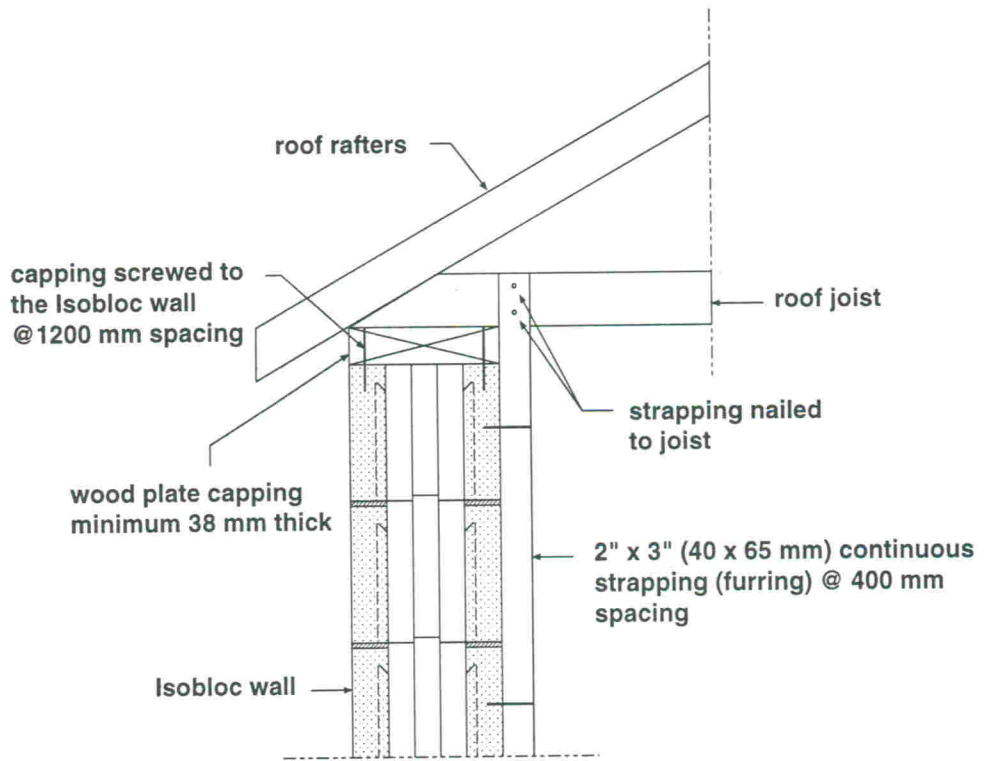
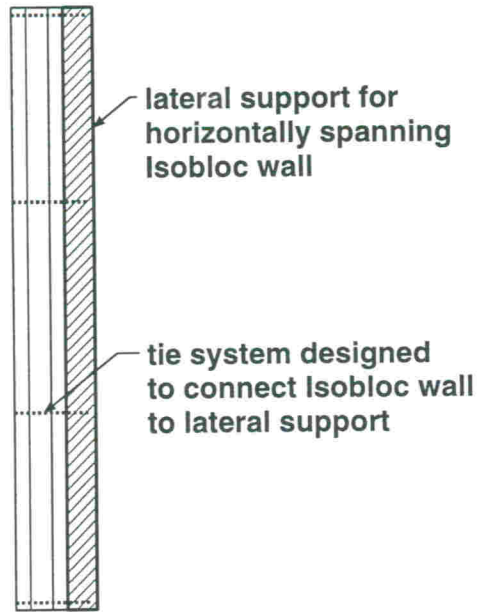
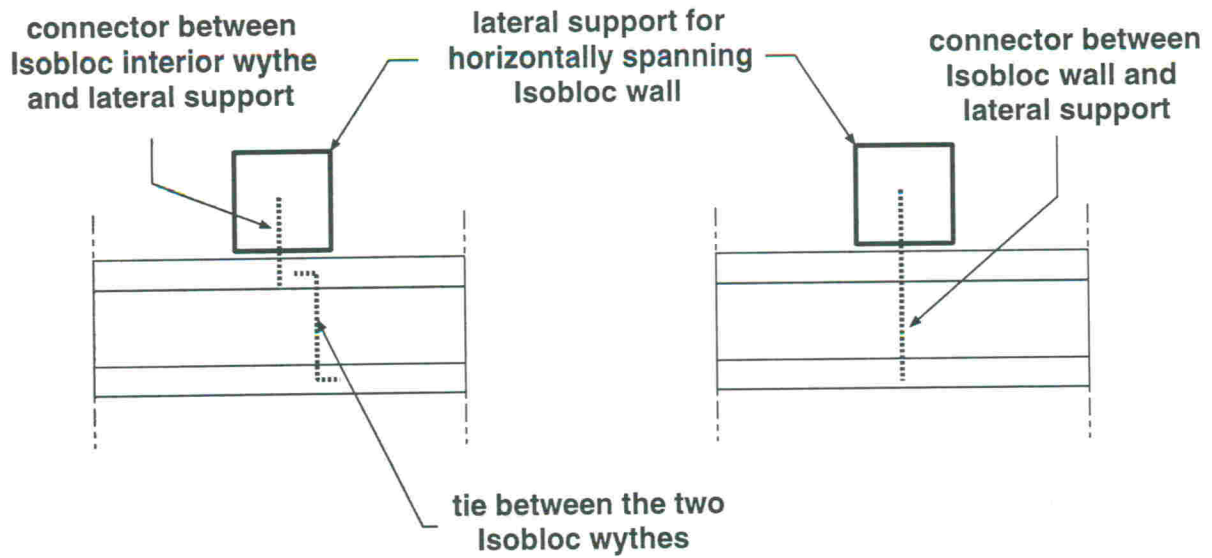


Fig. 19 Roof supported on Isobloc wall



Elevation



(a) Option 1 Section

(b) Option 2 Section

Fig. 20 Schematic connection details between Isobloc wall and lateral support

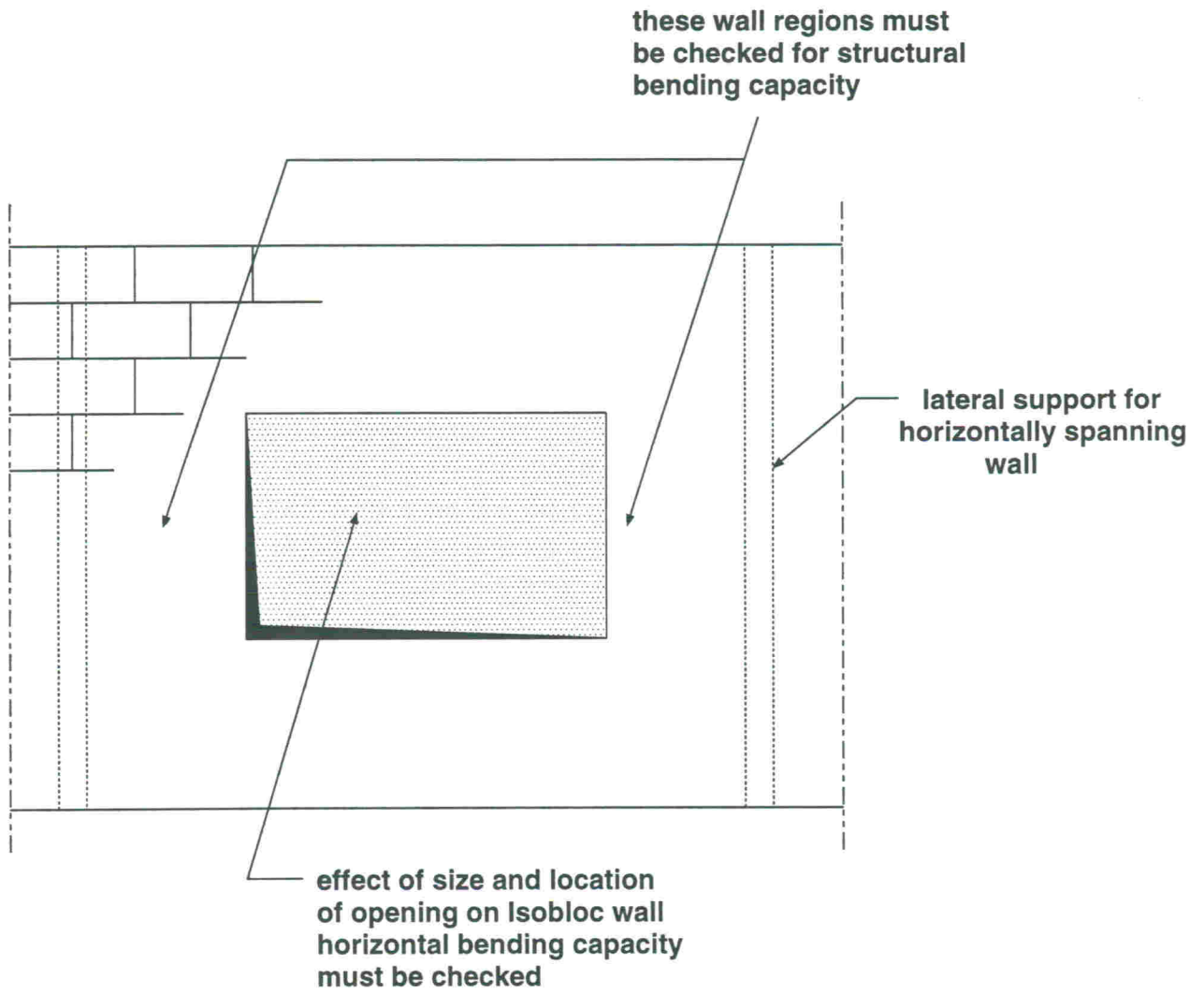


Fig. 21 Elevation showing opening in Isobloc wall

APPENDIX A

ISOBLOC TESTS PHASE I



SUTER CONSULTANTS INC *Consulting Engineers*

38 Auriga Drive, Suite 200, Nepean, Ontario Canada K2E 8A5
TEL: (613) 224-4426 FAX: (613) 224-6055

**ISOBLOC TESTS
PHASE I**

**REPORT FOR
LES PRODUITS ISOBLOC INC.
526, Ch. du Parc Industriel
Bromptonville, Quebec
JOB 1H0**

PROJECT 94119

FEBRUARY 8, 1995

ISOBLOC TESTS - PHASE I

1. INTRODUCTION

The Phase I test program dealt with in this report was carried out to establish the behaviour and capacity of firstly, four assemblages subjected to concentric and eccentric compression and secondly, two full height single storey walls subjected to lateral loading. A key variable in both the assemblage and wall tests was the absence or presence of standard Z ties between the two block faceshells. The presence of Z ties would establish to what extent such easily installed connectors could provide a measure of composite action between the face shells.

The test program was carried out during December 1994 and January 1995 in the Structures Laboratories at Carleton University, Ottawa, under the direct supervision of the author.

2. TYPES OF SPECIMENS

The following types of specimens were prepared for testing:

- (1) Six 50mm cubes for compressive strength testing of the mortar.
- (2) Twelve - 75 x 150mm cylinders for split-tensile and stress-strain testing of the mortar.
- (3) Four 3-course high assemblages for concentric and eccentric compressive strength testing. Two assemblages contained no ties while two assemblages contained 2 Z-ties placed as shown in Fig. 1.
- (4) One seven-unit high assemblage without ties for concentric compressive strength testing. This assemblage was not originally planned but was added to provide additional information.
- (5) Two 1200 x 2800 mm walls for flexural load testing. One wall contained no ties and the other wall contained 10 Z-ties placed as shown in Fig. 2.

3. MATERIALS

The mortar used for construction was a type S mortar, typical for concrete block construction. The masons chose a premixed mortar and included a small quantity of Sealbond which is typical of construction practice. The proportions are listed below:

2 bags - Betomix Plus, Type S mortar, ANCOR-CSA A 179M

1/3 bag - Sealbond Plasticizer for Mortar, CSA A179 or ASTM C270.

The walls and prisms were constructed with standard Isobloc blocks supplied to us by Les Produits Isobloc Inc.. The masonry wall ties were 178 mm (7in.) 4.76 mm (3/16 in.) diameter hot-dipped galvanized Z ties provided by Block-Lok Limited.

4. SPECIMEN CONSTRUCTION

Construction of all specimens was carried out on December 15, 1994. All masonry specimens were constructed by a skilled mason under the supervision of Suter Consultants Inc. The workability of the mortar was left to the judgement of the mason.

For the first seven days of curing, all specimens were kept moist by means of wet rags and polyethylene wrapping. After seven days, the specimens were uncovered to cure under laboratory conditions until testing at about 28 days. Laboratory conditions consisted of a relative humidity of about 25% and an air temperature of about 20°C.

5. TESTING

5.1 Mortar Testing

Compressive, split-tensile, and stress-strain testing of mortar specimens was carried out in a Tinius Olsen Universal testing machine. Testing took place at an age of 36 days on January 20, 1995.

A summary of the mortar test results is given in Table 1. It should be noted here that samples 1 to 3 were taken from the first batch of mortar made for construction, and samples 4 to 6 were taken from the second batch of mortar made. They are however basically the same mix.

The following comments apply to Table 1:

1. While the results vary slightly from one batch to another, they are close enough to be grouped together.
2. The average compressive strength of 12.13 MPa is close to the 12.5 MPa required strength for Type S mortar at 28 days (for laboratory prepared mortar in accordance with CSA A179-94 "Mortar and Grout for Unit Masonry") and is therefore judged as satisfactory.
3. The average split-tensile strength of 2.12 MPa provides a good level of strength for this mortar and is therefore acceptable. CSA Standards do not require a certain minimum tensile strength for mortar.

5.2 Assemblage Properties Tests

5.2.1 General

Compressive testing of the four 3-course high and one 7-course high assemblages was carried out in a Tinius Olsen Universal testing machine. Testing took place between January 10 and 16, 1995 at ages of 26 to 32 days.

First, two 3-course high assemblages (one assemblage without ties and the other with ties) were tested concentrically as shown in Fig. 1. Each assemblage was instrumented with stainless steel discs for deformation readings by means of a Demec extensometer (200 mm gauge length) as follows: two sets of discs on both the front and back faces for vertical deformations and two sets of discs at half height across the wythes to monitor potential spreading deformations between the two shells. The instrumentation setup is illustrated in Photo 1. Loading was applied gradually in about ten load steps to failure. After each load increment, a set of Demec readings was taken. The typical duration of a test was about one hour.

Second, two 3-course high assemblages (one assemblage without ties and the other with ties) were tested eccentrically; the eccentric load was centered on one wythe as shown in Fig. 1. Again a set of six Demec readings was taken for each load increment. The duration of a test and the number of load increments were similar as for the concentric tests.

Finally, one 7-course high assemblage without ties was tested concentrically. The lower four courses were built vertically while the upper three courses were built with an out-of-plane eccentricity of 22 mm at the top of the assemblage. Only two Demec readings were taken for each load increment to monitor the spreading deformation between the two wythes. Loading was applied gradually in 14 load steps to failure.

5.2.2 Compressive Behaviour of Assemblages

The following comments apply for concentric compression:

1. During the uncracked stage, both the assemblage without ties and the assemblage with ties behaved in a linearly elastic manner; this behaviour is as expected. Compressive stress-strain relationships for both assemblages are illustrated in Fig. 3. Note that the stress-strain data of Fig. 3 indicate a modulus of elasticity for the masonry, E_m , equal to about

$$E_m = 12\,500 \text{ MPa for the assemblage without ties, and}$$

$$E_m = 6600 \text{ MPa for the assemblage with ties.}$$

The spread in E_m values is likely caused by the inherent stiffness variability of the concrete block masonry rather than by the presence or absence of ties. The average E_m value for the two assemblages is equal to 9600 MPa.

2. The ultimate compressive capacities of the assemblages without ties and with ties were almost identical and equal to 700 kN and 650 kN respectively (16.9 MPa and 15.7 MPa stress over net area respectively). The capacities are not influenced by the absence or presence of ties and are deemed to be satisfactory.
3. Both the assemblage with ties and the assemblage without ties exhibited almost equal spreading deformations as illustrated in Fig. 5. The fact that the spreading deformation for the assemblage with ties is negative (i.e. the two faceshells or wythes moved closer together) while the other is positive, at first appears to indicate that the Z-ties are effective in controlling spread. As later test results for eccentric compression and the 7-course high specimen will indicate, the spread (whether outward or inward) may be more dependent on the exact filling conditions of the bedjoints rather than the presence of ties.
4. While no significant cracking was observed before ultimate failure for the assemblage without ties, the assemblage with ties exhibited a small crack at 400 kN.

Photos 1 and 4 illustrate testing details for the assemblages subjected to concentric compression. Final failure of both the specimens without ties and with ties was relatively sudden but that is to be expected for unreinforced concrete masonry.

The following comments apply for eccentric compression:

1. During the uncracked stage, both the assemblage without ties and the assemblage with ties behaved in a linearly elastic manner; this behaviour is as expected. Compressive stress-strain relationships for both assemblages are illustrated in Fig. 5. Note that the stress-strain data of Fig. 5 indicate a modulus of elasticity for the directly loaded wythe of the masonry equal to about

$$E_m = 12\,000 \text{ MPa for the assemblage without ties, and}$$

$$E_m = 10\,700 \text{ MPa for the assemblage with ties.}$$

As for the concentrically loaded assemblages, the spread in E_m values is likely caused by the inherent stiffness variability of the concrete block masonry rather than by the presence or absence of ties. The average E_m value for the two assemblages is equal to 11 400 MPa.

2. The ultimate compressive capacities of the assemblages without ties and with ties were similar and equal to 385 kN and 335 kN respectively (18.6 MPa and 16.1 MPa respectively over net area of the loaded shell). The capacities apparently are not significantly influenced by the absence or presence of ties and are deemed to be satisfactory. Ultimate failure of both assemblages occurred relatively suddenly as the loaded wythe crushed. Note that the ultimate capacities of the eccentrically loaded specimens are about half those of the concentrically

loaded specimens. This indicates that there is no composite action between the two wythes even when Z ties are present.

3. Both the assemblage with ties and the assemblage without ties exhibited almost equal spreading deformations as illustrated in Fig. 6. Note that both spreads are small and positive.

The following comments apply for the 7-course high assemblage loaded concentrically:

1. The ultimate compressive capacity of the assemblage was equal to 585 kN (14.1 MPa stress over net area). The attainment of such a high load and stress level is somewhat surprising firstly, due to the increased slenderness of the 7-course high wythes and secondly, due to the pre-existing out-of-plane eccentricity of 22 mm.
2. The assemblage exhibited relatively small spreading deformations as illustrated in Fig. 7. Note that the spreading is negative and the wythes therefore moved closer together. These spread findings for a relatively slender specimen without ties as well as those for the 3-course high assemblages indicate that the presence or absence of ties has no major influence on the direction and magnitude of the spread; it is likely that the nature of the bedjoints (i.e. the filling and uniform thickness) has a more direct influence on the spread behaviour. At any rate, the small amounts of spread that would be exhibited at working stress levels of say 3 or 4 MPa would be of no structural significance.
3. As shown in Photo 5, significant cracking developed at 450 kN and extended over most of the specimen's height by 550 kN. The ultimate failure was sudden as depicted in Photo 6.

5.2.3 Mode of Failure Summary Comment

All five assemblages regardless of whether they were loaded concentrically or eccentrically and regardless of whether they contained ties, failed in a relatively sudden crushing, spalling and outward buckling failure mode characteristic of unreinforced slender concrete block masonry. The capacities were not significantly influenced by the absence or presence of the Z ties.

5.3 Flexural Wall Testing

5.3.1 General

Two 1200 x 2800 mm walls were constructed on rigid steel channels for flexural testing in the vertical direction. One wall was built without ties and the other had 10 Z-ties distributed as indicated in Fig. 2. Flexural wall testing was carried out according to ASTM Standard E 72 in a test setup shown in Photo 7. In order to

measure the deflections, four dial gauges were installed, two on each side of the wall at mid-height. By providing deflection gauges on both sides of the wall, potentially different movements of the two wythes of the wall could be monitored. Also, three dial gauges, two mounted at the bottom of the wall and one mounted at the top of the wall, were employed to monitor support movements.

An MTS 50-kip hydraulic actuator was used to apply load to the walls through a distributing beam as shown in Photo 8. After each load increment, the load level was maintained constant for 5 minutes. Deformation readings were taken as soon as practical after load application, at the end of the 5-minute period under constant load, immediately upon release of the load, and again after 5 minutes. No significant variations between the dial gauge 0-min and 5-min readings were recorded.

5.3.2 Wall Behaviour

The following wall behaviour was observed:

1. During the uncracked stage, the wall with no ties and the wall with ties behaved in a linearly elastic manner and deflections were very small.
2. Both the walls with no ties and with ties exhibited cracking at 1000 N (cracking moment = 325 N.m). Cracking consisted of one major crack at mid-height of the wall. Crack widths at the cracking load were determined as about 0.1 mm for both walls; such a crack width is considered a hairline crack.
3. As loading increased, crack widths increased and additional cracks developed in other high moment regions. Crack widths at 2000 N were measured as 0.8 mm for the wall without ties and 0.25 mm for the wall with ties; the widths pertain to the mid-height crack location and represent maximum crack widths. It is noteworthy, that the wall with ties exhibited a significantly smaller crack width.
4. At loads exceeding the cracking load, the wall with ties displayed significantly smaller deflections than the wall without ties; this deflection behaviour is shown in Fig. 8. Note that at 2500 N, which represents 83 percent of ultimate capacity, the wall with ties exhibited only about one quarter of the deflection of the wall without ties. The ties therefore provide a measure of wall stiffening which is beneficial.
5. The deflection behaviour shown in Fig. 8 clearly indicates that the two wythes deflect different amounts even when ties are present, i.e. the front face exhibits increased deflections as compared to the back face. From the makeup of the Isobloc and the compressibility of the insulation core such behaviour is to be expected.
6. The ultimate flexural capacity of both walls was identical and equal to 3000 N

(ultimate moment = 975 N.m). This indicates that the presence of ties had no effect on lateral load capacity.

5.3.3 Mode of Failure of Walls

1. No difference in mode of failure between the wall with no ties and the wall with ties was observed.
2. The mode of failure consisted of a relatively sudden rotation of one larger wall element versus the rest of the wall at a major flexural crack in a bed joint. A typical wall failure is illustrated in Photo 8.

6. KEY CONCLUSIONS

Regarding the flexural wall tests, the following conclusions are reached:

1. Both cracking and ultimate load capacities of the walls are small and are not influenced by the presence or absence of ties.
2. The ties provide a measure of crack control and wall stiffening for the post-cracking stage which is beneficial.
3. Both walls without and with ties do not display composite behaviour and hence are weak in resisting lateral loads when spanning vertically.

Regarding the compressive assemblage tests, the following conclusions are reached:

1. For concentric loading, the ultimate capacity corresponding to an ultimate stress of about 16 MPa for both the assemblages without and with ties is considered as satisfactory.
2. For concentric loading, the ultimate capacity and mode of failure are not influenced by the presence or absence of ties.
3. For eccentric loading, the ultimate capacity and mode of failure are not influenced by the presence or absence of ties.
4. No conclusive evidence exists of the effect of the presence of ties on the spreading deformation of the assemblages. The spreading deformations at working stress levels are small at any rate and are judged to be of no structural significance.



Dr. G.T. Suter, P.Eng.



Table 1 Mortar test results

Sample	Compressive Strength (MPa)	Split-Tensile Strength (MPa)
1	10.97	2.22
2	10.97	2.31
3	10.88	2.11
4	12.50	2.04
5	12.75	2.01
6	14.71	2.07
Average	12.13	2.12
COV %	12.00	5.00

Note: COV : Coefficient of variation

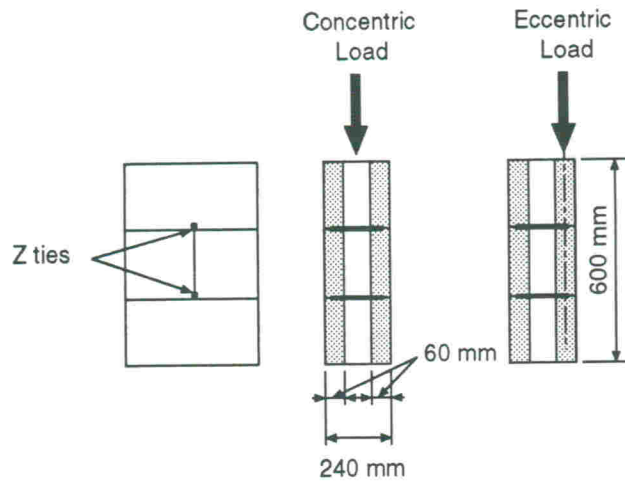


Fig. 1 Assemblage properties test

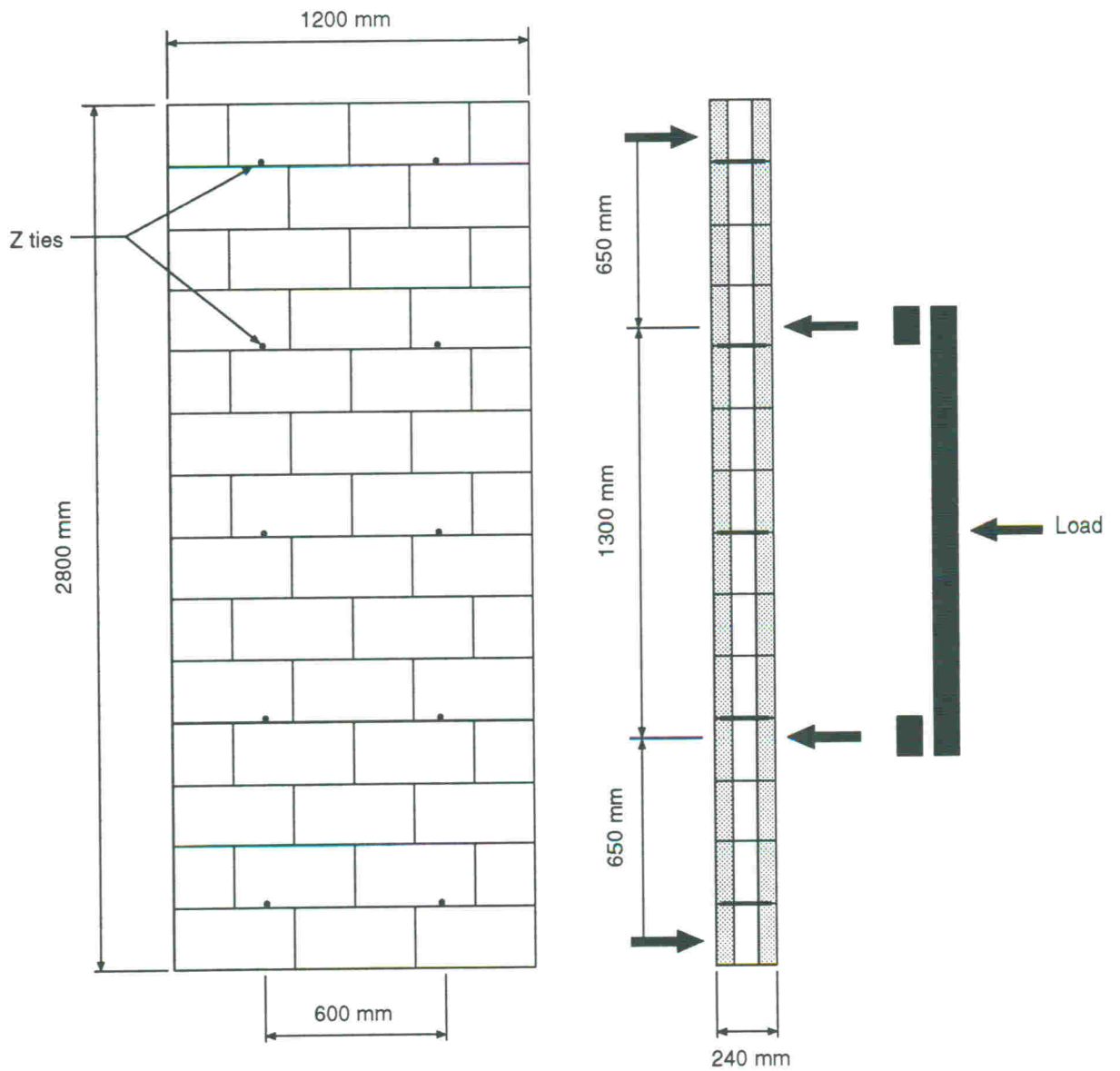


Fig. 2 Wall flexural test

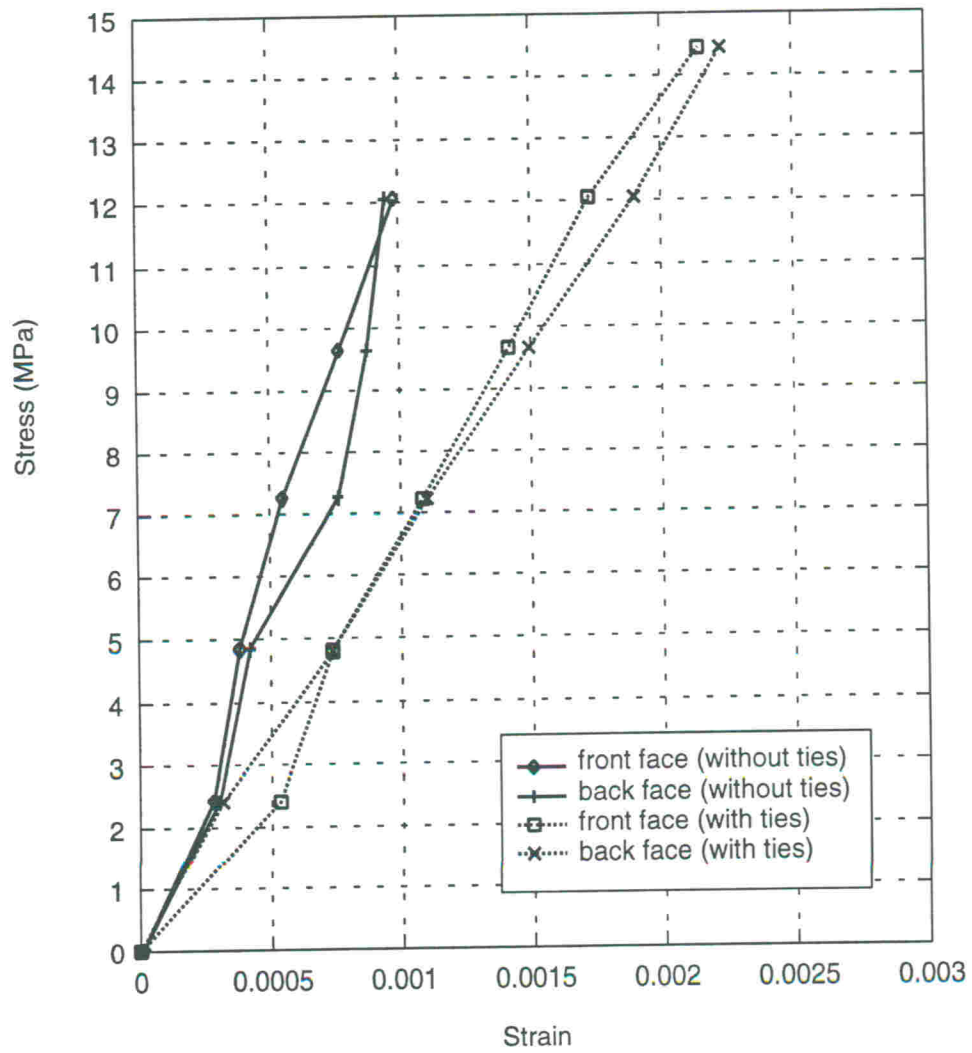


Fig. 3 Compressive stress-strain relationships for assemblages with and without ties loaded concentrically

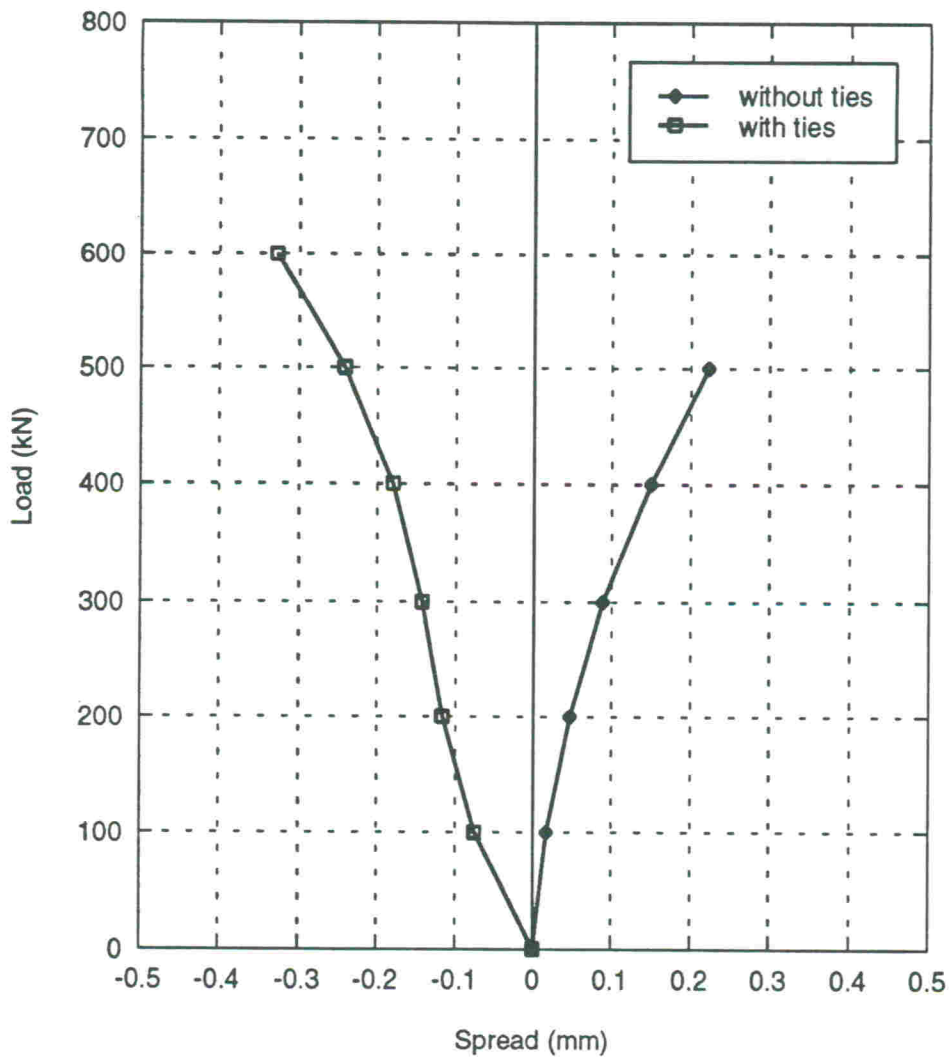


Fig. 4 Spreading deformations for assemblages with and without ties loaded concentrically

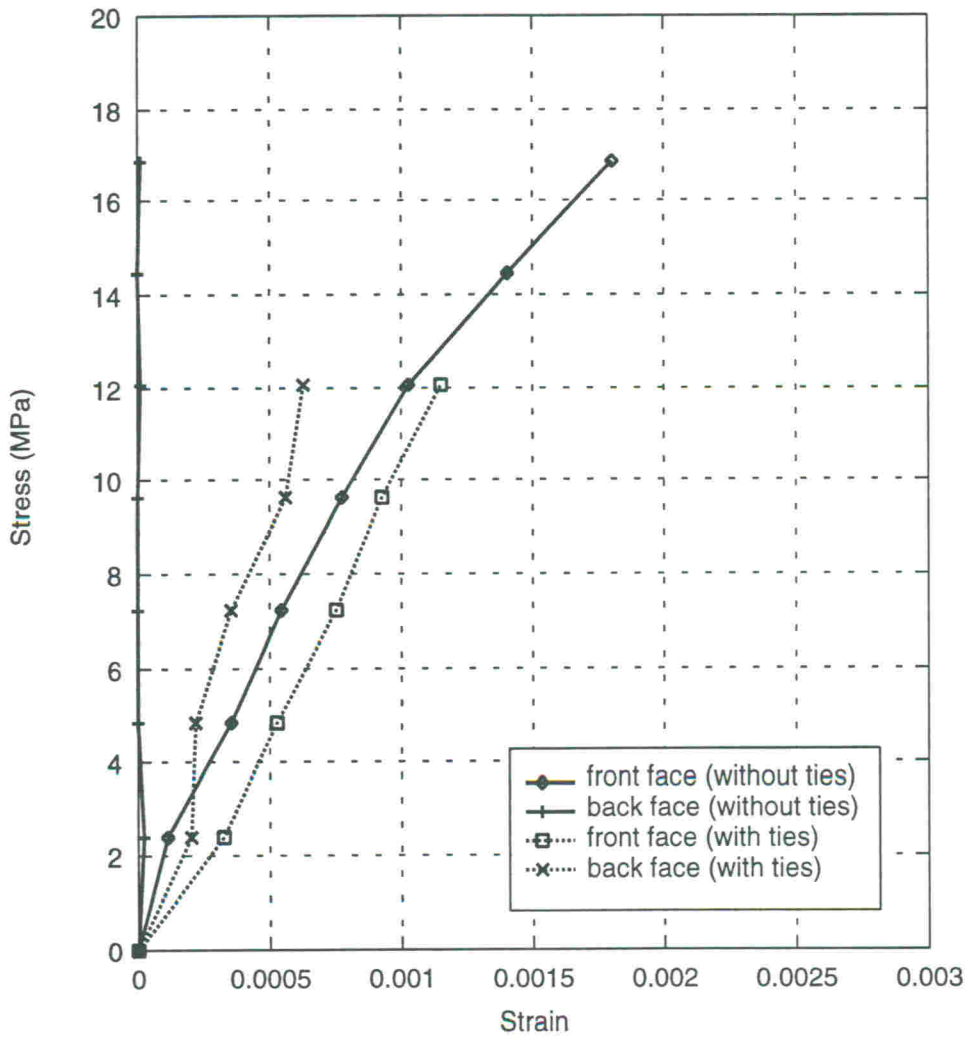


Fig. 5 Compressive stress-strain relationships for assemblages with and without ties loaded eccentrically

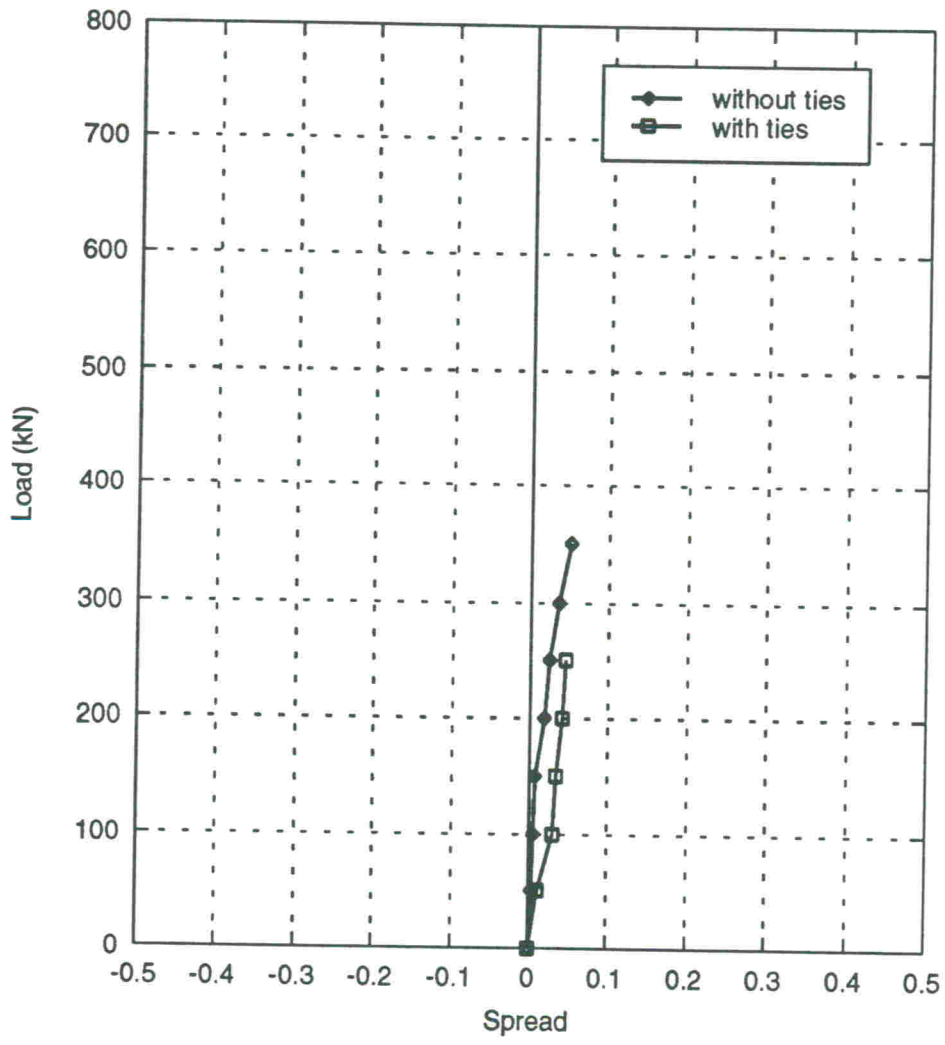


Fig. 6 Spreading deformations for assemblages with and without ties loaded eccentrically

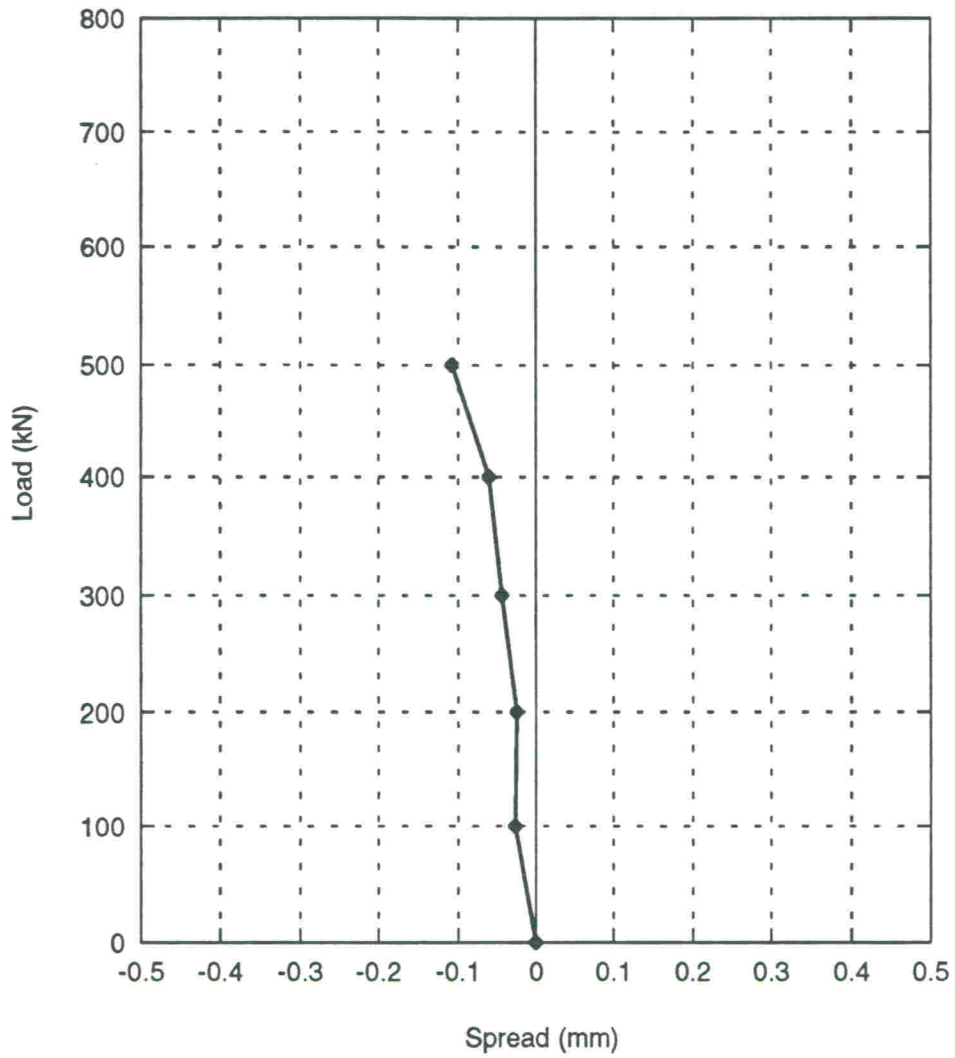


Fig. 7 Spreading deformations for the 7-course high assemblage loaded concentrically

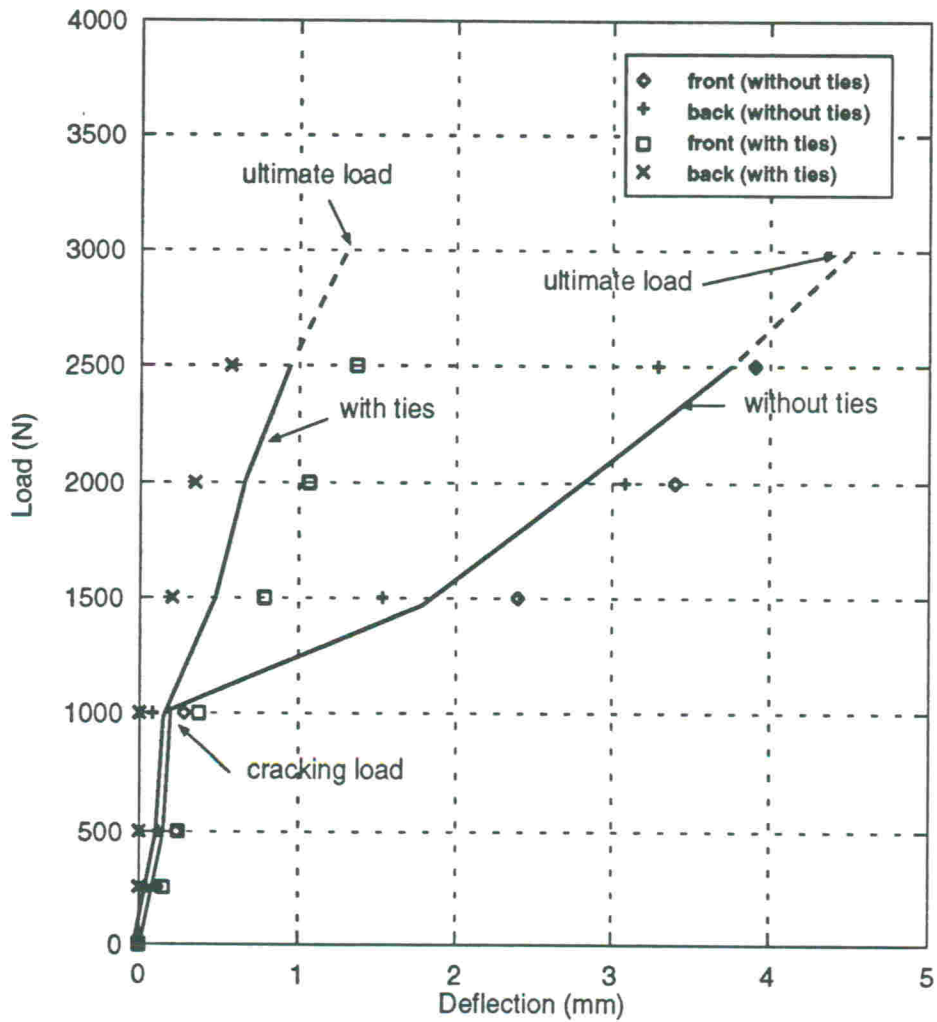


Fig. 8 Deflection response of the walls without and with ties

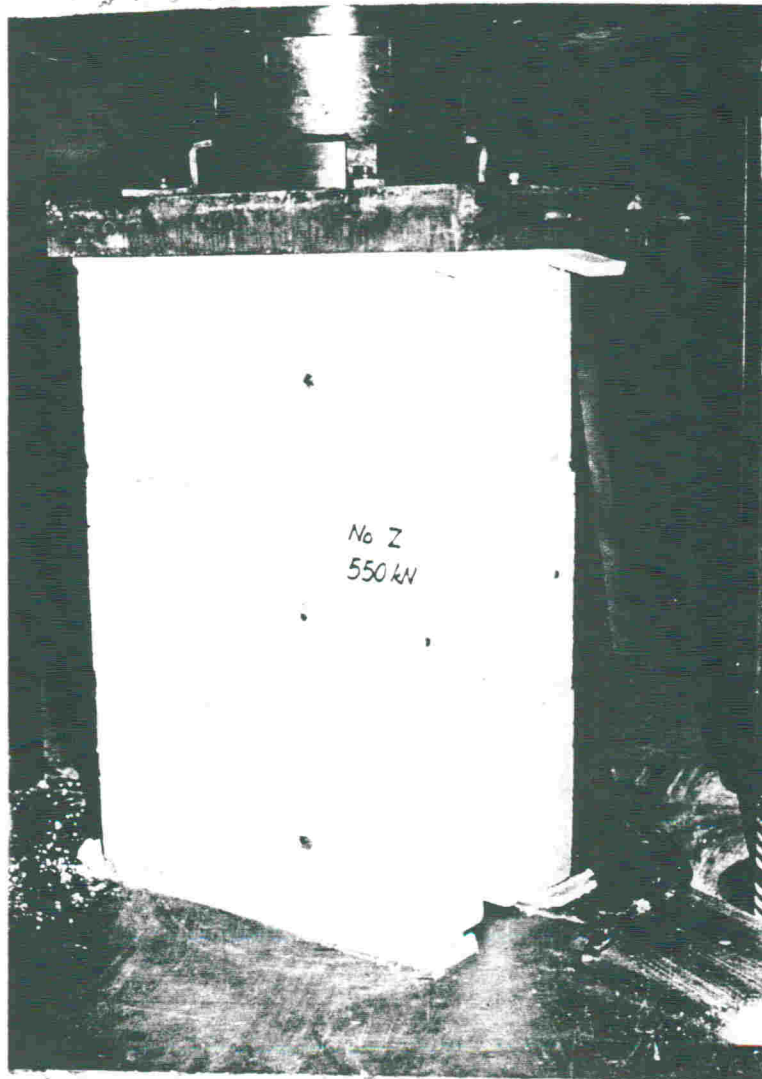


Photo 1 View of the 3-course high assemblage without Z-ties under a concentrated load of 550 kN. No cracking was observed at this load level close to 80% of ultimate capacity. Note the presence of Demec extensometer points on the concrete block surfaces to provide vertical strain and spread of faceshell readings.

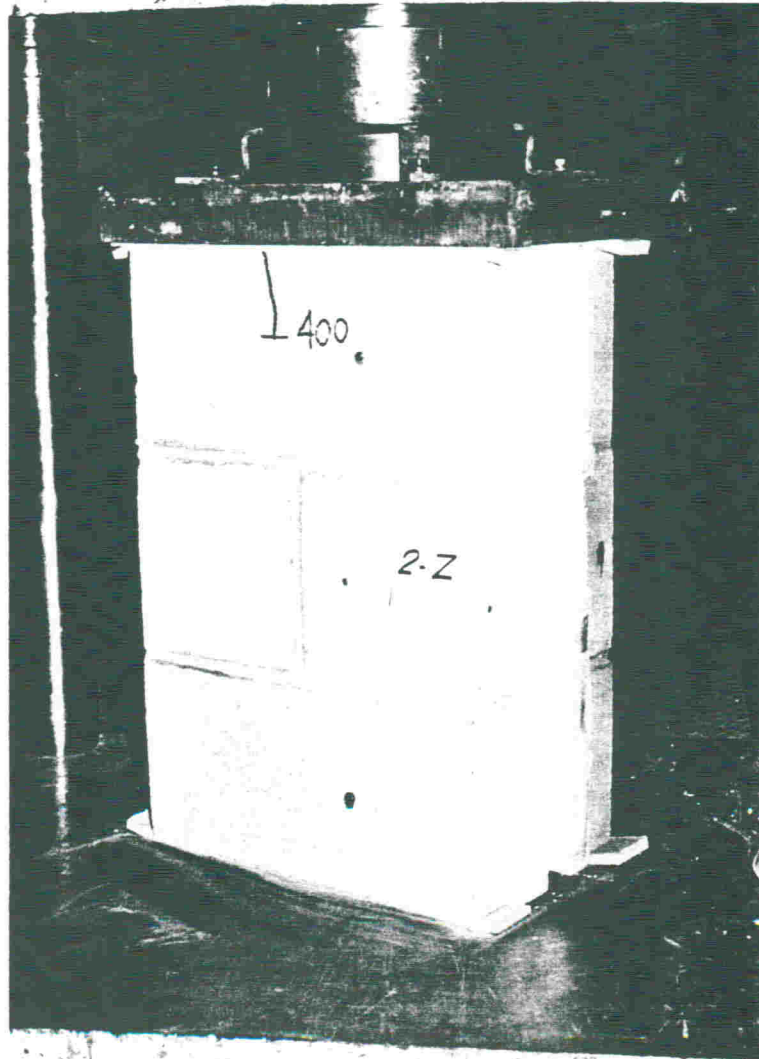


Photo 2 View of the 3-course high assemblage with 2 Z-ties under a concentrated load of 400 kN. At this load level close to 60% of ultimate capacity only one minor crack was observed. The provision of 12 mm thick strips of fibreboard at the top and bottom of the assemblage helped ensure uniform loading under reduced platen constraint.

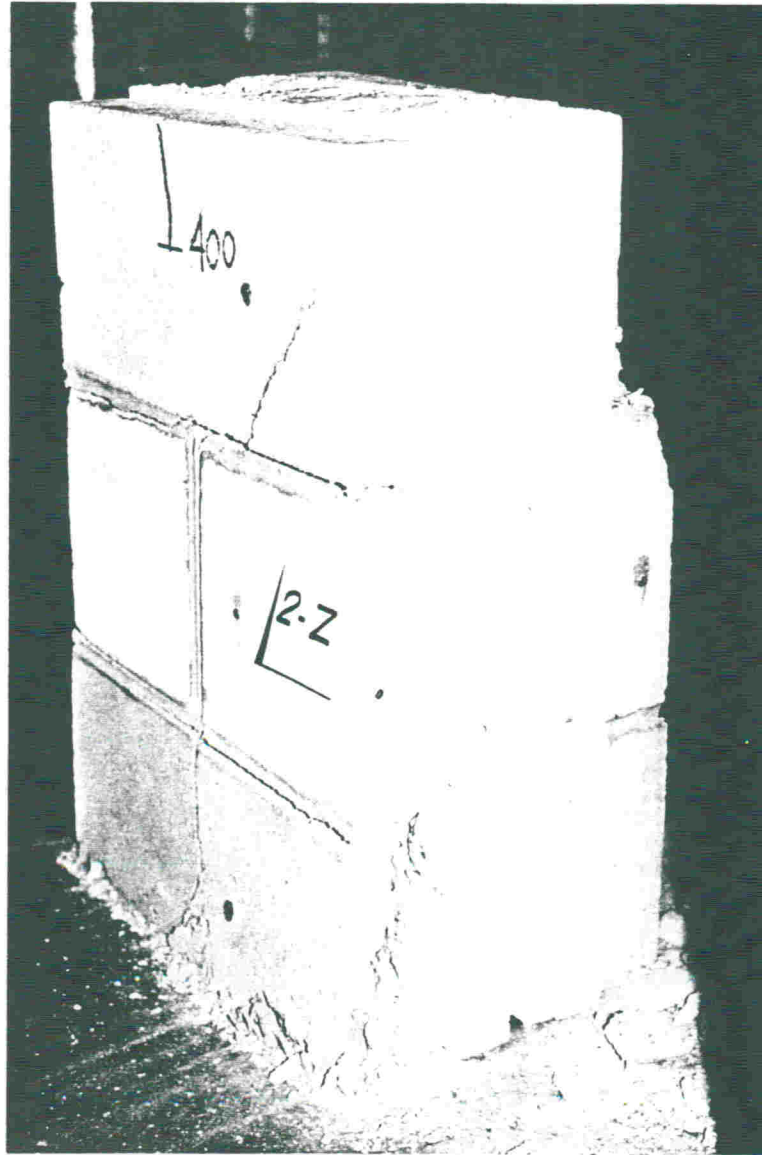


Photo 3 This view of the Photo 2 assemblage after failure shows the typical crushing compressive failure mode of an assemblage.

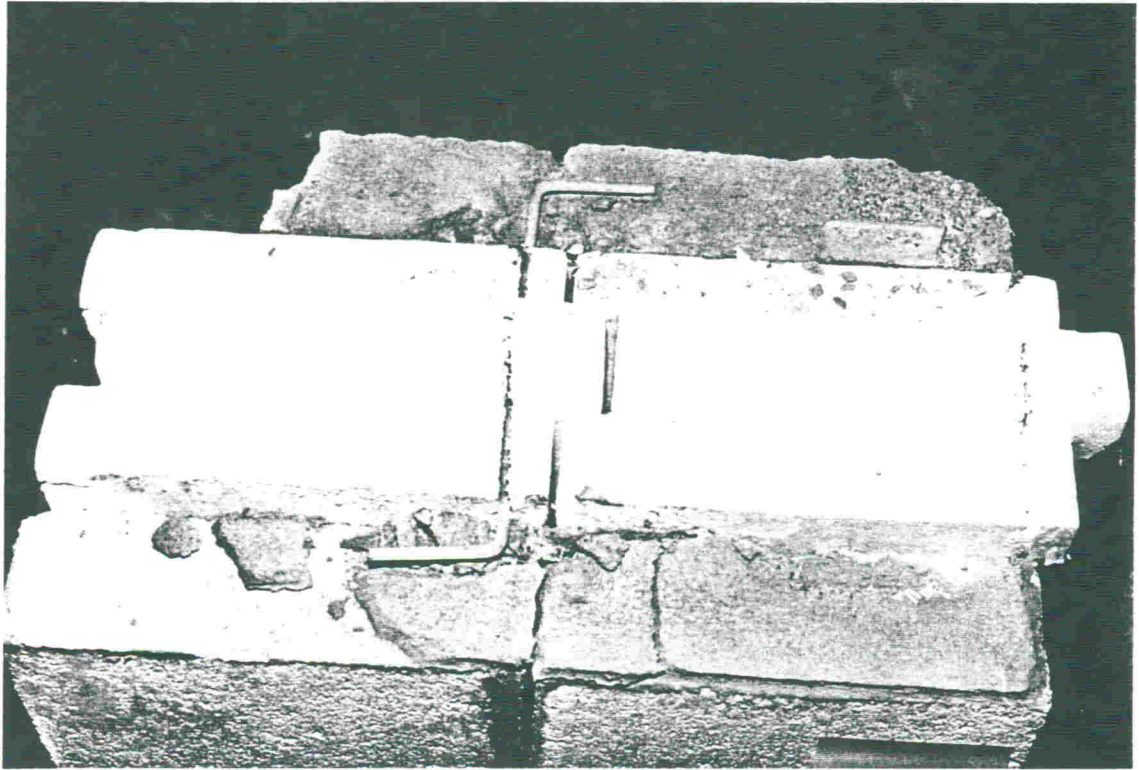


Photo 4 Examination of Z-ties after failure of the assemblage of Photo 3 indicated that the ties were properly embedded in the bedjoints.

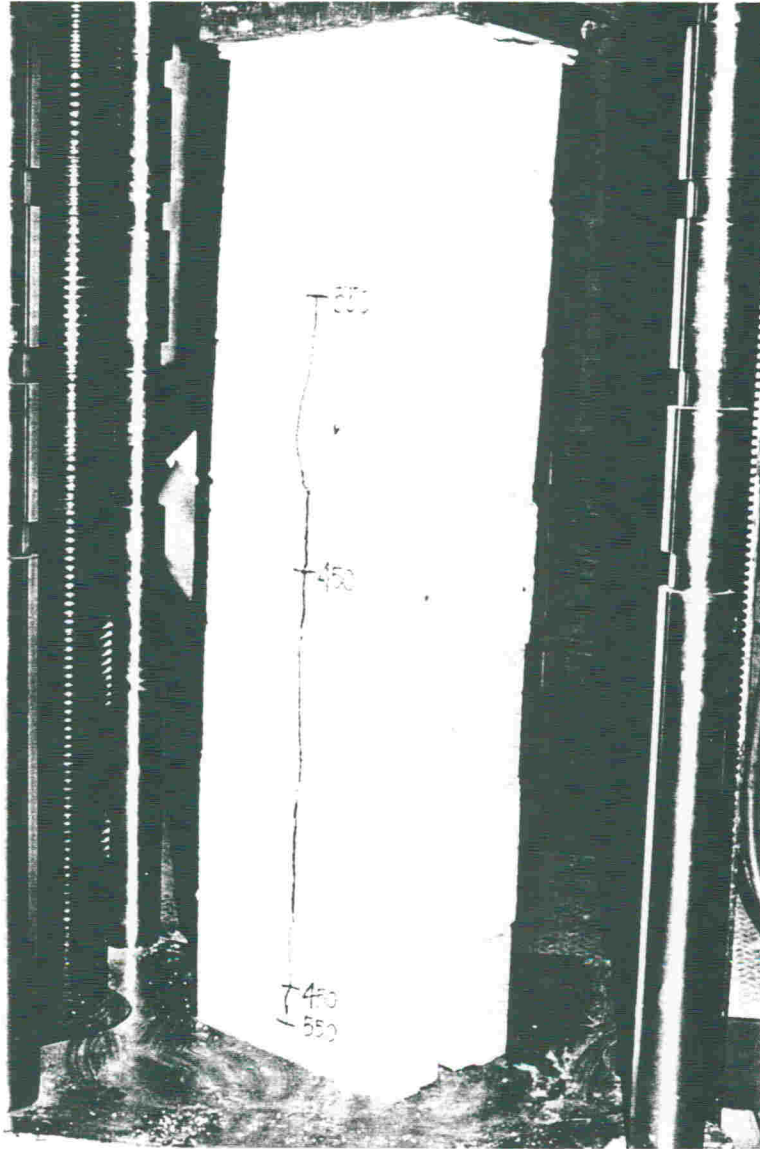


Photo 5 This view of the 7-course high assemblage under concentric loading indicates that significant cracking started at 450 kN (77% of ultimate capacity) and extended over most of its height at 550 kN (94% of ultimate capacity). The assemblage failed at 585 kN.

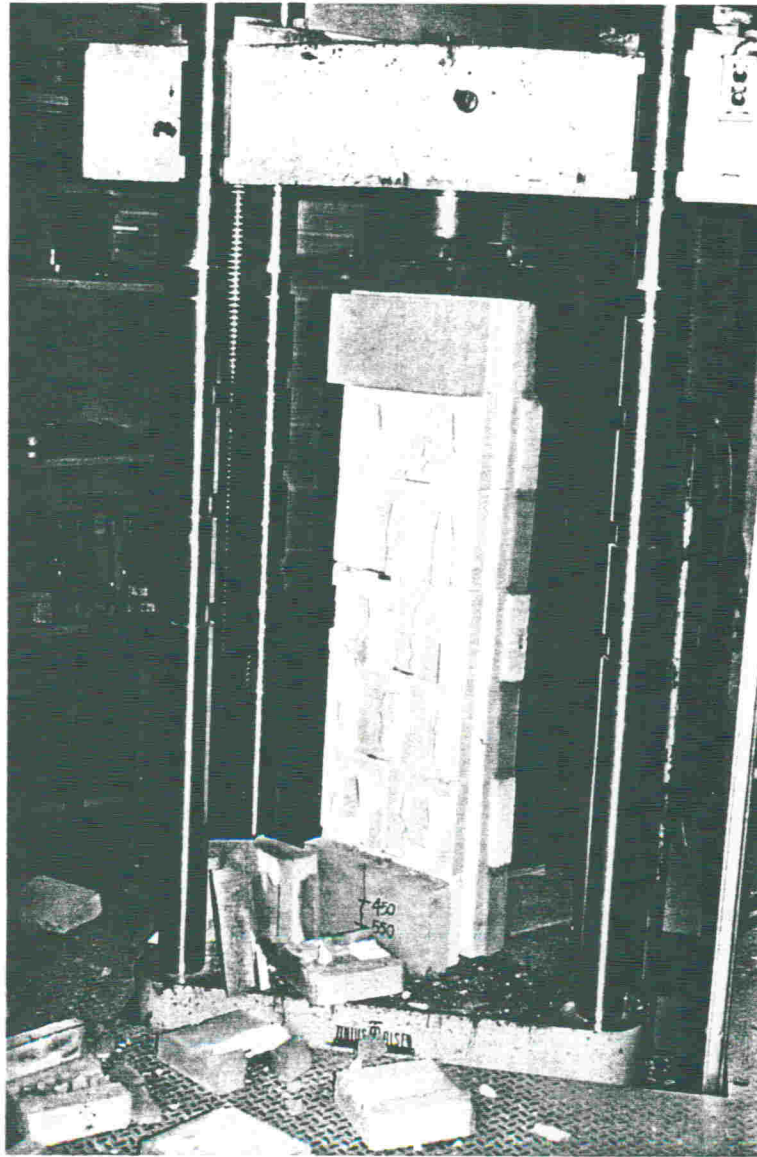


Photo 6 As expected from slenderness considerations and as shown on this photo, the failure of the 7-course high assemblage was sudden.

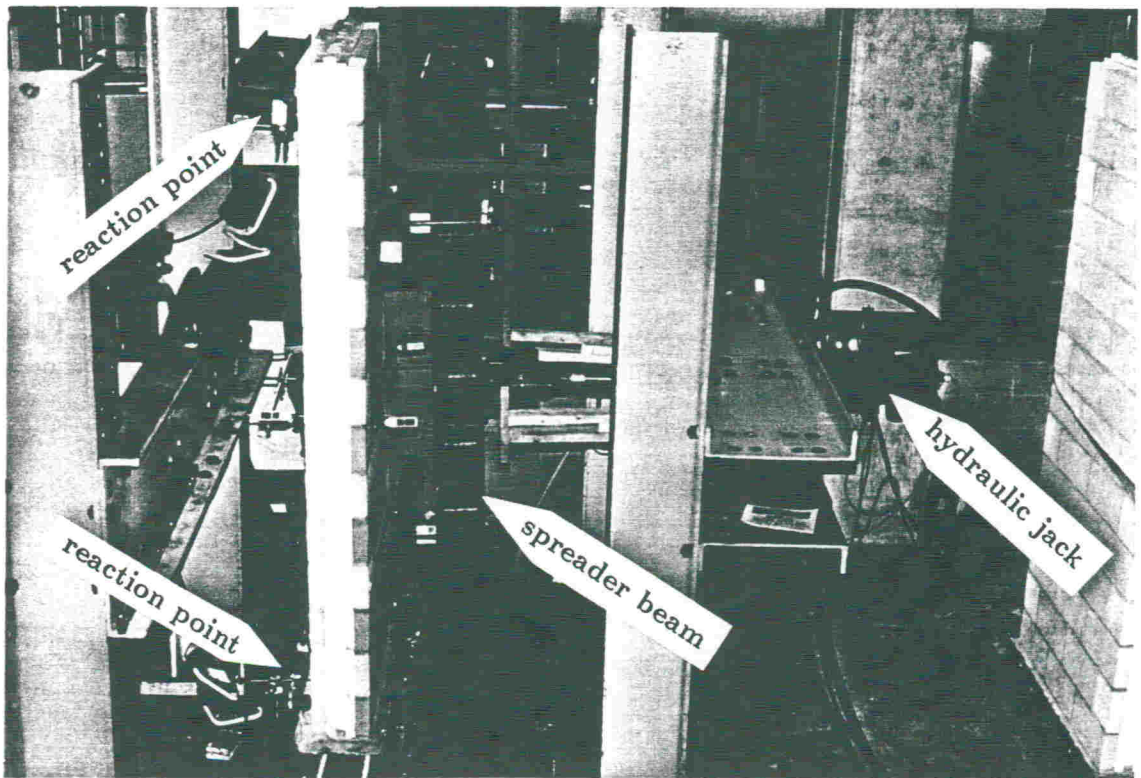


Photo 7 This view of the flexural wall test setup shows the hydraulic jack, the spreader beam and reaction points at top and bottom of the wall.

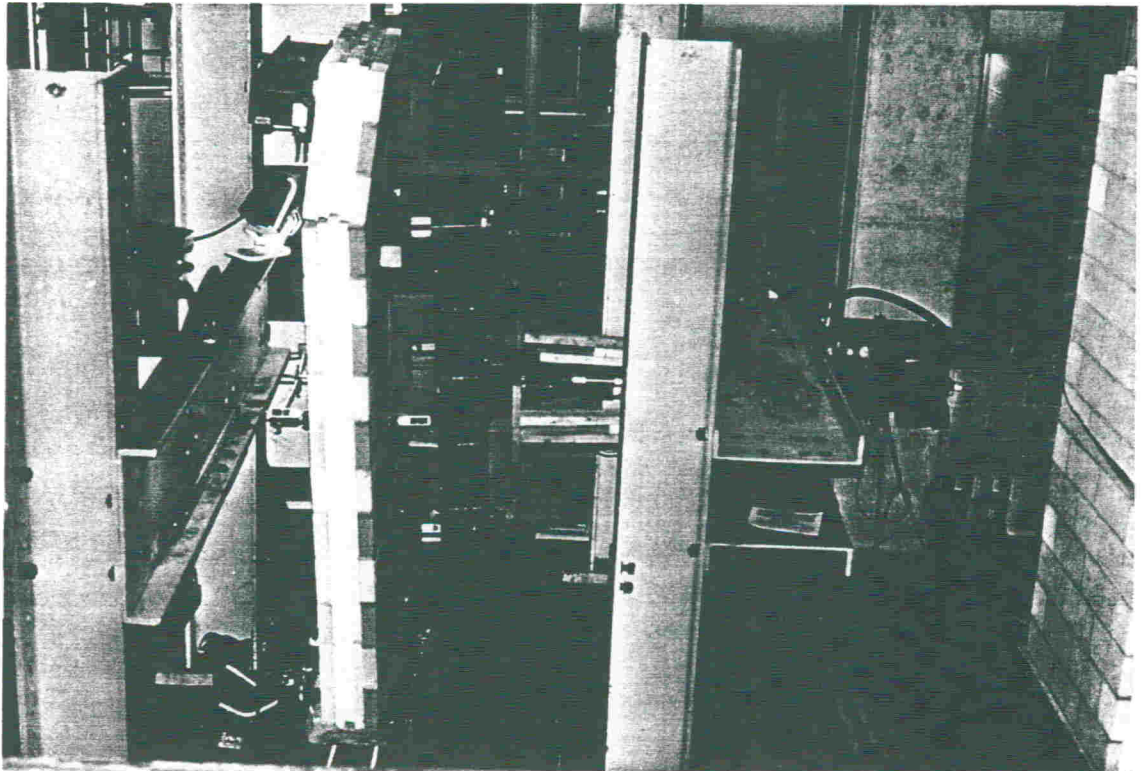


Photo 8 Typical view of a wall after failure.

APPENDIX B

ISOBLOC TESTS PHASE II



SUTER CONSULTANTS INC *Consulting Engineers*

38 Auriga Drive, Suite 200, Nepean, Ontario Canada K2E 8A5
TEL: (613) 224-4426 FAX: (613) 224-6055

**ISOBLOC TESTS
PHASE II**

**REPORT FOR
LES PRODUITS ISOBLOC INC.
BROMPTONVILLE, QUEBEC
526, Ch. du Parc Industriel
JOB 1H0**

PROJECT 94119

JUNE 27, 1995

ISOBLOC TESTS - PHASE II

1. INTRODUCTION

The Phase II test program dealt with in this report is in general agreement with the technical requirements specified by CCMC for approval of Isobloc as a National Building Code of Canada, Part 9, building material. The test program was carried out between March and May 1995 in the Structures Laboratories at Carleton University, Ottawa, under the direct supervision of the author.

2. TYPES OF SPECIMENS AND TYPES OF TESTS

The following types of specimens were prepared for testing:

- (1) Five blocks (190 x 240 x 390 mm) to determine their average compressive strength and variability.
- (2) Six 3-unit high assemblages for eccentric compressive strength testing to determine average strength, variability and deformational behaviour. Three assemblages each were tested for top and bottom eccentricities of $t/6$ and $t/3$ as shown in Fig. 1a.
- (3) Two 5-unit high assemblages for creep testing under eccentric compression. One assemblage each was tested for top and bottom eccentricities of $t/6$ and $t/3$ as shown in Fig. 1b to determine their strength and deformational behaviour. Both assemblages were originally planned for an eccentricity of $t/6$ but this was altered based on the satisfactory experimental findings at $t/6$ as will be discussed later.
- (4) Two 1 m high x 2 m wide walls for flexural load testing in the *strong direction* to determine their horizontal bending capacity and their deformational behaviour as shown in Fig. 2.
- (5) Two 1.2 m wide x 2.8 m high walls reinforced with wood studs for flexural load testing in the *weak direction* to determine their vertical bending capacity and deformational behaviour as shown in Fig. 3. Note that the two walls were tested under simulated wind pressure and wind suction.
- (6) One joist hanger concentrated load test to determine Isobloc wall behaviour and capacity under concentrated loading as shown in Fig. 4.

3. MATERIALS

The mortar used for construction was a type S mortar, typical for concrete block construction. The mason chose a premixed mortar and included a small quantity of Sealbond which is typical of construction practice. The proportions are listed below:

2 bags - Betomix Plus, Type S mortar, ANCOR-CSA A 179M

1/3 bag - Sealbond Plasticizer for Mortar, CSA A179 or ASTM C270.

The walls and prisms were constructed with standard Isobloc blocks supplied to us by Les Produits Isobloc Inc. Five random samples of the block were checked for dimensions. The height, width and length of the 5-block sample were found to vary between 189 to 190, 240 to 241, and 390 to 391 mm respectively; average values were determined as 189.6, 240.2 and 390.8 mm. Similarly, the thickness of a shell or wythe was found to vary between 59 and 60 mm with an average of 59.8 mm. Based on these measurements, Isobloc calculations in this report will be based on the following block dimensions: 190 x 240 x 390 mm with a 60 mm shell thickness. Allowing for the six dovetail slots in each block, a net area of 41 500 mm² per block was calculated and used for stress calculations; the equivalent shell thickness is reduced to 53.2 mm from the nominal 60 mm value due to the material lost by the dovetail slots.

4. SPECIMEN CONSTRUCTION

Construction of all specimens was carried out on March 10, 1995. All masonry specimens were constructed by a skilled mason under the supervision of Suter Consultants Inc. The workability of the mortar was left to the judgement of the mason. In spite of being skilled in normal masonry construction, the mason had no experience with Isobloc masonry and as a result produced occasional bedjoints which were too thick and did not allow the insulated core to fit snugly together as shown in Photo 1. These workmanship deficiencies were accepted as part of the test program since on-site construction practices also will vary. Overall workmanship was judged as average with occasional below average masonry regions.

For the first seven days of curing, all specimens were kept moist by means of wet rags and polyethylene wrapping. After seven days, the specimens were uncovered to cure under laboratory conditions until testing at ages between about one and two months. Laboratory conditions consisted of a relative humidity of about 25% and an air temperature of about 20°C.

5. TESTING

5.1 Mortar Testing

Twelve 50 mm cubes were tested to determine the compressive strength of the

mortar. Compressive testing of mortar specimens was carried out in a Tinius Olsen Universal testing machine. Testing took place at an age of 38 days on April 19, 1995. A summary of the mortar test results is given in Table 1.

The following comments apply to Table 1:

1. While the coefficient of variation at 24% is fairly large (this is mainly due to the first batch of mortar having a relative high strength), the results are close enough to be grouped together.
2. The average compressive strength of 15.4 MPa at 38 days is higher than the required 12.5 MPa strength for laboratory prepared Type S mortar at 28 days (CSA A179 - 94 "Mortar and Grout for Unit Masonry") and is therefore judged as satisfactory.

5.2 Block Compressive Strength Test

Compressive testing of Isobloc masonry units was carried out in a Tinius Olsen Universal testing machine. A summary of the masonry unit test results is given in Table 2.

The following comments apply to Table 2:

1. While the results vary slightly from one unit to another, they are close enough to be grouped together. The coefficient of variation at 6% is judged to be small.
2. The Isobloc units' average compressive strength of 22.9 MPa is higher than the required 15 MPa strength for exterior walls according to the technical requirements of CAN3 - A165 Series-M85 "CSA Standards on Concrete Masonry Units" specified by CCMC and is therefore judged as satisfactory.

5.3 Assemblage Properties Tests

5.3.1 General

Compressive testing of the six 3-unit high and two 5-course high assemblages was carried out in a Tinius Olsen Universal testing machine. Loads were introduced into each assemblage through stiff (50 mm thick) steel plates and steel rollers; 12 mm thick strips of fibreboard were used between steel plates and block shells to distribute stresses. Testing took place between May 2 and 5, 1995 at ages of 52 to 55 days.

First, three 3-unit high assemblages were tested eccentrically as shown in Fig. 1a. The load was applied at top and bottom eccentricities of $t/6$ (t is the total thickness of the block). Each assemblage was instrumented with stainless steel discs for deformation readings by means of a Demec extensometer (200 mm gauge length) as follows: two sets of discs on both the front and back faces for vertical deformations

and two sets of discs at half height across the wythes to monitor potential spreading deformations between the two shells. Loading was applied gradually in about ten load steps to failure. After each load increment, a set of Demec readings was taken. The typical duration of a test was about one hour.

Second, three 3-unit high assemblages were tested eccentrically with top and bottom eccentricities of $t/3$ (t is the total thickness of the block) as shown in Fig. 1a. Again a set of six Demec readings was taken for each load increment. The duration of a test and the number of load increments were similar as for the $t/6$ eccentric tests.

Finally, as shown in Fig. 1b, two 5-unit high assemblages were tested eccentrically to determine their creep behaviour under eccentric compressive load. As called for in the CCMC Technical Requirements, the applied eccentric load was equal to an equivalent concentric load based on the allowable compressive stress plus 25%. In testing the first assemblage, the eccentric load was applied at an eccentricity of $t/6$ (t is the total thickness of the block) while in testing the second assemblage, the load was applied at an eccentricity of $t/3$. Each assemblage was instrumented for deformation readings by means of a Demec extensometer (200 mm gauge length) as follows: one set of discs on both the front and back faces for vertical deformations and two sets of discs at half height across the wythes to monitor potential spreading deformations between the two shells. Load was applied gradually and then kept constant for the 24-hour duration of the test. Specimen deformation was monitored and sets of Demec readings were taken at several time intervals. Note that the larger eccentric creep test at $t/3$ would result in much higher stresses and hence larger creep deformations than the $t/6$ test. This choice was made intentionally to study creep behaviour under extreme conditions.

5.3.2 Compressive Behaviour of Assemblages

The following comments apply for eccentric compression with an eccentricity equal to $t/6$:

1. During the uncracked stage, all the assemblages behaved in a linearly elastic manner; this behaviour is as expected. Compressive load and stress-strain relationships for all three assemblages are illustrated in Figs. 5a, 5b and 5c. In these figures, while the right hand side vertical axis represents the applied vertical eccentric load, the left hand side vertical axis represents the stresses calculated based on the assumption that plane sections remain plane; while this assumption requires full composite action between the two wythes, which in reality is known not to be present (see Phase I report), it nevertheless represents a simplified approach to deal with stresses. Such a simplification is deemed reasonable due to the size and loading conditions of the assemblages.
2. The ultimate compressive capacities of the assemblages were similar and equal to 650 kN, 627 kN, and 722 kN (15.7 MPa, 15.1 MPa and 17.4 MPa *average* stress over net area respectively). The variability in strength is judged to be

satisfactory for concrete masonry. Note that the average failure capacity of 666 kN is virtually identical to the Phase I average failure capacity of 675 kN obtained for *concentrically* loaded assemblages. This indicates that a small eccentricity of $t/6$ has no significant effect on overall load capacity.

3. All assemblages exhibited minor spreading deformations not exceeding an average value of 0.31 mm.
4. No significant cracking was observed before ultimate failure. All assemblages exhibited a relatively sudden failure which occurred mainly at the wythe having the maximum compressive stress. The highly loaded wythe would crack, crush and buckle in a somewhat similar manner to faceshells failing in plain concrete block assemblages.
5. From the stress-strain relationships illustrated in Figs. 5a, 5b and 5c, an average modulus of elasticity of 10 200 MPa was determined. This value represents about 74% of the modulus of elasticity E_m determined according to the S304.1 formula for E_m equal to $850 f'_m$ (f'_m was determined as 16.3 MPa from the test results of Phase I and S304.1 refers to CSA Standard S304.1-94 "Masonry Design for Buildings, Limit States Design").

The following comments apply for eccentric compression with an eccentricity equal to $t/3$:

1. During the uncracked stage, all the assemblages behaved in a linearly elastic manner; this behaviour is as expected. Compressive load and stress-strain relationships for all three assemblages are illustrated in Figs. 6a, 6b and 6c. In these figures, while the right hand side vertical axis represents the applied vertical eccentric load, the left hand side vertical axis represents the stresses calculated based on the assumption that plane sections remain plane after deformation and full composite action between the two wythes exists; again, this assumption is known to represent a simplified approach.
2. The ultimate compressive capacities of the assemblages were equal to 260 kN, 474 kN, and 450 kN (6.3 MPa, 11.4 MPa and 10.8 MPa *average* stress over net area respectively). The results indicate significant variability in ultimate capacity between the three specimens; note that two of the results are closely grouped together while the 260 kN value represents only about 56% of the other two results. The low value may be partly due to the inherent strength variability of concrete block assemblages (especially the incomplete and unequal filling of bed joints would have an effect) and partly due to experimental difficulties in closely aligning specimens for the rather large $t/3$ eccentricity. Note that the average failure capacity of 395 kN represents about 58% of the 675 kN average capacity established for concentric compression in Phase I work.

3. All assemblages exhibited minor spreading deformations not exceeding an average value of 0.29 mm.
4. Ultimate failure of all assemblages occurred relatively suddenly as the wythe with the higher compressive stress failed by cracking, crushing, and buckling.
5. From the stress-strain relationships illustrated in Figs. 6a, 6b and 6c, an average modulus of elasticity of 10 600 MPa was determined. This value represents about 77% of the modulus of elasticity E_m determined according to the S304.1 formula for E_m equal to $850 f'_m$ (f'_m was determined as 16.3 MPa from the test results of Phase I).

5.3.3 Creep Behaviour of Assemblages

The following comments apply to the 5-unit high assemblages loaded eccentrically for creep behaviour over a 24-hour period:

1. The applied eccentric load was calculated based on the masonry allowable compressive stress ($0.25 f'_m$) plus 25% according to the CCMC Technical Requirements; an average ultimate compressive stress (f'_m) of 13.0 MPa was assumed in calculating the creep test load. Note that the $f'_m = 13.0$ MPa assumption is close to the 16.3 MPa value determined in Phase I for concentric compression.
2. For the $t/6$ eccentric creep assemblage, Fig. 7 shows that the strain behaviour with time remains unchanged for both the more highly and the less highly loaded shells of the block assemblage. This indicates that creep during 24 hours under working load conditions is negligible for the small eccentricity of $t/6$.

Also shown on Fig. 7 are the creep recovery values immediately after unloading as well as 24 and 48 hours after unloading. The recovery values ranged between 60 to 69% for the more highly loaded shell and between 83 and 90% for the less highly loaded shell; these values are judged to indicate satisfactory behaviour.

Because of the satisfactory creep behaviour at $t/6$, it was decided to test the second creep assemblage under the much more severe eccentric conditions of $t/3$.

3. For the $t/3$ eccentric creep assemblage, Fig. 8 shows firstly, that the two shells exhibit markedly different strains and that both shells experience increased strains with time; both of these responses are as expected. Based on the assumption of plane sections remaining plane upon loading, calculations indicate that the maximum stress in the more highly loaded shell would amount to 8.4 MPa; such a high stress represents about 52% of the ultimate concentric stress of 16.3 MPa (from Phase I work) and far exceeds the allowable stress of $0.25 f'_m = 3.25$ MPa. This then explains why the $e = t/3$ assemblage displayed significant 24-hour creep deformations.

As also shown on Fig. 8, the creep recovery upon unloading ranged between 45 and 67% for the more highly loaded shell and between 96 and 100% for the less highly loaded shell. The reduced recovery for the shell loaded to about twice the working stress range is to be expected.

4. As illustrated in Figs. 9 and 10, both assemblages exhibited relatively constant and small spreading deformations which with a maximum value of 0.53 mm are deemed to be satisfactory.

5.4 Wall Flexural Strength Test in Strong (Horizontal) Direction

5.4.1 General

Two 1 x 2 m walls were constructed on rigid steel channels for flexural testing in the horizontal direction as indicated in Fig. 2. Both walls were built in a similar fashion and were tested in the same manner for simulated wind pressure or simulated wind suction. Testing was carried out on April 24 to 26, 1995 at an age of about 46 days.

In order to measure the deflections, six dial gauges were installed, one on each side of the wall at lower course, mid-height and top of the wall. By providing deflection gauges on both sides of the wall, potentially different movements of the two wythes of the wall could be monitored. Also, four dial gauges were mounted at the top and bottom of the wall at both ends to monitor support movements.

An MTS 50-kip hydraulic actuator was used to apply load to the walls through a transversal vertical beam as shown in Photo 2. Deformation readings were taken as soon as practical after load application and after the readings had stabilized, typically within one minute.

5.4.2 Wall Behaviour

The following horizontal wall behaviour was observed:

1. During the uncracked stage, both walls behaved in a linearly elastic manner and deflections were very small. This behaviour is as expected.
2. The dial gauges installed at the bottom of the wall at its mid-length indicated lower deflection values as compared to the mid-height gauge deflection readings due to the friction between the wall lower edge and the supporting channel. A similar relationship was detected between the mid-height and the wall top edge gauges. In essence, the mid-height deflections represent an average of all deflections and it will be these mid-height deflections that will be utilized in the report.
3. The walls cracked at 4750 N and 6000 N respectively. Cracking consisted of very fine horizontal and vertical cracks at or near midspan. Crack widths at

the cracking load were determined as less than 0.1 mm; such a crack width is considered a hairline crack.

4. As loading increased, the initial cracks widened and more fine horizontal and vertical cracks developed at various locations of the wall.
5. The deflection behaviour shown in Figs. 11 and 12 indicates that the two wythes deflect different amounts, i.e. the front face exhibits increased deflections as compared to the back face. From the makeup of the Isobloc and the compressibility of the insulation core such behaviour is to be expected. Both walls exhibited relatively small deflections prior to ultimate failure.
6. The ultimate flexural capacity of the walls was equal to 6380 N and 7850 N respectively. Such variability in bending capacity is to be expected for unreinforced concrete block masonry.
7. Both walls failed in the same manner as a major flexural staggered crack extended along the wall height. A typical wall failure is illustrated in Photo 3. This failure pattern is as expected for unreinforced concrete block masonry.

5.5 Wall Flexural Strength Test in Weak (Vertical) Direction

5.5.1 General

Two 1.2 x 2.8 m walls were constructed on rigid steel channels for flexural testing in the vertical direction as indicated in Fig. 3. Each wall was reinforced with three nominal 50 x 75 mm (2 x 3 in.) wood studs (Spruce, construction grade) screwed vertically to the wall surface at horizontal spacings measuring 400 mm on centres as depicted in Fig. 3. Tapcon pre-drilled screws (3/16 in. diameter, 2 3/4 in. length) were used to connect the wooden studs to both walls at spacings of 400 mm starting from the middle of the first course. One wall (designated wall no. 1) was tested for simulated wind pressure (wood straps on tension side, see Fig. 3b) and the other (designated wall no.2) for simulated wind suction (wood straps on compression side, see Fig. 3a).

Flexural wall testing was carried out on April 12 to 13, 1995 at an age of about 33 days according to ASTM Standard E 72 in a test setup shown in Photo 4. To measure deflections, two dial gauges were installed, one on each side of the wall at mid-height. By providing deflection gauges on both sides of the wall, potentially different movements of the two wythes of the wall could be monitored. Also, four dial gauges (two mounted at the bottom of the wall and two mounted at the top of the wall) were employed to monitor support movements. Further, two sets of discs at half height across the wythes were installed at each end of the wall to monitor the relative deformation between the front and back faces by means of a Demec extensometer.

An MTS 50-kip hydraulic actuator was used to apply load to the walls through a

transversal horizontal beam as shown in Photo 4. It was decided to replace the two-point loading system used in Phase I by a one-point loading system to ensure symmetrical loading of the wall.

In Phase I work, after each load increment the load level was maintained constant for 5 minutes. Deformation readings were taken as soon as practical after load application, at the end of the 5-minute period under constant load, immediately upon release of the load, and again after 5 minutes. As no significant variations between the dial gauge 0-min. and 5-min. readings were recorded in Phase I work, it was decided for Phase II to record deformation readings after they stabilized, typically within one minute.

5.5.2 Wall Behaviour

Wall No. 1 (wood studs in tension)

The following wall behaviour was observed:

1. During the uncracked stage, the wall behaved in a linearly elastic manner and deflections were very small.
2. The wall cracked at 500 N (cracking moment = 325 N.m). Cracking consisted of a single crack at mid-height of the wall. The crack width at the cracking load was determined as about 0.1 mm; such a crack width is considered a hairline crack.
3. As loading increased, the crack width of the mid-height crack increased and additional cracks developed in other high moment regions. Crack width at 5000 N was measured as 2.0 mm; this width pertains to the mid-height crack location and represents the maximum crack width.
4. The deflection behaviour shown in Fig. 13 indicates that the two wythes deflect slightly different amounts, i.e. the front face exhibits somewhat increased deflections as compared to the back face. From the makeup of the Isobloc and the compressibility of the insulation core such behaviour is to be expected.
5. At loads exceeding the cracking load, the wall exhibited a relatively ductile behaviour; it was loaded up to 7500 N before being unloaded. The crack width and deflection at the mid-height of the wall were measured as about 2.5 mm and 25 mm respectively at 7500 N.

In the vertical wall test described so far, the wood studs had extended for the full length of the wall beyond the supporting line as illustrated in Figs. 3 and 13. As this arrangement could add strength and stiffness to the wall and would not represent common practice, it was decided to free both ends of the wood studs by cutting the studs at the mid-height of the 2nd and 13th courses; the wall was then reloaded again.

Final testing of the wall was carried out in two steps. First, just prior to cutting the studs the wall was loaded in a number of increments to 6000 N again to provide a second load-deflection response. This response proved to be largely similar to the initial loading of the wall. Second, both ends of the studs were cut at the selected locations and the wall was loaded to failure. The final test response of the wall before and after cutting the studs is shown in Fig. 14.

From the final test and Fig. 14, the following wall behaviour was observed:

1. The freeing up of the studs at their ends slightly reduced the stiffness of the wall, i.e. at a load of 6000 N the wall deflection increased by about 28%. The overall load-deflection response continued to be relatively ductile.
2. The wall failed suddenly at 7000 N due to fracture of the three screws connecting the three studs at the uppermost wall location. As the wall was now no longer reinforced, the upper three courses rotated out of the vertical alignment as shown in Photo 5 and Fig. 15.

Wall No. 2 (wood studs in compression)

The following wall behaviour was observed:

1. During the uncracked stage, the wall behaved in a linearly elastic manner and deflections were very small.
2. The wall cracked at 500 N (cracking moment = 325 N.m). Cracking consisted of a single crack at mid-height of the wall. The crack width at the cracking load was determined as about 0.1 mm; such a crack width is considered a hairline crack.
3. As loading increased, the crack width of the mid-height crack increased and additional cracks developed in other high moment regions. Crack width at 1000 N was measured as 0.6 mm; this width pertains to the mid-height crack location and represents the maximum crack width.
4. The deflection behaviour shown in Fig. 16 indicates that the two wythes deflect slightly different amounts, i.e. the front face exhibits somewhat increased deflections as compared to the back face. From the makeup of the Isobloc and the compressibility of the insulation core such behaviour is to be expected.
5. At loads exceeding the cracking load, the wall exhibited a relatively ductile behaviour as the reinforcing studs held the cracked wall segments together.
6. The wall was subjected to an ultimate load of 1750 N (ultimate moment = 1138 N.m). Although the wall could have sustained a higher load, the test was stopped at that load level due to the large wall deflection of 32 mm (see Fig. 16) and the large crack width at mid-height (see Photo 6).

5.6 Joist Hanger Concentrated Load Test

5.6.1 General

This test was designed to determine the Isobloc wall behaviour and capacity under concentrated loading and at a very large eccentricity as shown in Fig. 4. To achieve this objective, a wooden flooring system of 6 m span was constructed from three 2 x 10 in. wood joists at spacings of 400 mm on centres. Plywood sheets of 20 mm thickness were nailed to the top of the joists. This flooring system was supported by three joist hangers at each end which were sitting on two 7-unit high Isobloc walls of 1.2 m width constructed on two channels. The joist hangers were made to fit the width of the inner shell of the Isobloc wall and were supplied to us by Les Produits Isobloc Inc. The test setup is shown in Photo 7.

The following instrumentation was installed to determine Isobloc wall behaviour when subjected to the concentrated load test from a joist hanger at a large eccentricity:

1. Demec extensometer discs to measure potential spreading deformations of the two Isobloc shells. The discs were installed at both ends of the two walls at two locations: at the top of the wall and at the top of the fourth course.
2. Dial gauges at the back face of both walls to monitor overall wall movements.

Additional instrumentation consisted of dial gauges at various floor locations to determine floor system deflections and of Isobloc crack width monitoring by means of a crack width comparator.

An MTS 50-kip hydraulic actuator was used to apply the load to the flooring system through a transversal steel beam. The load was applied at the third point as shown in Fig. 4 in order to subject the two Isobloc walls to different loading and rotation conditions; the East wall (see Fig. 4) was obviously subjected to higher concentrated loads than the West wall. Loading was applied in a number of steps to simulate floor loading increments of about 10 psf (pound per square foot).

5.6.2 Wall Behaviour

The following wall behaviour was observed:

1. The West wall exhibited a horizontal crack at the uppermost joint of the exterior shell between the 6th and 7th course at a floor load of 11 psf or 4 kN. A hairline shrinkage crack was noted at the same location before loading.
2. As loading increased beyond 11 psf or 4 kN, the West wall's initial crack widened and the East wall experienced progressive spreading behaviour between the two shells of the top Isobloc course; for the East wall this meant a gap opened

between the inner shell and the insulated core exactly where the lip of the joist hanger was inserted.

3. At 11 psf or 4 kN, limited hairline vertical cracks were observed in the interior wythe of the East and West walls in the region of the joist hanger locations. As loading progressed, these cracks remained as hairline cracks of less than about 0.2 mm width.
4. As the total load reached 5.2 kN, the joist hangers at the highly loaded East wall failed prematurely by a bending failure as shown in Fig. 17 and Photo 8.

At this stage, it was decided to tie down the horizontal part of each joist hanger at its contact with the top of the block by means of two Tapcon pre-drilled screws of 3/16 in. diameter and 1 in. length as illustrated in Fig. 18 and Photo 9. The test then was continued and the following wall behaviour was observed:

1. Tying down the joist hangers proved to be satisfactory in that no further problems were encountered with respect to the hangers as much higher concentrated wall loads were achieved.
2. Under progressive load increments, the Isobloc walls exhibited two deformational mechanisms as shown in Fig. 19; the gap at the top of the East wall continued to widen and the crack in the top joint of the West wall continued to enlarge. The load-dependent widening of the gap and crack is illustrated in Fig. 20. Note firstly, that both walls were otherwise not structurally damaged by the concentrated and highly eccentric loading and secondly, that the particular loading of the walls with no wall extensions present above the joist hangers represented a worst case condition which would be unrealistic in practice.
3. At a total applied vertical load of 21 kN or about 60 psf, a total floor deflection of 62 mm was recorded, the average deflections of the joists at the joist hanger locations were 9.3 mm at the East wall and 4.6 mm at the West wall, and a maximum East wall gap opening of 9 mm was observed.
4. The spreading deformations between the two wythes of the lower courses of both East and West walls were very minor indicating that only the top blocks experienced the aforementioned spreading deformations and cracking.
5. At 22 kN or about 61 psf the test was stopped due to the large floor deflections and imminent failure of the floor joists. Also, as can be seen from Fig. 20, the gap and crack widths were very large. The final gap width under the maximum test load is illustrated in Photo 10.

Also, a pullout test was conducted on two specimens to determine the ultimate pullout strength of joist hangers attached to an Isobloc unit by means of two screws as detailed in the concentrated load test. An average value of 3.9 kN was found as an ultimate strength for a joist hanger attached by two screws (1.95 kN per screw).

6. KEY CONCLUSIONS

Regarding the compressive strength test of Isobloc masonry units, the average ultimate compressive strength of 22.9 MPa exceeds the CCMC Technical Requirements of 15 MPa and is therefore considered as satisfactory.

Regarding the eccentric compressive assemblage tests, the following conclusions are reached:

1. For the relatively small eccentricity of $t/6$, no significant strength reduction as compared to concentric loading was determined.
2. For the larger eccentricity of $t/3$, the strength reduction as compared to concentric loading amounted to about 42 %.
3. The modulus of elasticity, E_m , was determined as about 10 200 MPa and 10 600 MPa for the $t/6$ and $t/3$ assemblages respectively. These values are very close to the overall average modulus of 10 500 MPa determined in Phase I testing.
4. Spreading deformations between the two Isobloc shells were found to be satisfactorily small regardless of the eccentricity.

Regarding the creep tests of assemblages under eccentric compression, the following conclusions are reached:

1. For the relatively small eccentricity of $t/6$, no significant creep deformation was determined while the assemblage was subjected to stress levels about 25% higher than working stress levels over a 24-hour period. This stable behaviour is judged as satisfactory.
2. For the much larger eccentricity of $t/3$ and resultant maximum stresses more than twice working stress levels, significant creep deformations were determined after 24 hours. Note that this test was an exploratory test not called for by CCMC and that in design practice, stress limitations should not permit such applications.
3. Spreading deformations between the two Isobloc shells were found to be satisfactorily small regardless of the eccentricity.

Regarding the flexural wall tests in the strong (horizontal) direction, the following conclusions are reached:

1. Both cracking and ultimate load strengths of the walls were high as compared to similar strengths of walls tested in the weak (vertical) direction. From the makeup of typical masonry walls constructed in running bond such behaviour is to be expected.

2. Walls in horizontal bending did not display composite behaviour. This lack of composite behaviour had previously also been established in Phase I work for walls in vertical bending.

Regarding the flexural wall tests in the weak (vertical) direction, the following conclusions are reached:

1. Cracking load capacities of the walls were small and appeared to be slightly increased by the presence of the wood studs.
2. The presence of the wood studs on the tension side simulating the wind pressure case improved considerably the ultimate capacity of the wall and controlled the widening of major flexural cracks.
3. The presence of the wood studs on the compression side simulating the wind suction case slightly improved the ultimate capacity of the wall and prevented the sudden collapse of the wall by holding the cracked wall elements together.
4. The reinforcing of vertically spanning Isobloc walls by means of vertical studs provided a small but important amount of composite behaviour. Care must be taken in attaching the studs to the walls in order to be able to rely on the safety contribution of the studs.

Regarding the joist hanger concentrated load test, the following conclusions are reached:

1. The connection between the floor joist and Isobloc walls must be properly designed to prevent a premature failure of the joist hangers. The screwed connection used in the test program proved to be satisfactory.
2. With properly connected joist hangers, the Isobloc walls resisted ultimate floor loads in excess of normal residential floor loading without overall wall failure.



Dr. G.T. Suter, P.Eng.



Table 1 Mortar test results

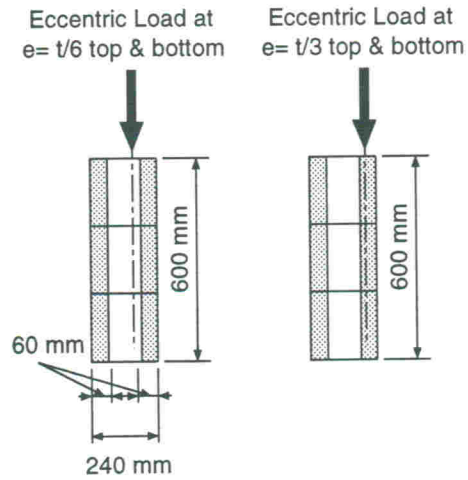
Sample	Compressive Strength (MPa)	Average (MPa)	COV. (%)
1	20.88	21.0	3.0
2	21.59		
3	20.53		
4	12.65	12.12	7.0
5	12.56		
6	11.15		
7	12.03	13.15	8.0
8	14.16		
9	13.27		
10	15.31	14.92	12.0
11	13.81		
12	16.64		
Average	15.40		
COV %	24.00		

Note:
COV : Coefficient of variation

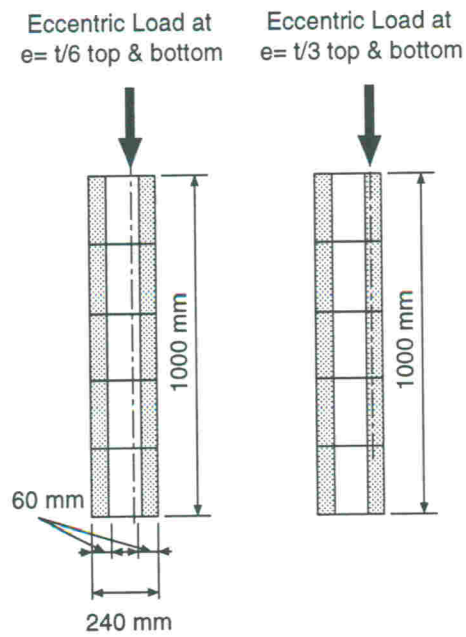
Table 2 Masonry unit test results

Sample	Compressive Strength (MPa)
1	23.7
2	23.9
3	20.7
4	24.0
5	22.1
Average	22.9
COV %	6.0

Note:
COV : Coefficient of variation
Net area = 41 500 mm²



(a) Eccentric compressive test



(b) Eccentric creep test

Fig. 1 Assemblage properties tests

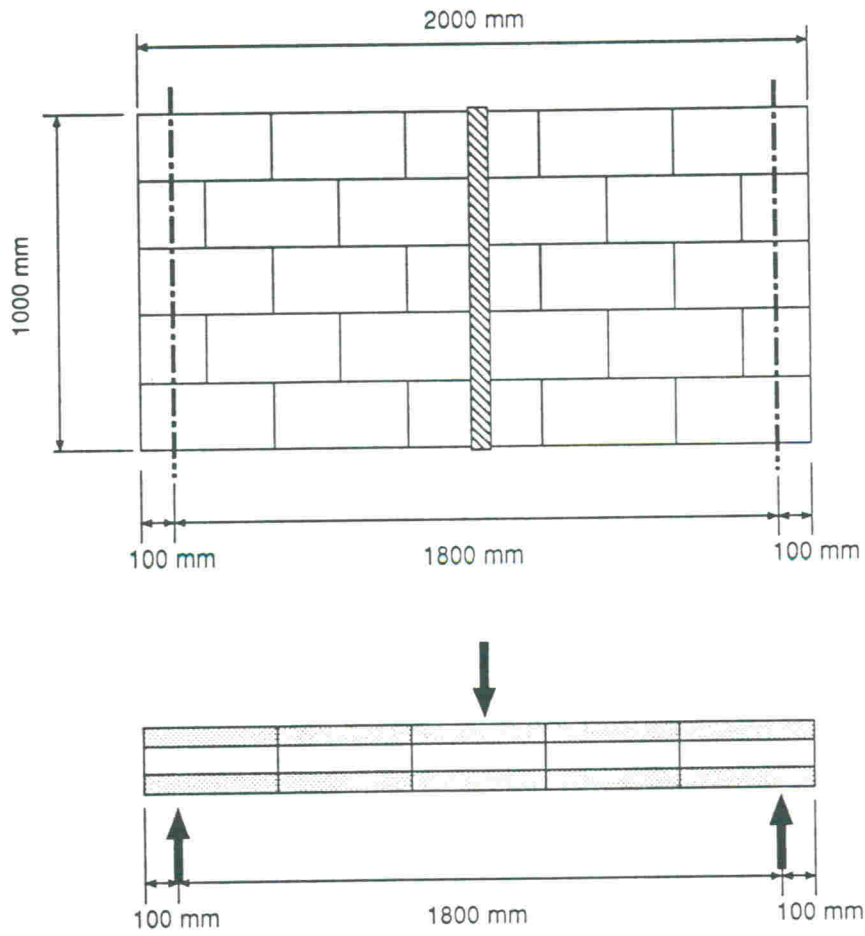
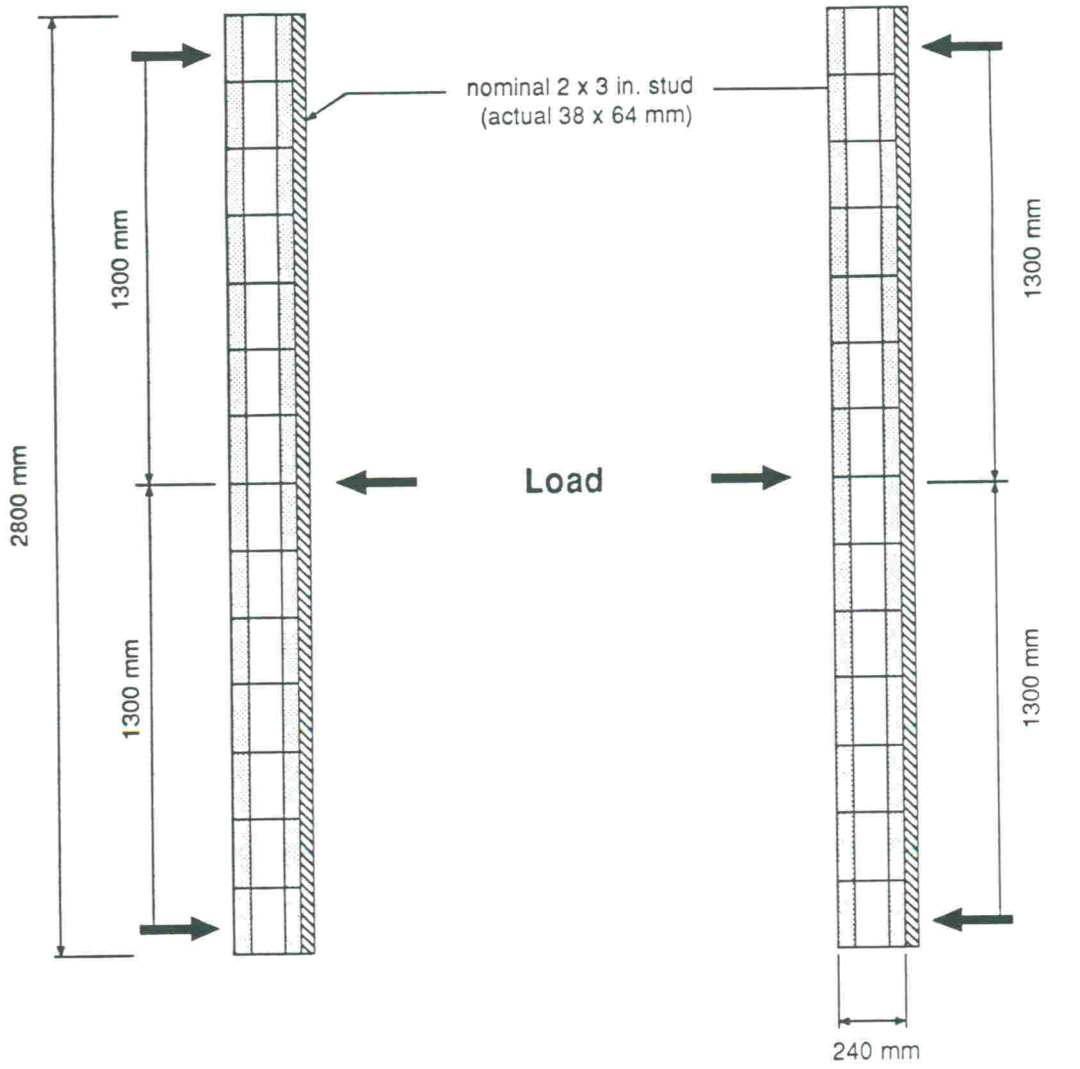
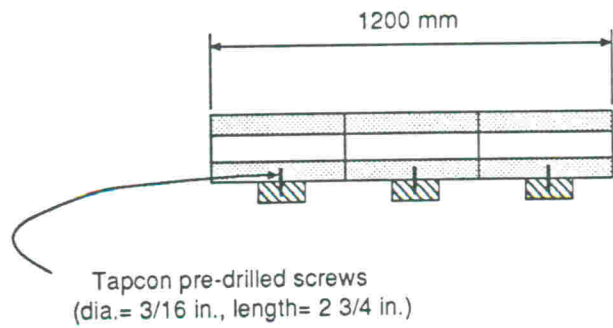


Fig. 2 Flexural wall test in strong direction (horizontal direction)



(a) Wind suction case

(b) Wind pressure case



Plan

Fig. 3 Wood -strapped flexural wall test in weak direction (vertical direction)

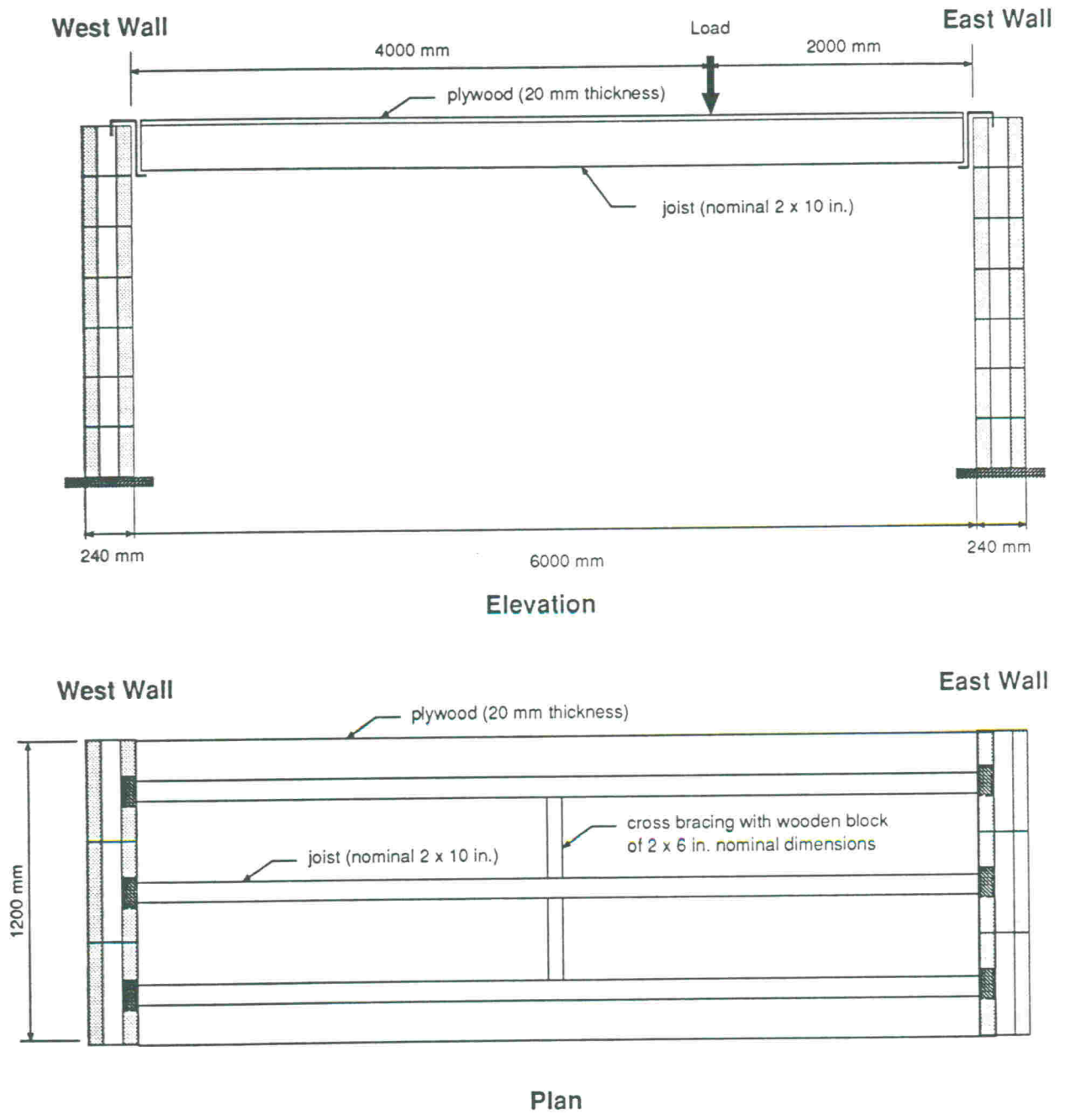


Fig. 4 Joist hanger concentrated load wall test

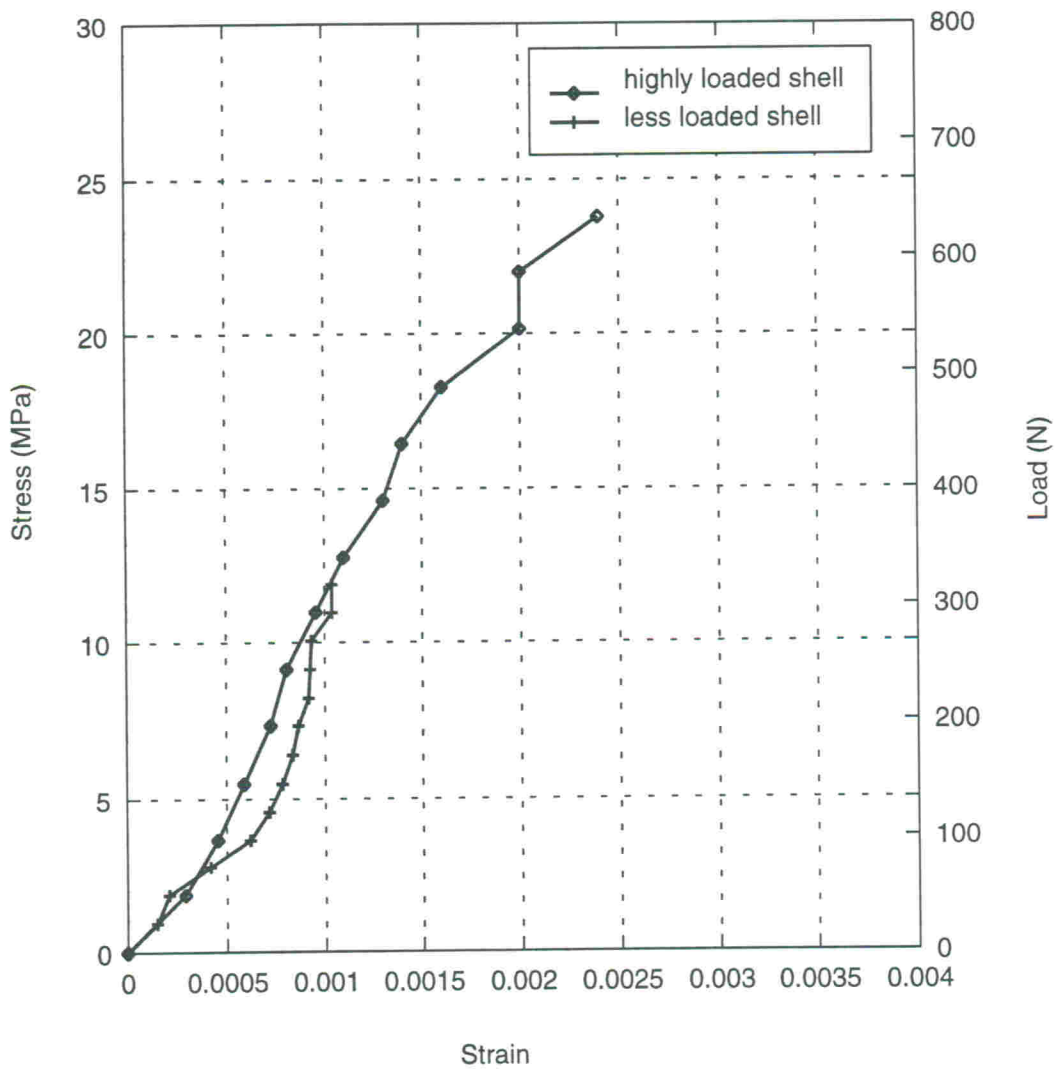


Fig. 5a Compressive stress-strain relationships for assemblage loaded eccentrically ($e = t/6$, specimen 1)

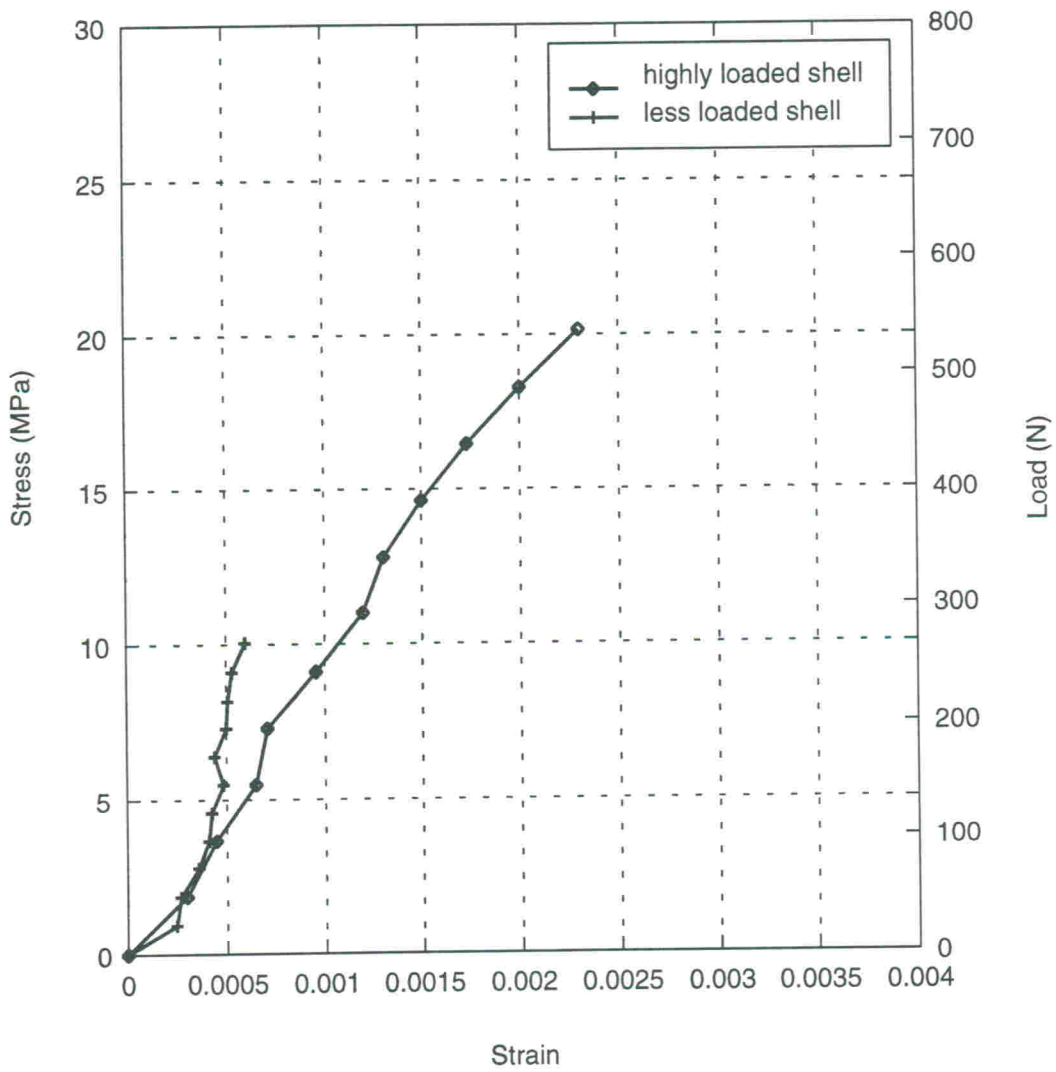


Fig. 5b Compressive stress-strain relationships for assemblage loaded eccentrically ($e = t/6$, specimen 2)

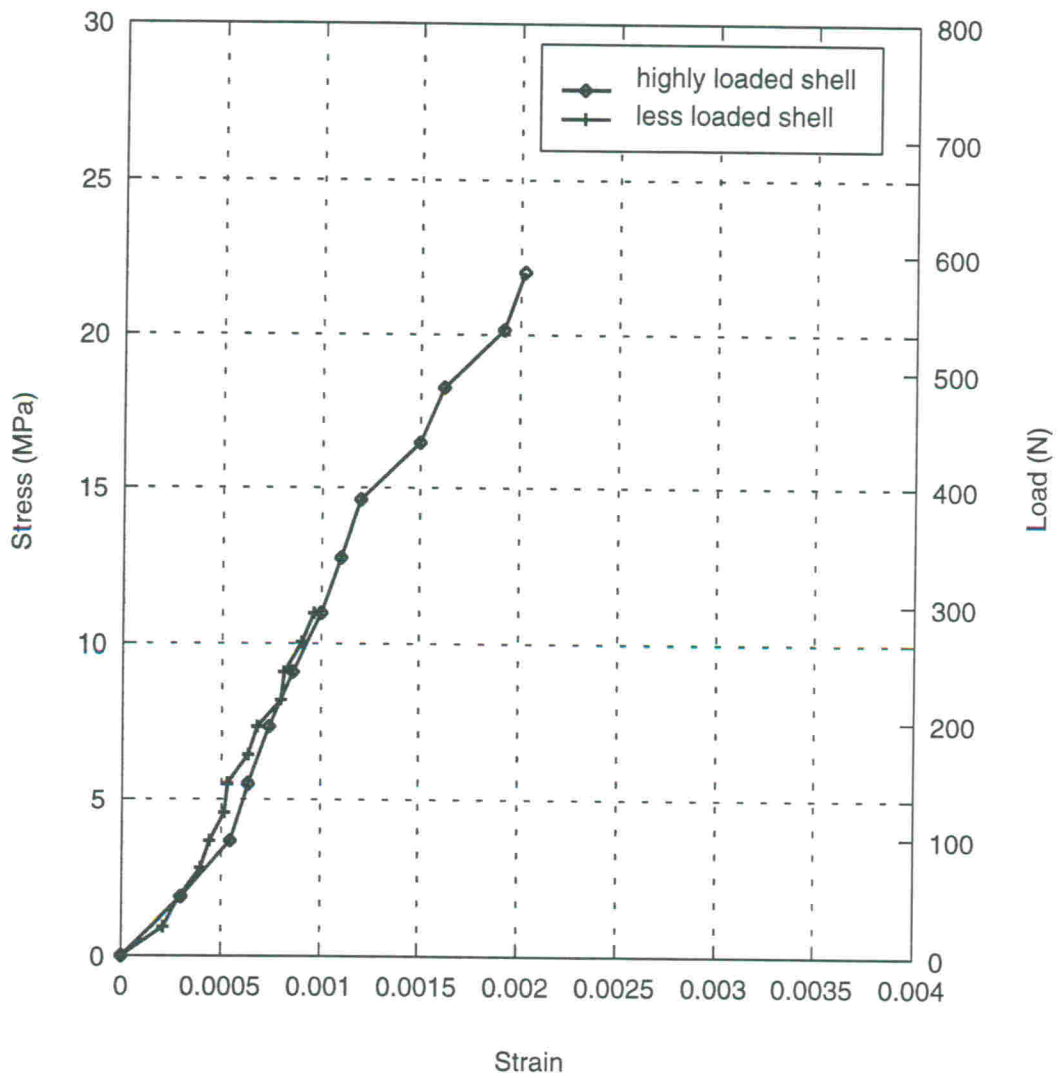


Fig. 5c Compressive stress-strain relationships for assemblage loaded eccentrically ($e = t/6$, specimen 3)

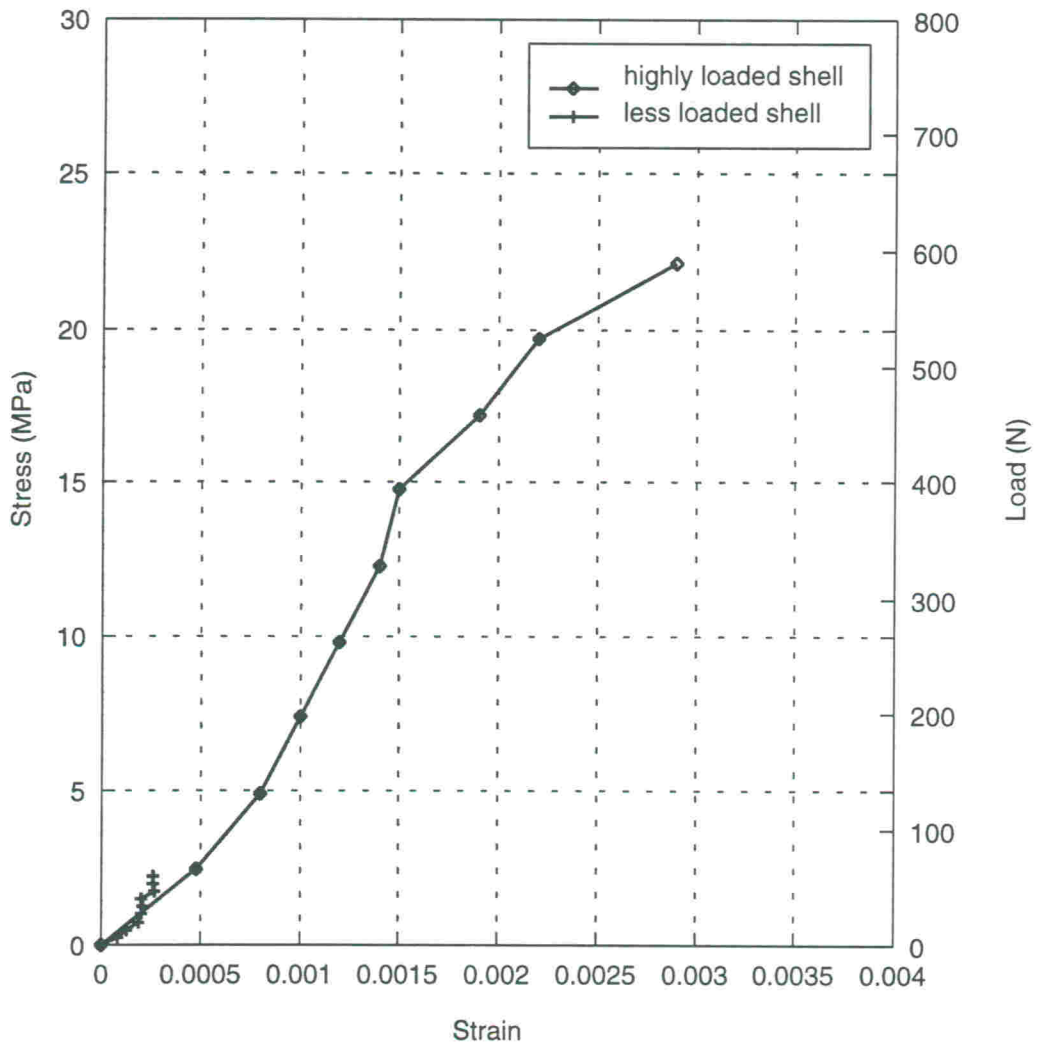


Fig. 6a Compressive stress-strain relationships for assemblage loaded eccentrically ($e = t/3$, specimen 1)

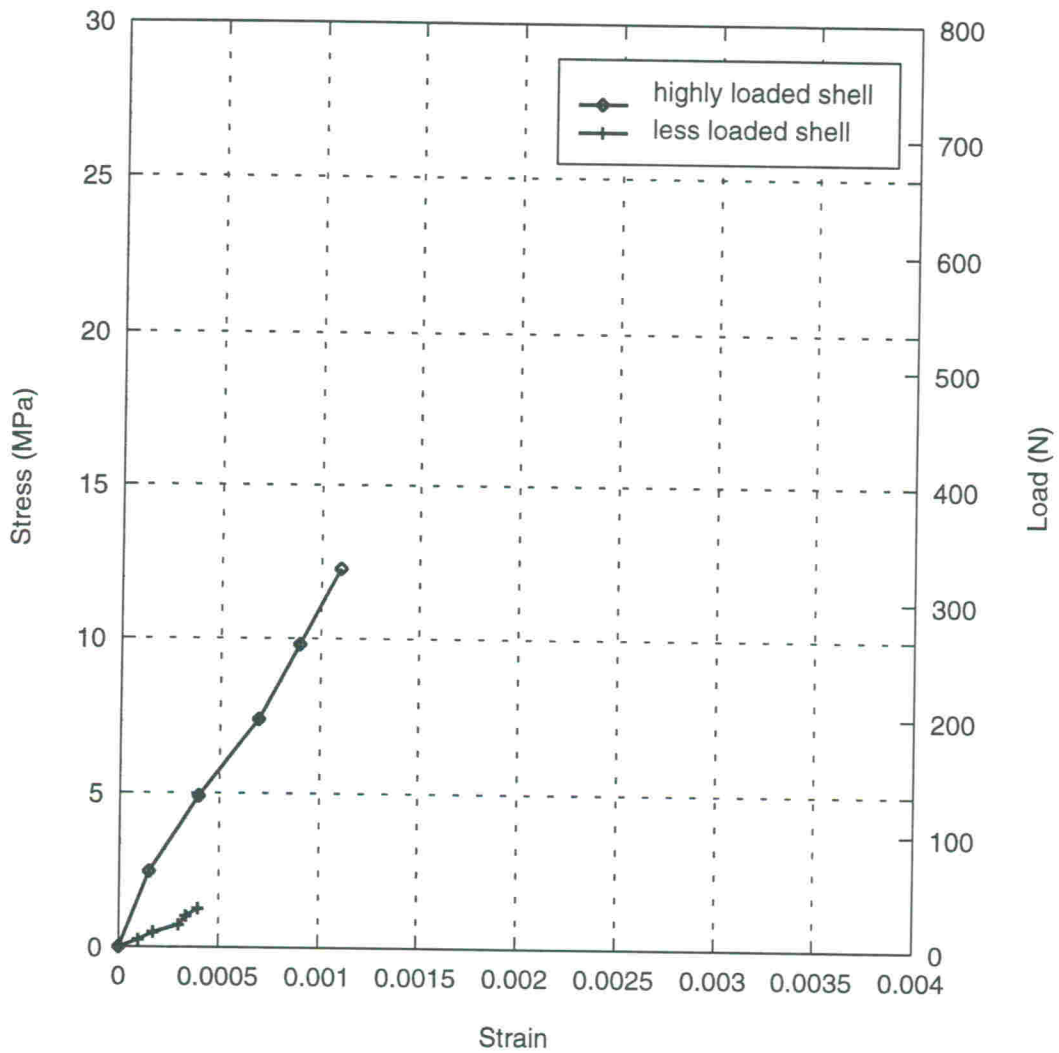


Fig. 6b Compressive stress-strain relationships for assemblage loaded eccentrically ($e = t/3$, specimen 2)

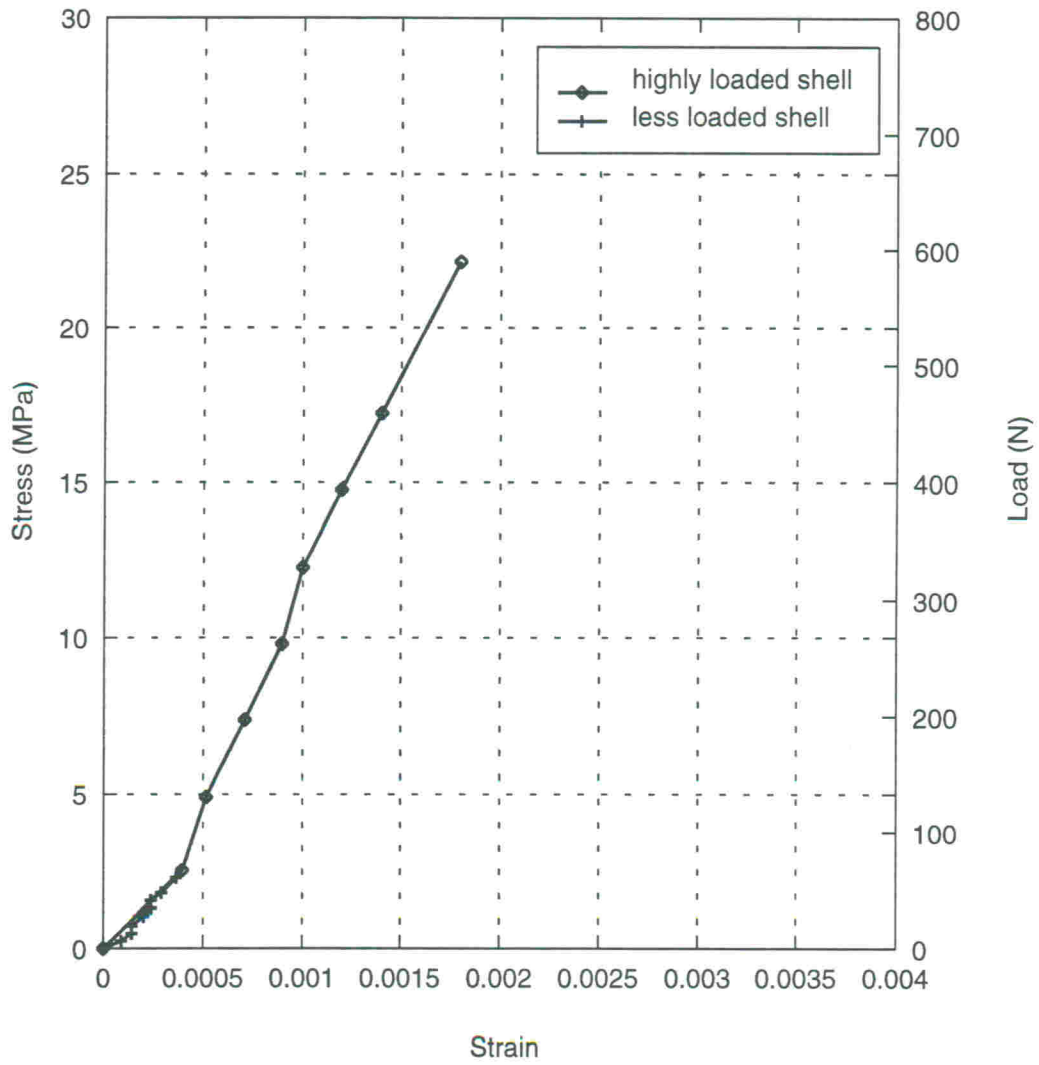


Fig. 6c Compressive stress-strain relationships for assemblage loaded eccentrically ($e = t/3$, specimen 3)

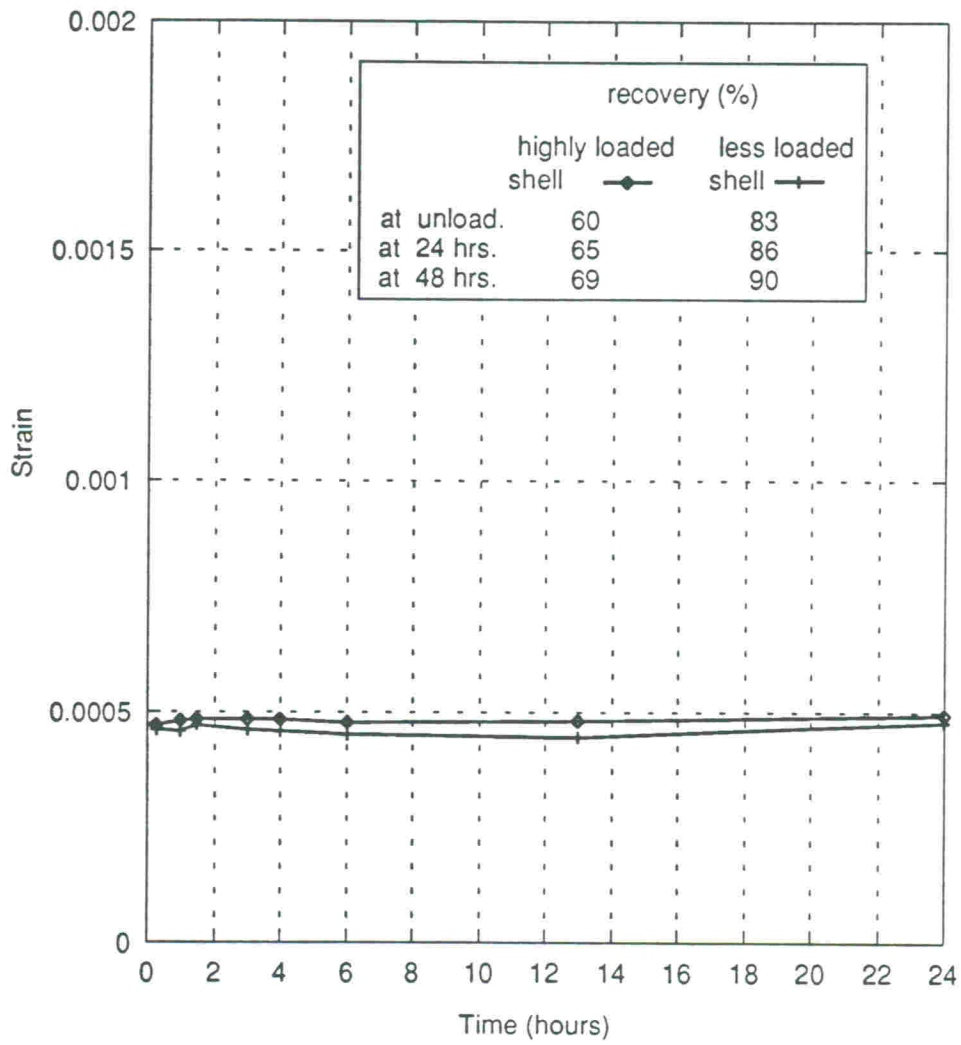


Fig. 7 Strain-time relationships for assemblage loaded eccentrically for creep behaviour ($e = t/6$)

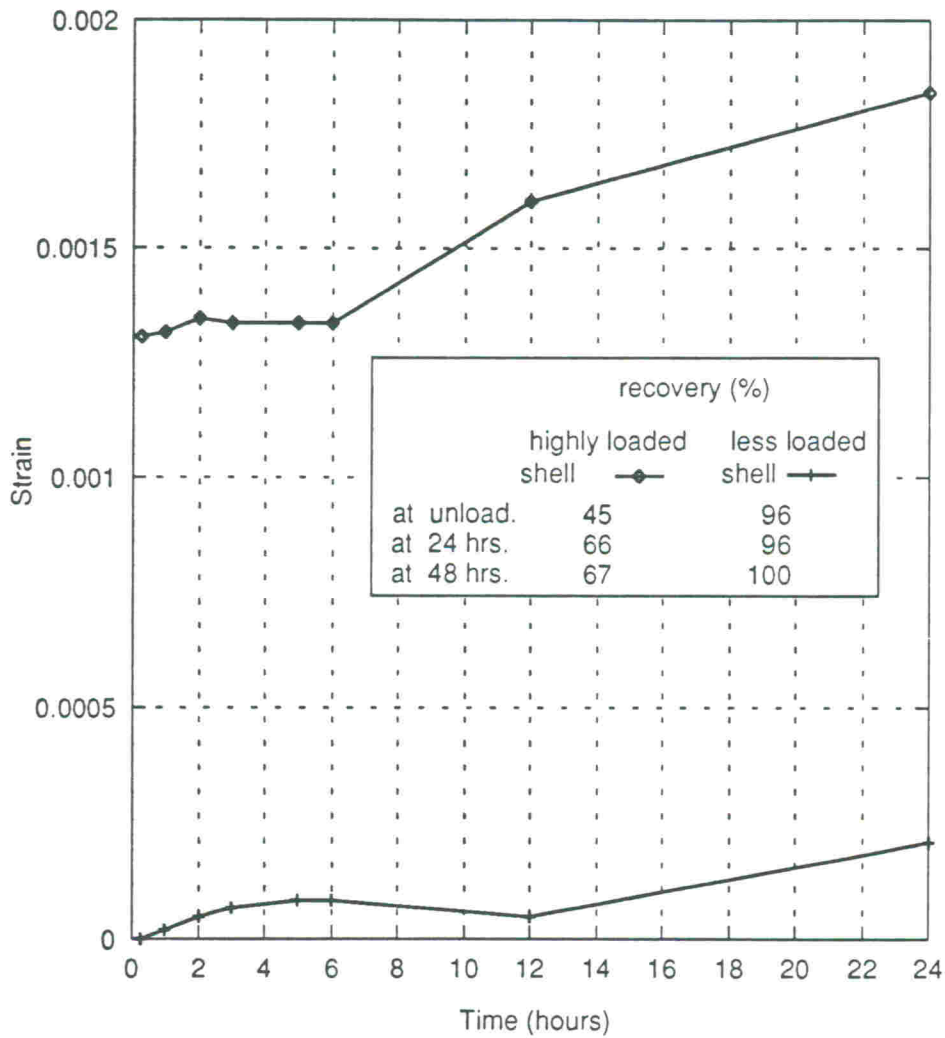


Fig. 8 Strain-time relationships for assemblage loaded eccentrically for creep behaviour ($e = t/3$)

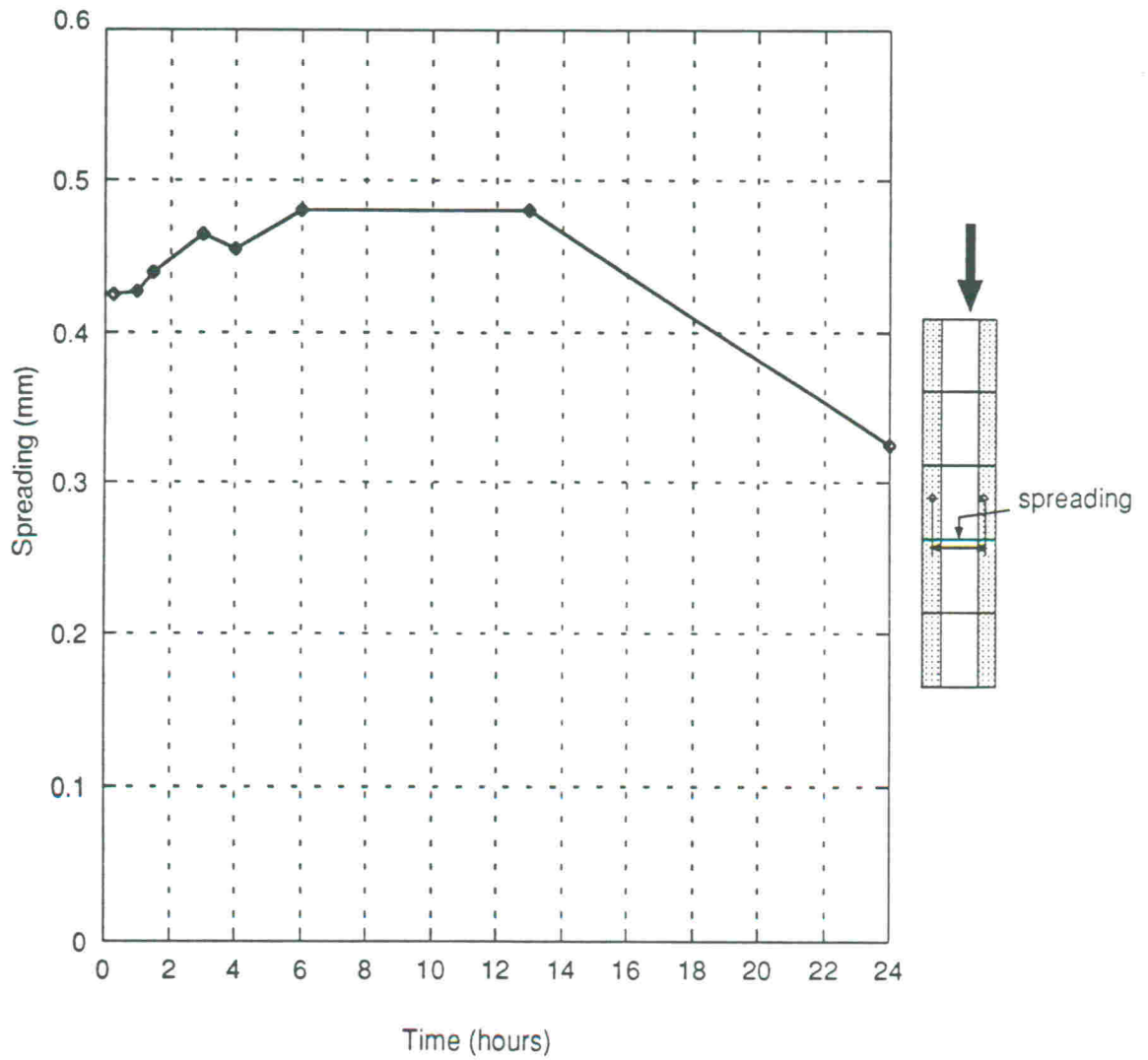


Fig. 9 Average spreading-time relationship for assemblage loaded eccentrically for creep behaviour ($e = t/6$)

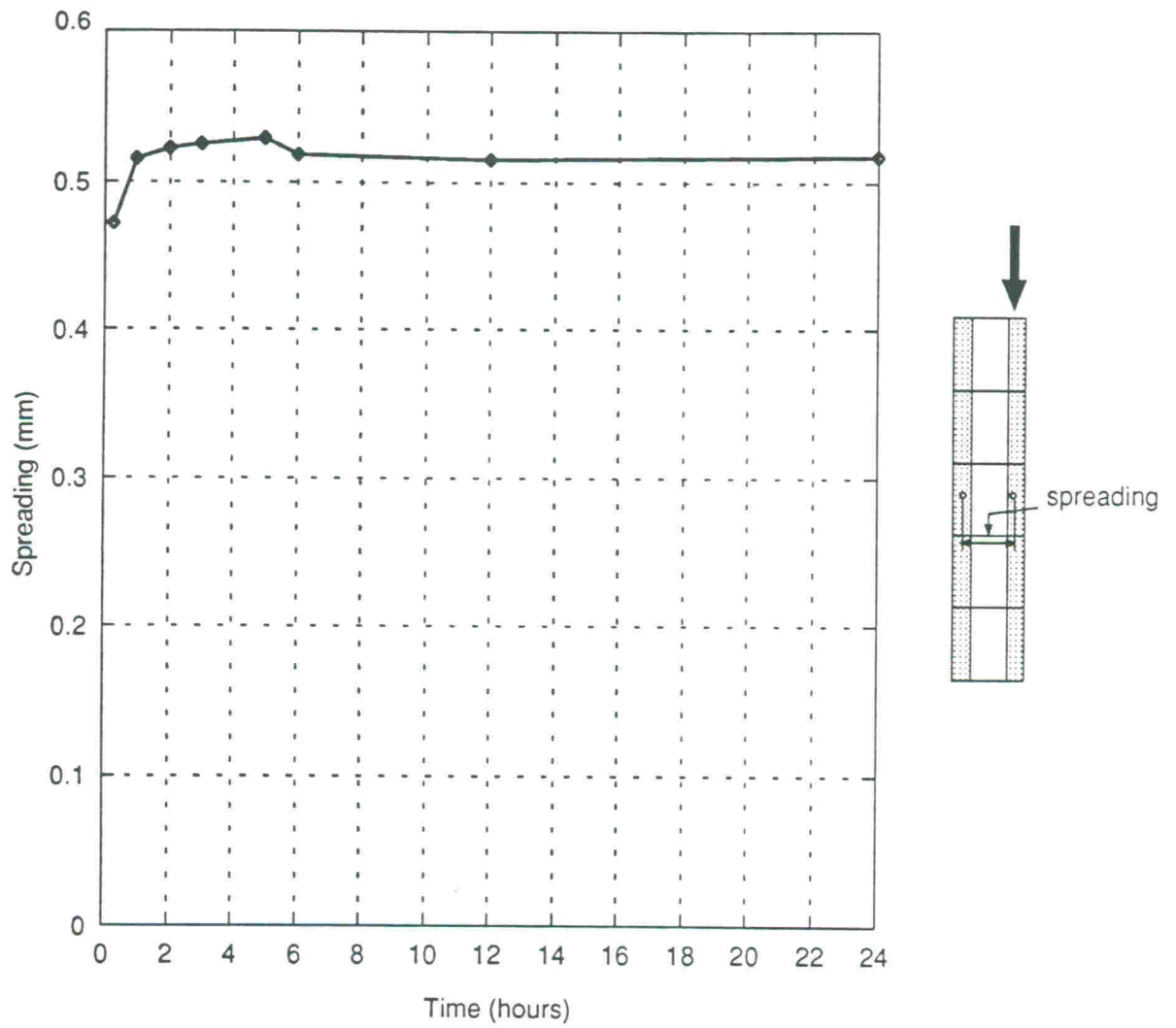


Fig. 10 Average spreading-time relationship for assemblage loaded eccentrically for creep behaviour ($e = t/3$)

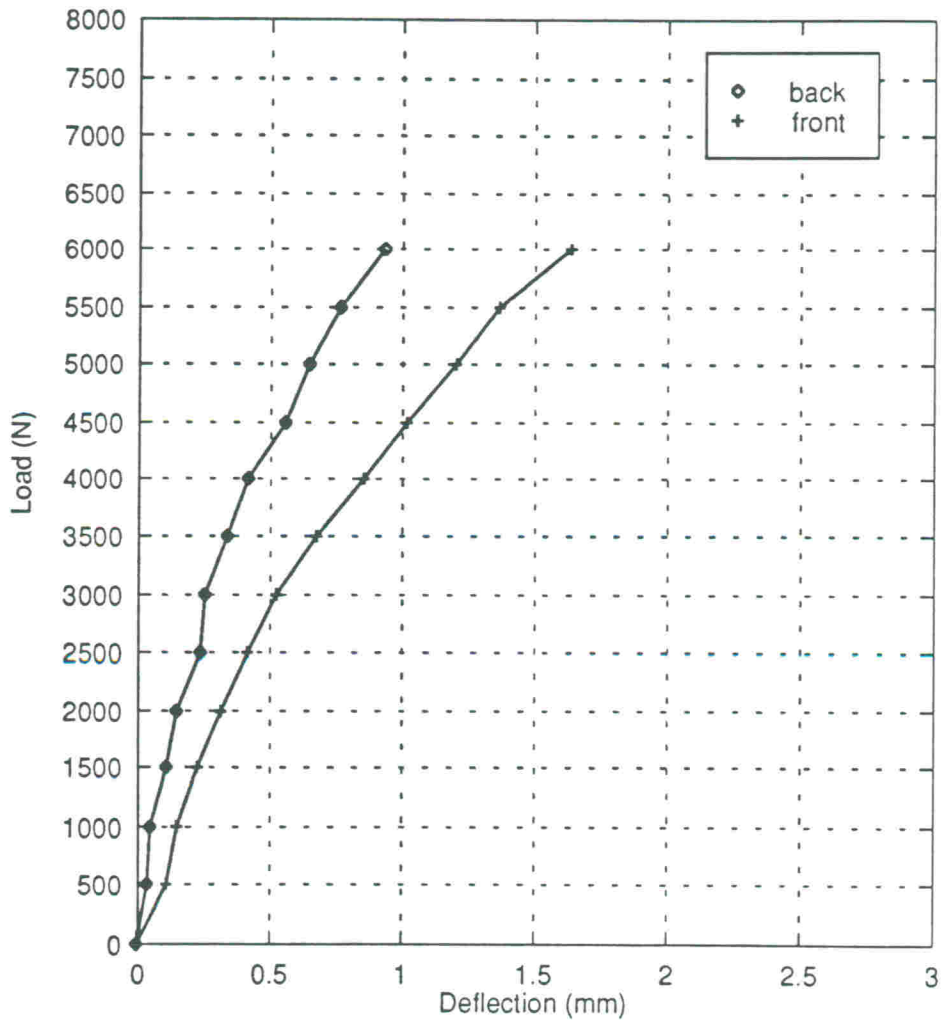


Fig. 11 Load-deflection response at the middle of wall No. 1 loaded in the strong direction (horizontal flexure)

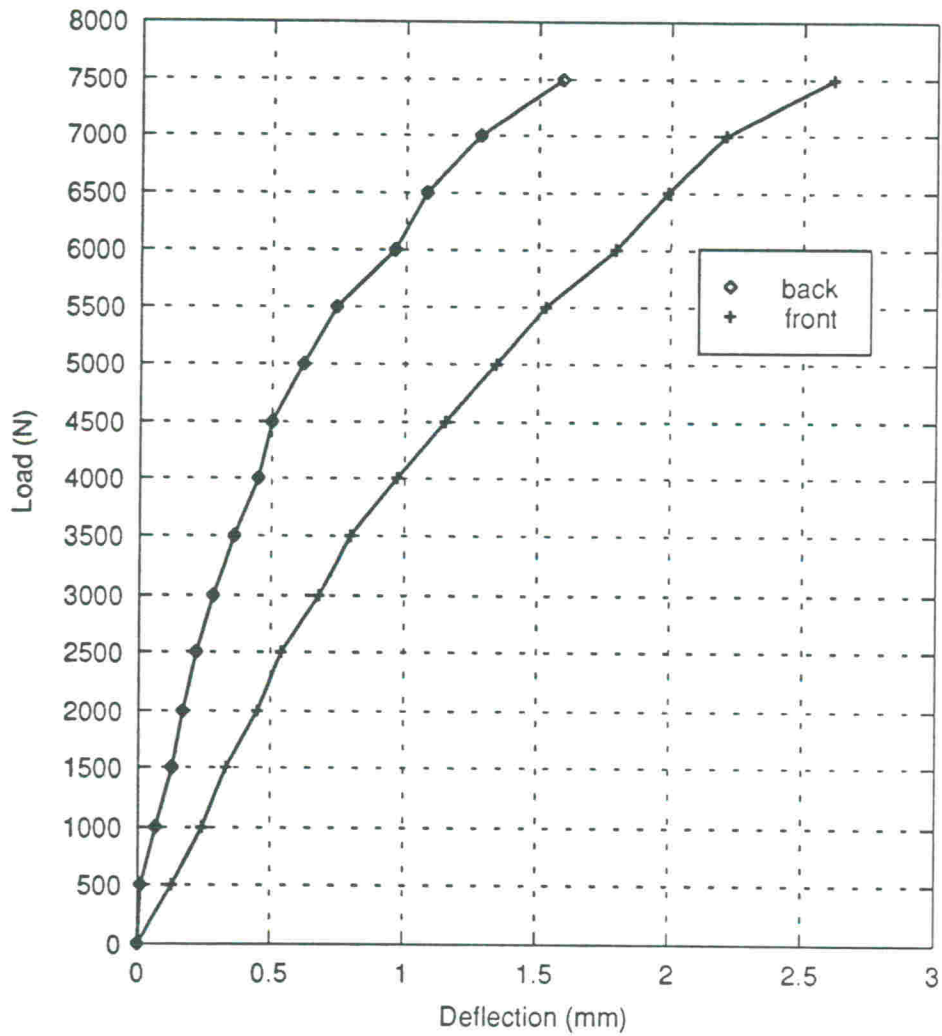


Fig. 12 Load-deflection response at the middle of wall No. 2 loaded in the strong direction (horizontal flexure)

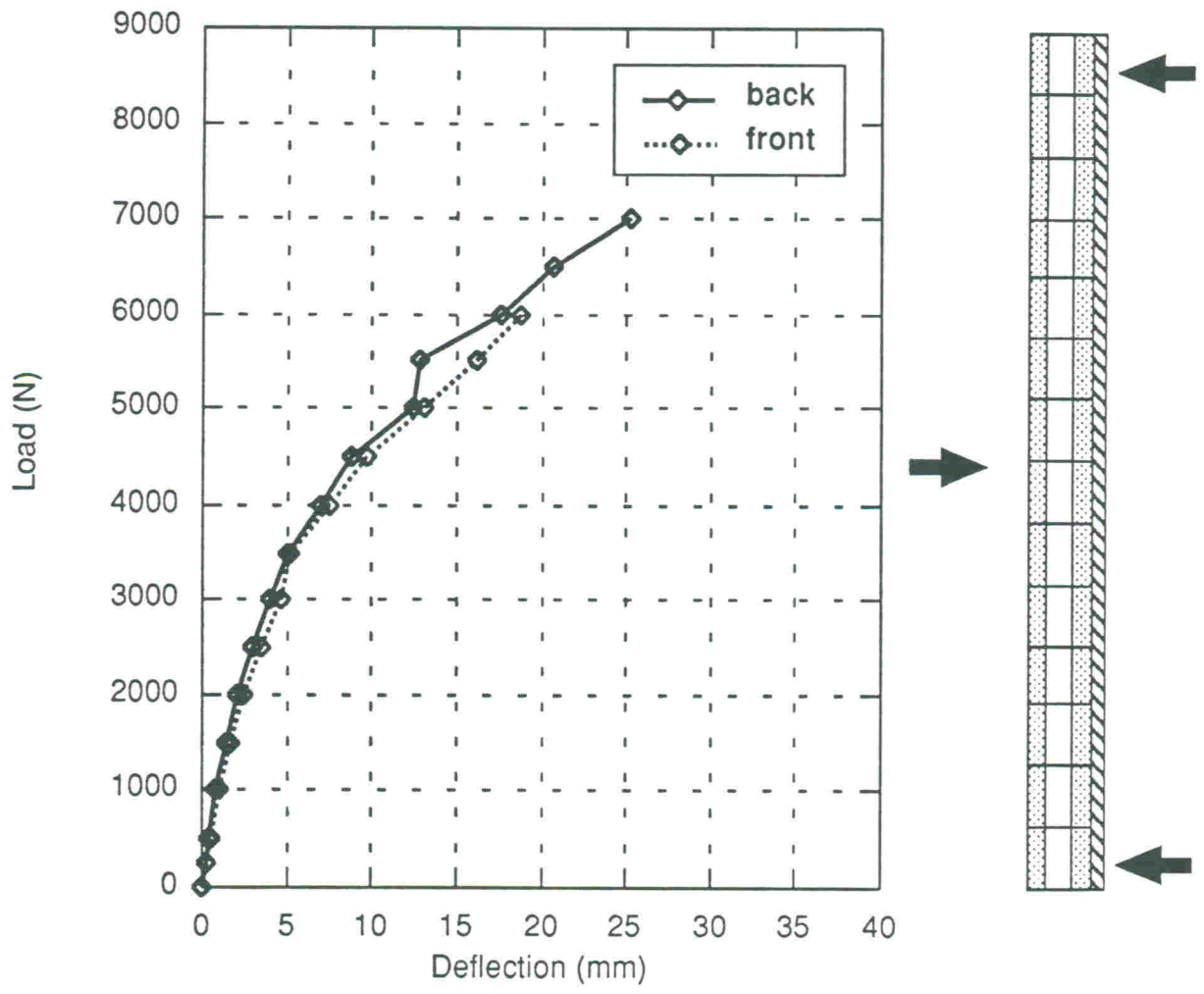


Fig. 13 Mid-height deflection response of the wall with wooden studs in tension (wind pressure case)

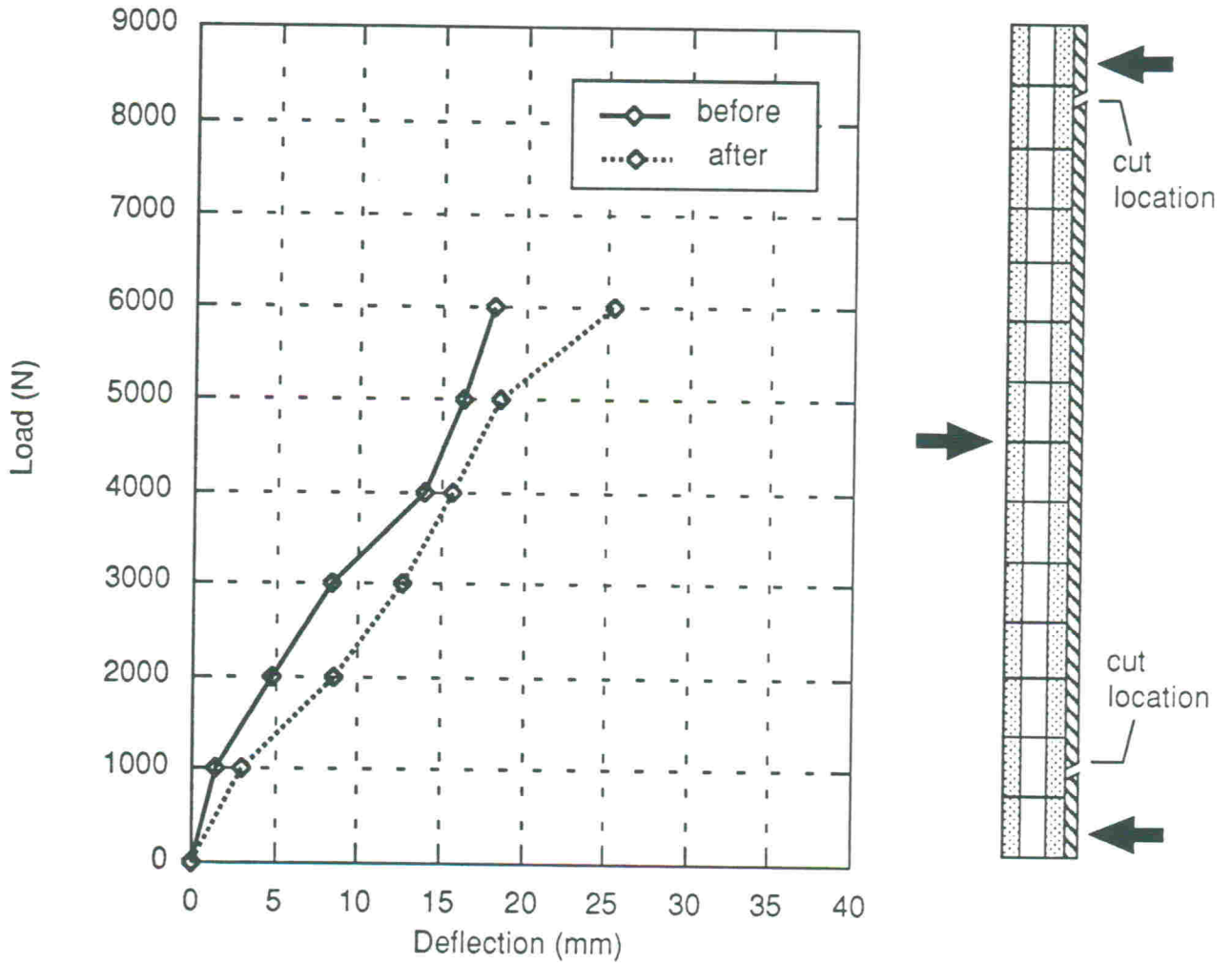


Fig. 14 Mid-height deflection at the back of the wall before and after cutting the wooden studs (wind pressure case)

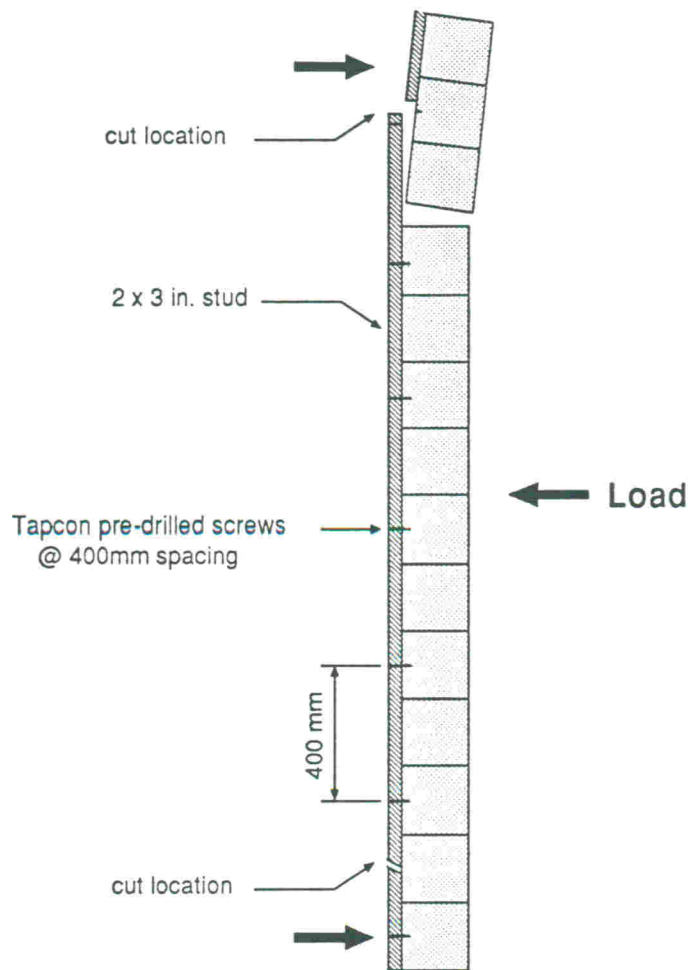


Fig. 15 Failure of the wall after cutting the reinforcing wooden studs (wind pressure case)

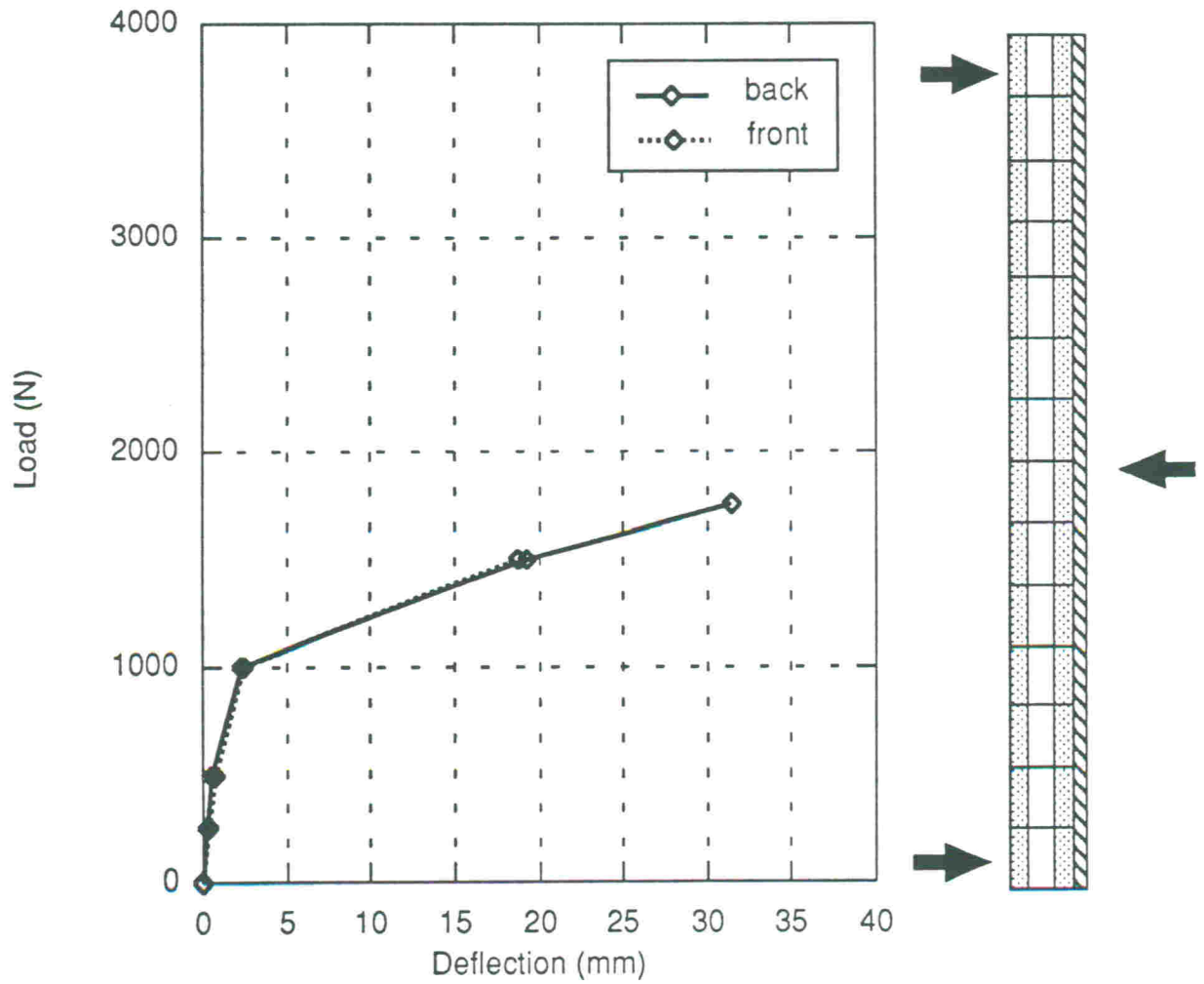


Fig. 16 Mid-height deflection response of the wall with wooden studs in compression (wind suction case)

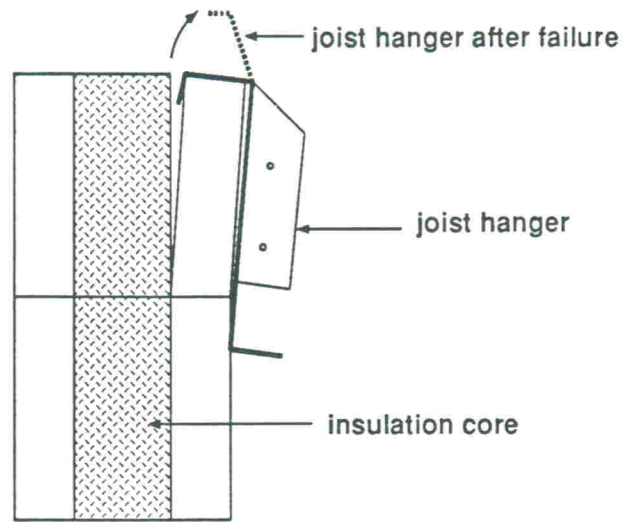


Fig. 17 Premature failure of joist hangers

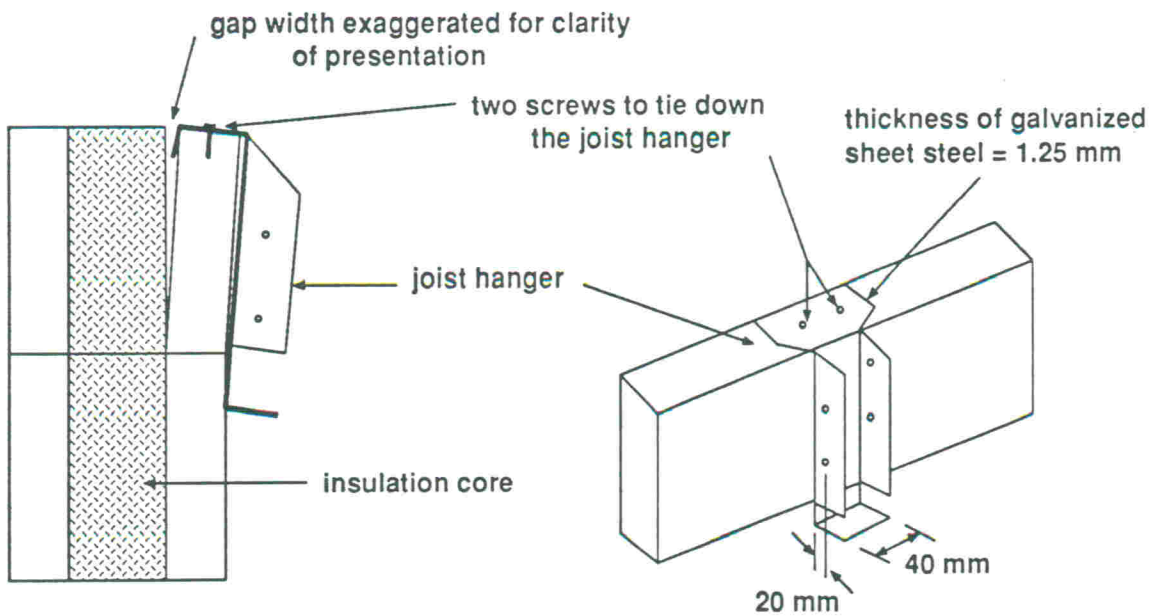
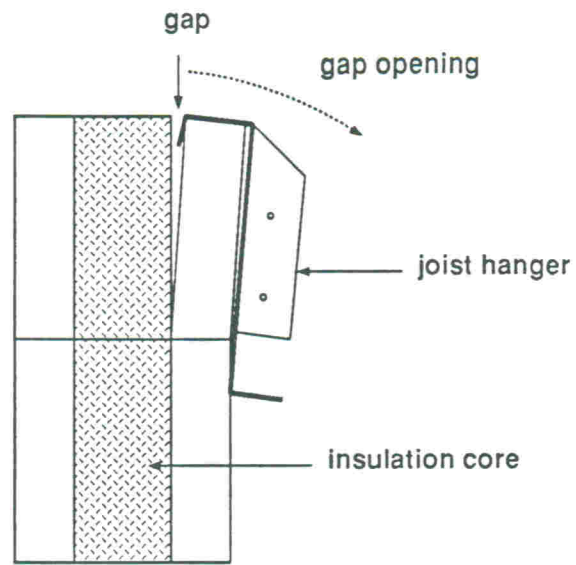
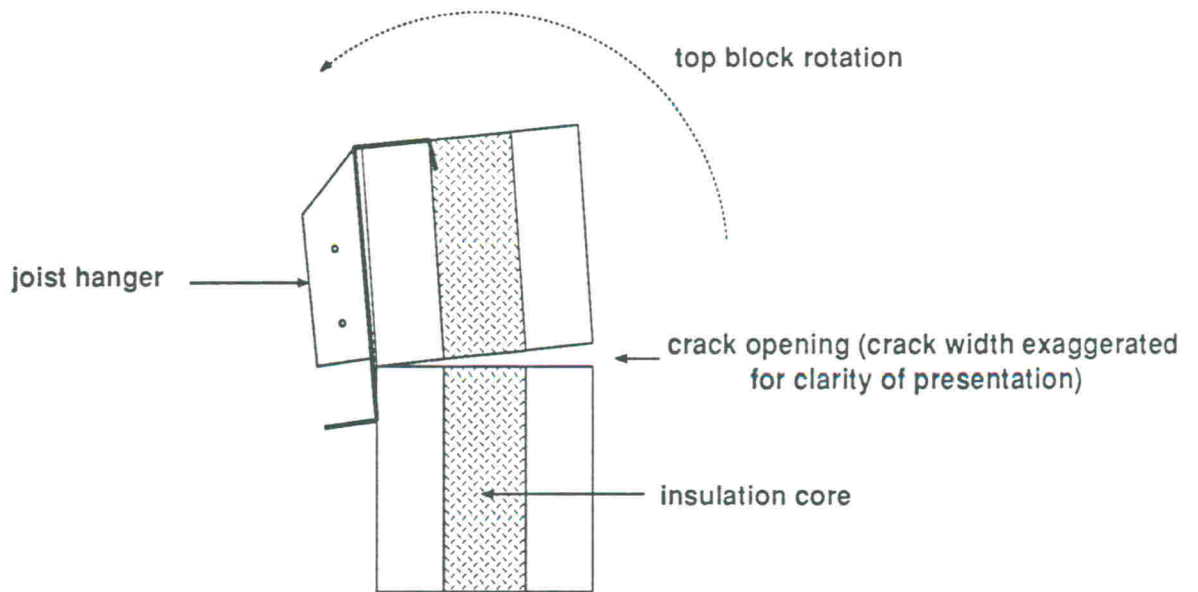


Fig. 18 Joist hanger tying down mechanism



(a) East wall



(b) West wall

Fig. 19 Wall behaviour under concentrated loads from joist hangers

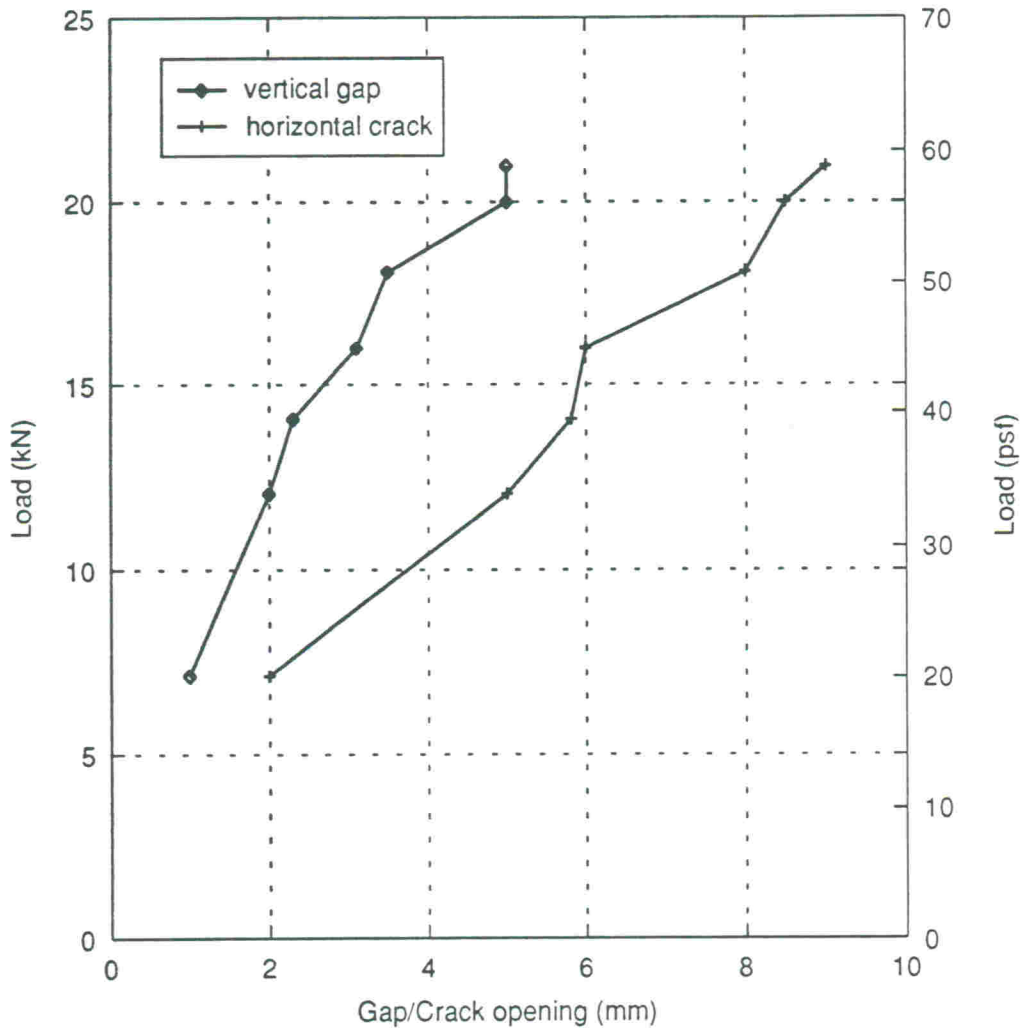


Fig. 20 Load gap/crack width relationships

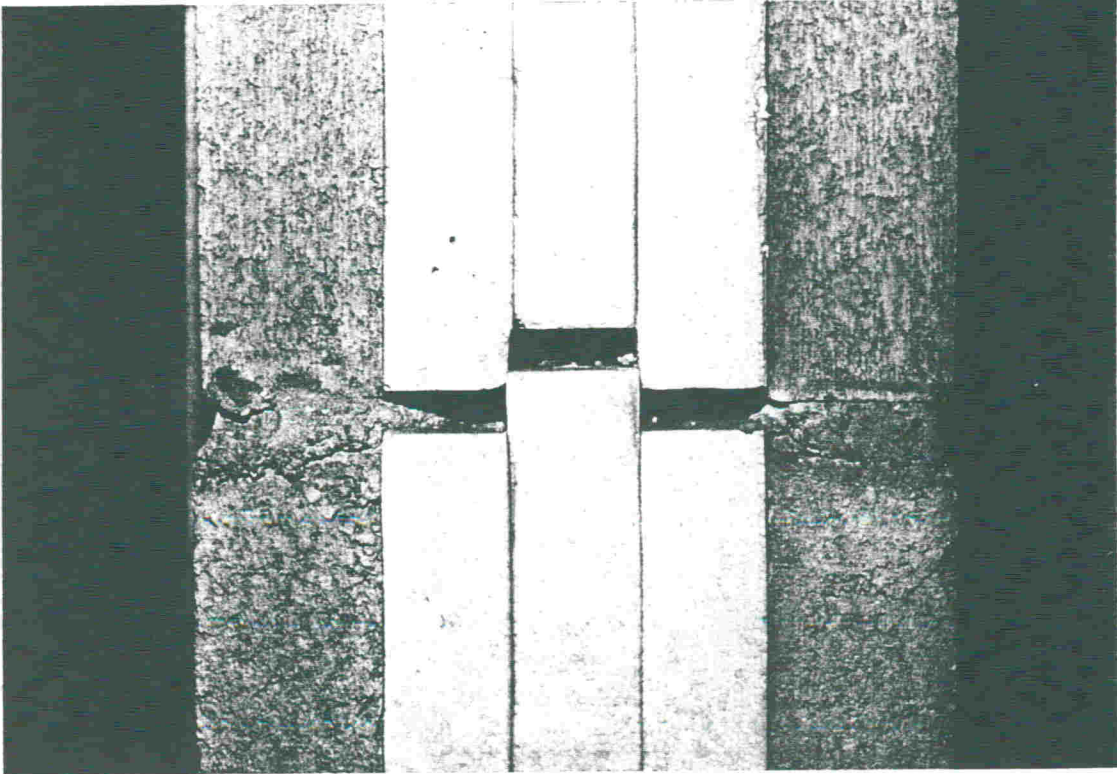


Photo 1 Below average workmanship resulted in some excessively wide bedjoints and poor continuity of the insulated core. Such occasional workmanship deficiencies were accepted as part of the test program.

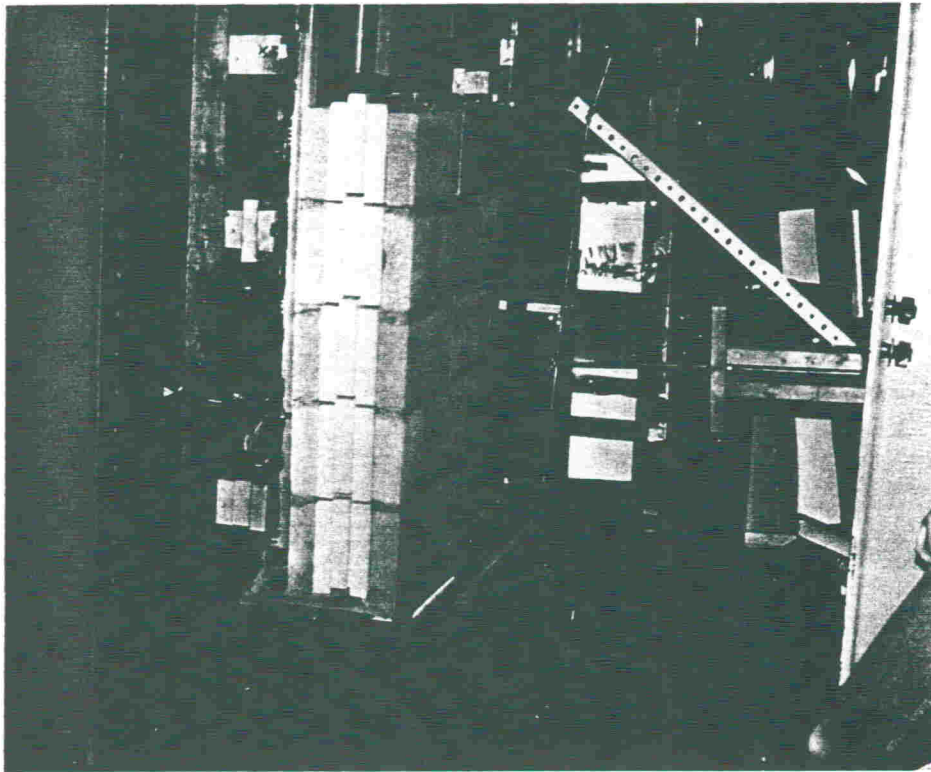


Photo 2 Horizontal bending test setup for 1 x 2 m wall

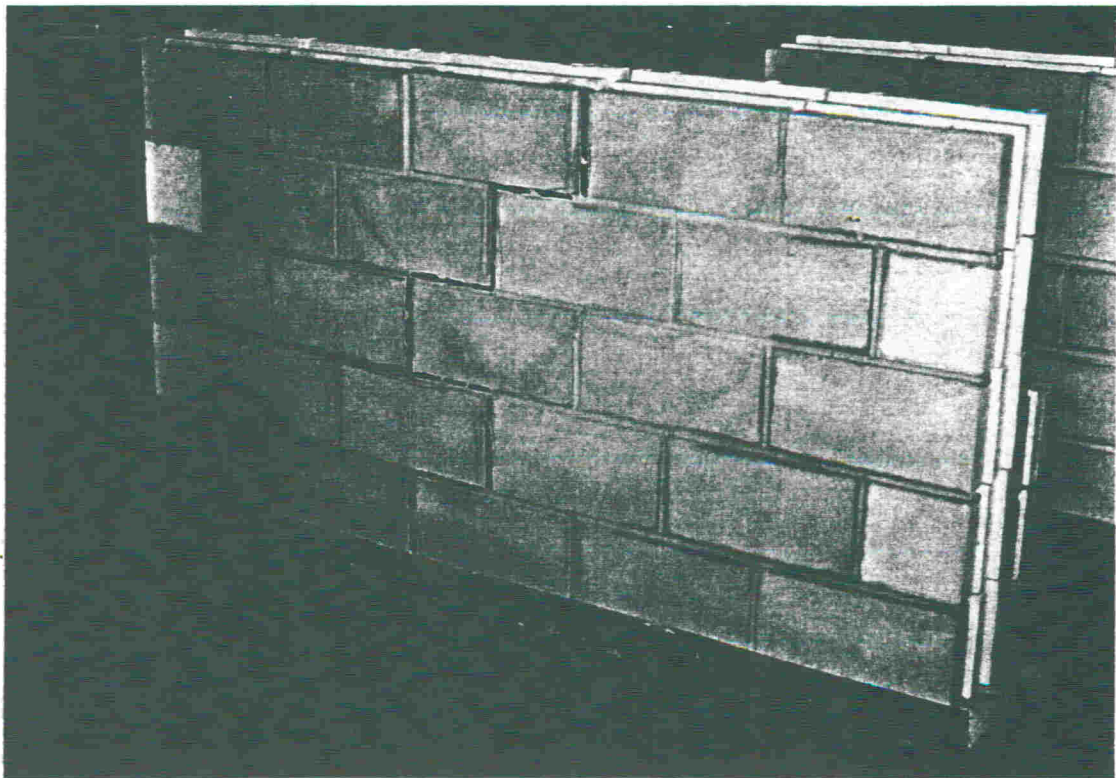


Photo 3 Typical failure pattern of 1 x 2 m wall after horizontal bending (strong direction) test

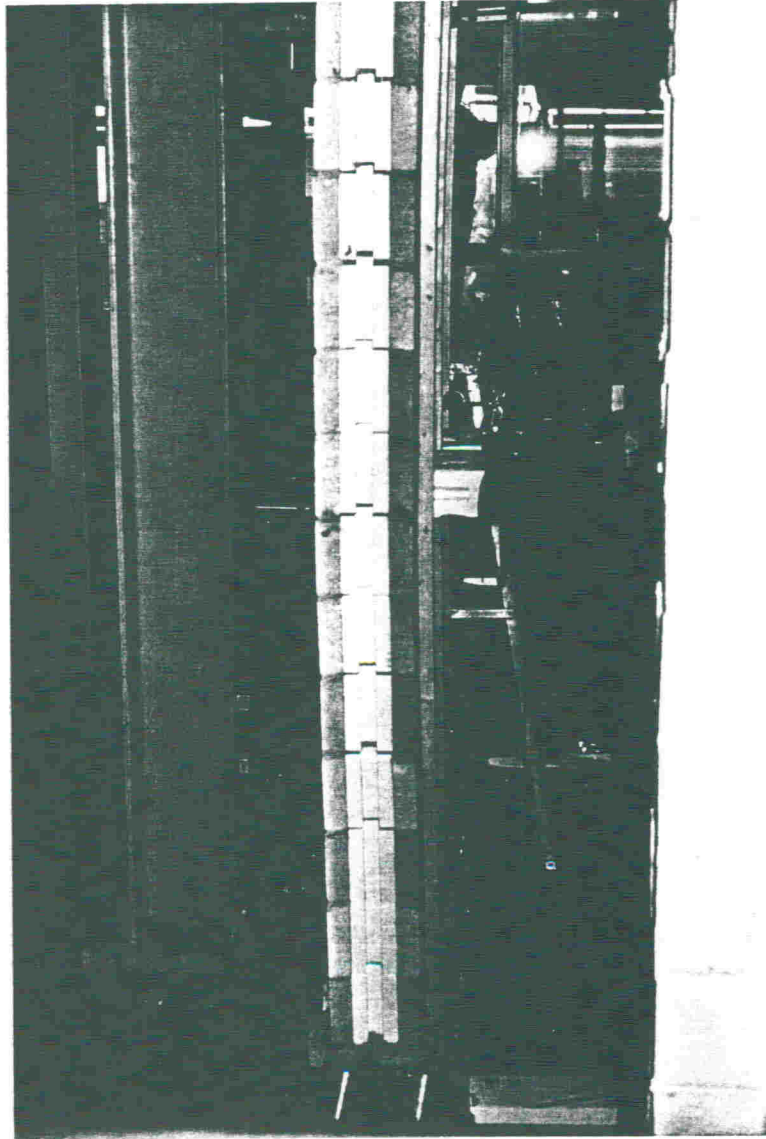


Photo 4 Vertical bending test setup for 1.2 x 2.8 m wall reinforced with wood studs for simulated wind suction case

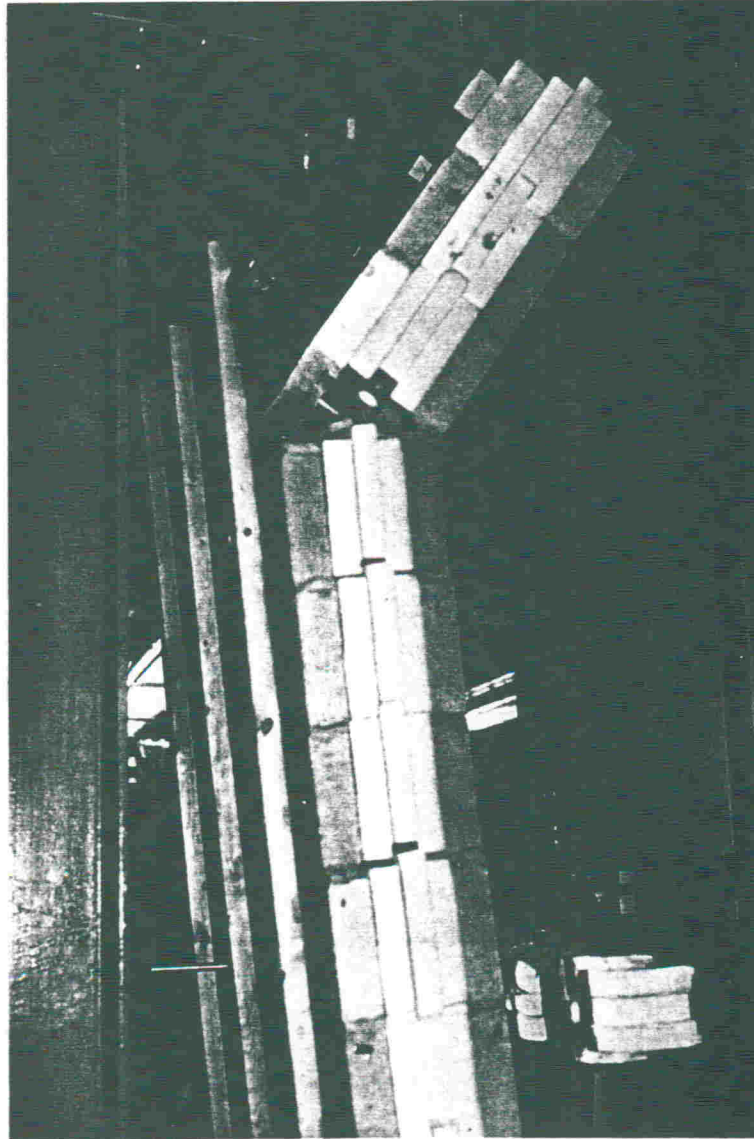


Photo 5 View of sudden wall failure as the screws reinforcing the vertical wall fractured at the uppermost wall location. Note the presence of studs on the tension side for a simulated wind pressure test.

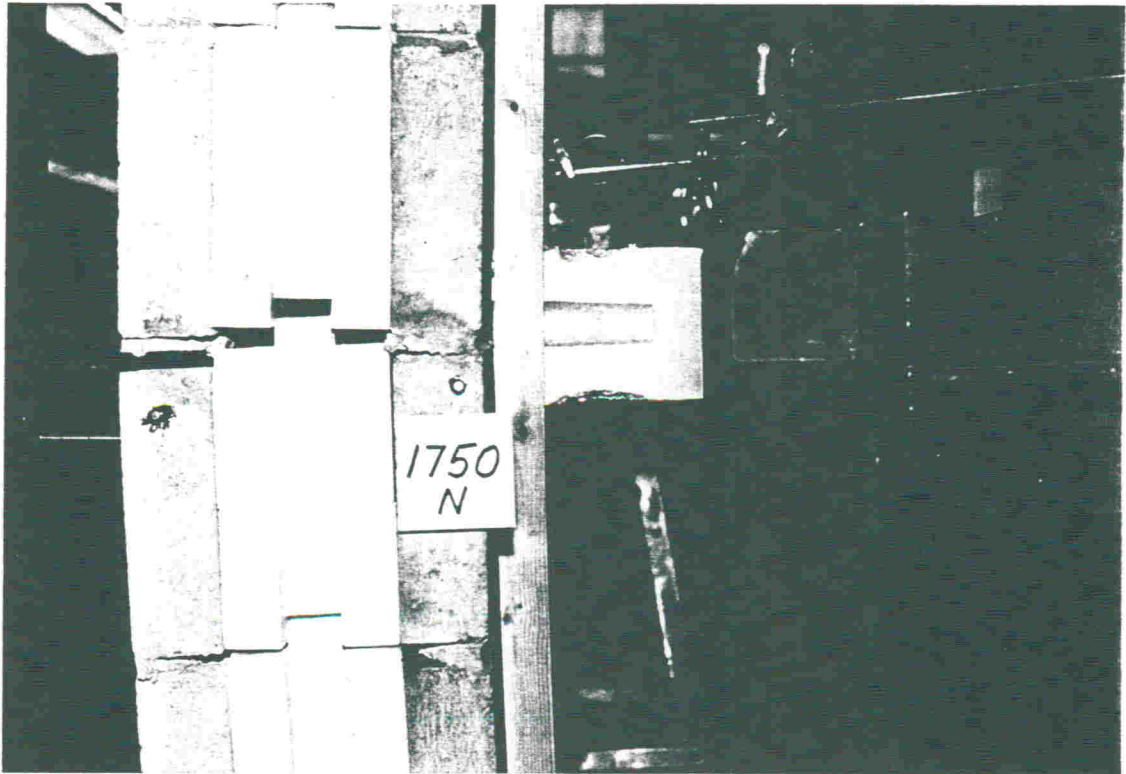


Photo 6 View of large mid-height crack width at ultimate load of the vertical wall with studs in compression for a simulated wind suction test.

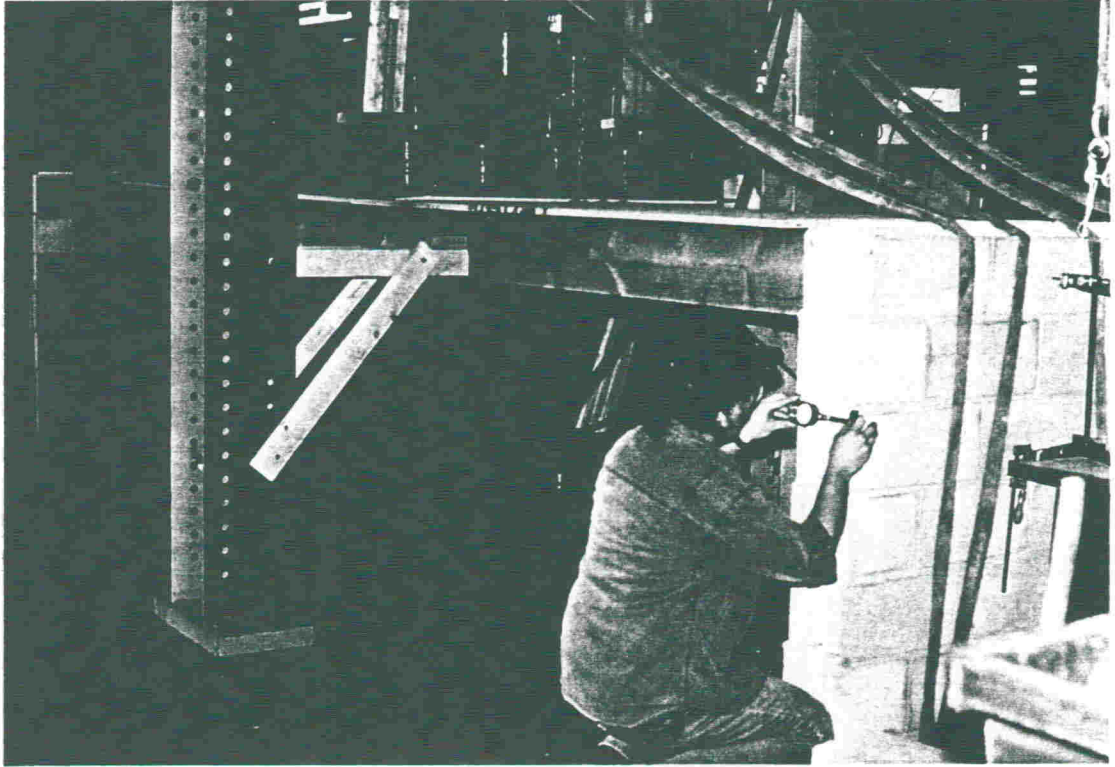


Photo 7 View of the two Isobloc walls subjected to the joist hanger concentrated load test at a very large eccentricity. The instrument being used on the right wall (East wall) is the Demec extensometer. It was used throughout the test program to measure potential spreading deformations between the two shells of the Isobloc unit. Note that the bracket extending out from the loading frame column represents a lateral safety catch in case the floor system moved sideways under high floor loadings. It was found that throughout the concentrated load test, the floor system did not move sideways and the bracket therefore never had to serve as a safety catch.

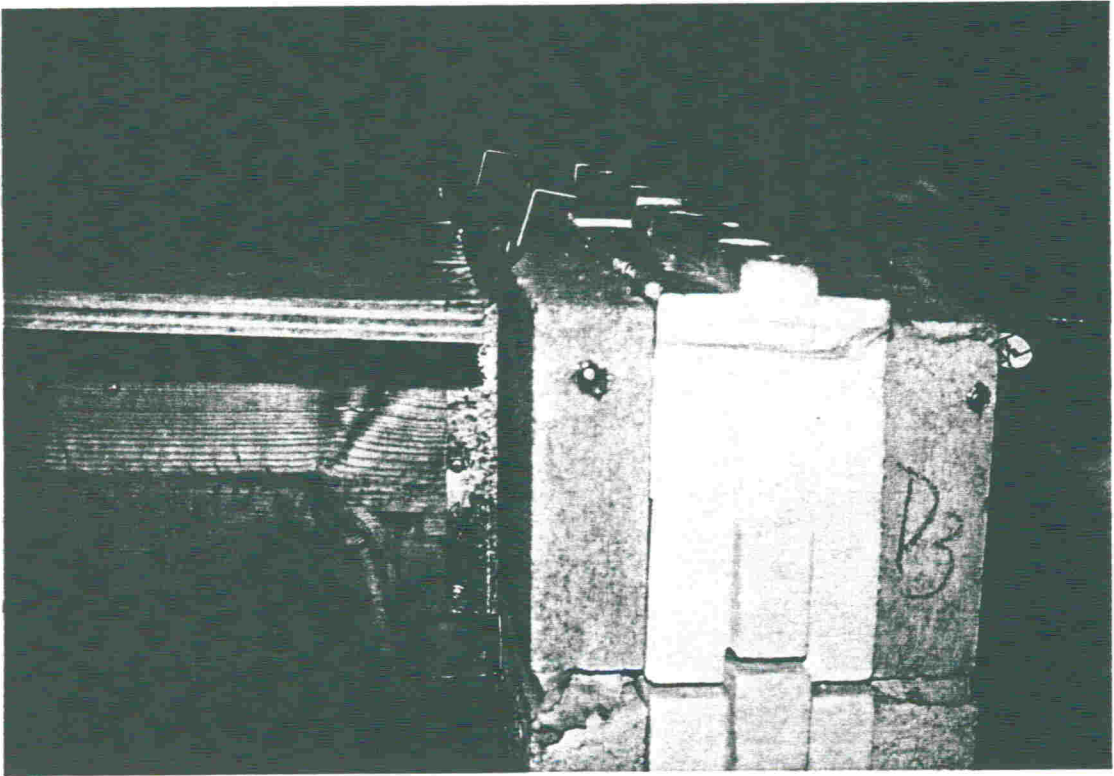


Photo 8 View of rotational bending failure of joint hangers at a total floor load of 5.2 kN

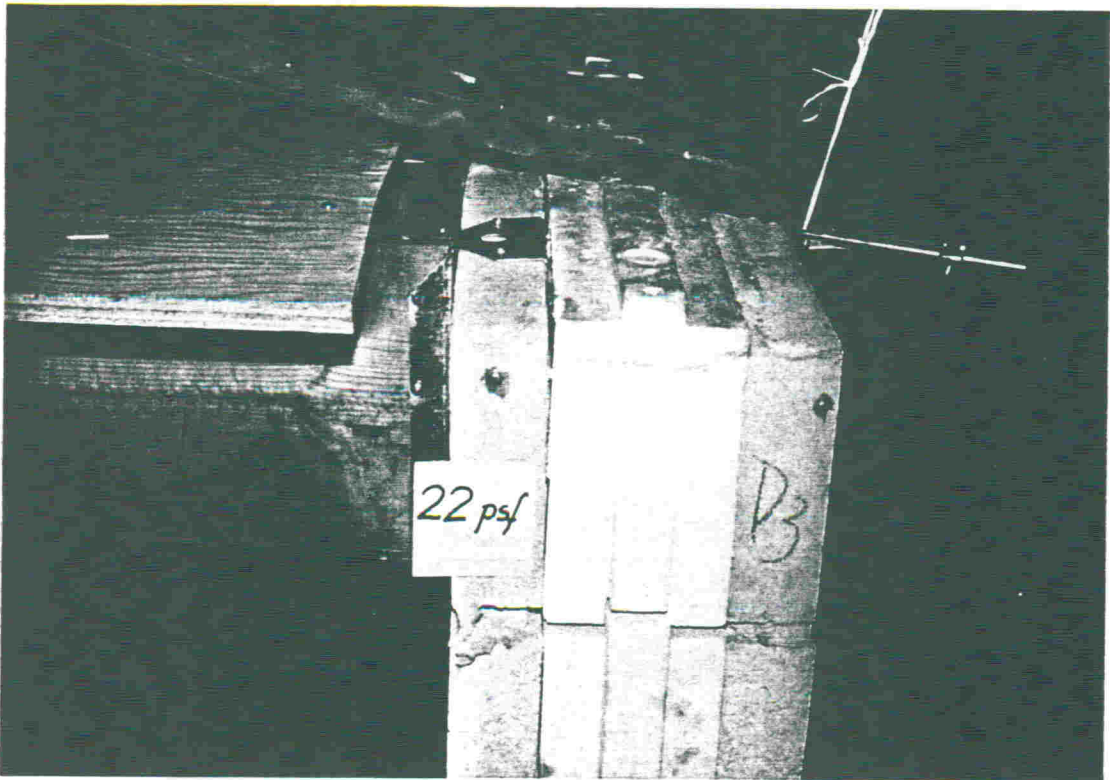


Photo 9 Screwed down joint hangers allowed continuation of concentrated load testing

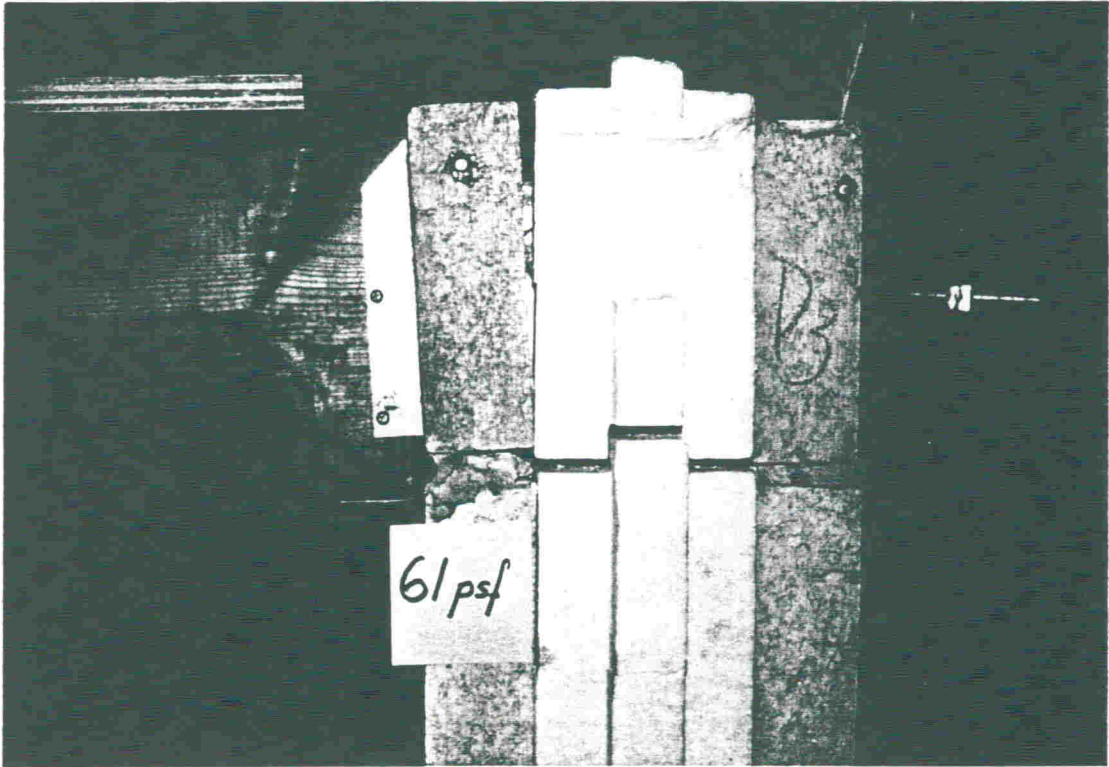


Photo 10 View of the gap opening at the top of the East wall under the maximum test load

APPENDIX C

SUPPLEMENTARY ISOBLOC TESTS



SUTER CONSULTANTS INC *Consulting Engineers*

38 Auriga Drive, Suite 200, Nepean, Ontario Canada K2E 8A5
TEL: (613) 224-4426 FAX: (613) 224-6055

**SUPPLEMENTARY
ISOBLOC TESTS**

REPORT FOR

**LES PRODUITS ISOBLOC INC.
BROMPTONVILLE, QUEBEC
526, Ch. du Parc Industriel
JOB 1H0**

PROJECT 94119

SEPTEMBER 1, 1995

SUPPLEMENTARY ISOBLOC TESTS

1. INTRODUCTION

This test report deals with two types of supplementary Isobloc tests to determine

1. strength and stiffness of the polystyrene core as part of the Isobloc unit, and
2. the concentrated loading performance of joist hanger assemblages without the screwed down joist hanger connection employed in Phase II testing.

2. POLYSTYRENE CORE STRENGTH AND STIFFNESS

2.1 General

A total of 10 Isobloc units were selected at random to determine strength and stiffness of the polystyrene insulation when tested as part of the block in a flatwise manner; five units each were tested in compression and tension as shown in Fig. 1. Testing was carried out during July 1995 in a Tinius Olsen Universal Testing Machine in the Structures Laboratories at Carleton University, Ottawa, under the direct supervision of the author. Demec extensometer discs were attached to the concrete shells of some of the specimens to monitor deformations under increasing load. The duration of each test was about half an hour.

2.2 Compression Results

Figs. 2 to 6 present the compressive load - deformation results for the five blocks. The following comments apply to the Figures and to other test evidence obtained:

1. The polystyrene core is able to withstand relatively high compressive loads while exhibiting a reasonable level of stiffness. Loading was stopped at a high level of 700 lbs due to the deformations at that load.
2. The deformations at the tongue end of the block are typically smaller than at the groove end. This behaviour is as expected since some material is absent at the groove .
3. The immediate recovery upon unloading varied between about 80 to 90% and therefore is quite high.

4. The average stiffness according to Fig. 6 is about 300 lbs at 1 mm. This 300 lb load over the flatwise block area of $390 \times 190 = 74\,100\text{mm}^2$ produces a stress of 0.018 MPa. Since a typical design wind pressure of 1 kN/m^2 produces a stress of 0.001 MPa, it can be seen that transient wind pressures can be effectively resisted by the Isobloc unit even without considering any beneficial effects from mortared construction and any in-plane axial loads.

2.3 Tension Results

Figs. 7 to 11 present the tensile load-deformation results for the five blocks. The following comments apply to the Figures and to other test evidence obtained:

1. The ultimate load capacities at pullout of the polystyrene core out of the dovetail slots were as follows for blocks 2 to 5: 200, 240, 100 and 170 lbs for an average of 177 lbs with a coefficient of variation of 33%. Block 1 was not tested to pullout failure because the first tension test concentrated on obtaining stiffness results. The fairly high variability in tensile capacity must be expected since the polystyrene core is discretely anchored in the six dovetail slots as shown in Fig. 1(a) and not uniformly attached to the total flatwise surface area of the concrete shells.
2. Under tensile loading, the tongue and groove deformations are seen to be very similar. This is as expected, since it is the dovetail slots that control the tensile response. The fact that the dovetail slots in an Isobloc unit stop at about 25mm from the unit's top surface must be expected to have a significant effect on the flatwise deformations under tensile loading. This is indeed so and can be observed from Figs. 9 to 11: the conventional bottom of the Isobloc unit exhibits much reduced deformations as compared to the top. Of course when the unit is mortared-in as part of an Isobloc wall, tensile loading as from wind suction will not produce such differential deformations between the top and bottom of a block; instead the mortar joints will resist and average out the differential deformations.
3. To arrive at a measure of tensile stiffness, Figs. 7 to 11 can be examined for loads corresponding to 1mm; the following approximate loads were determined: 13, 18, 50, 7, and 13 lbs for an average of 20.2 lbs at 1mm. Using the total flatwise block area of $390 \times 190 = 74\,100\text{mm}^2$, a stress of 0.0012 MPa is obtained. Since a typical design suction pressure of 0.8 kN/m^2 produces a stress of 0.0008 MPa, it can be seen that transient wind suction can be effectively resisted by the Isobloc

unit even without considering any beneficial effects from mortared construction and any in-plane axial loads. Also, since the average tensile pullout capacity is about 9 times higher than the 20.2 lb per 1mm stiffness value, the Isobloc system encompasses a satisfactory level of safety under flatwise tensile loading as from wind suction.

3. JOIST HANGER ASSEMBLAGE TESTS

3.1 General

The purpose of the joist hanger assemblage tests was to determine if a mortar joint between Isobloc units could provide adequate hold-down capacity to joist hangers to prevent a premature rotational bending failure of the hanger as experienced during Phase II testing prior to using two screws as hold-down devices.

A total of six pairs of Isobloc units were mortared together with the standard galvanized steel sheet metal joist hanger (thickness = 1.25mm) used during Phase II testing embedded in the mortar joint between each pair of blocks. The mortar was a type S mortar of the same materials and proportions as for Phase II work. Three assemblage tests were carried out at an age of four weeks. Prior to testing, paired blocks were moist cured for 2 weeks by covering the specimens with polyethylene sheeting; for the remainder of time, specimens were subjected to the laboratory conditions of about 22°C and 50% relative humidity.

Testing was carried out during August 1995 in a Tinius Olsen Universal Testing Machine in the Structures Laboratories at Carleton University, Ottawa, under the direct supervision of the author. For the test setup shown in Fig. 12, the 2 x 10 in. wood joist was attached to the joist hangers by means of four #10 - 1 in. long wood screws per hanger as in the previous Phase II work.

The average 28-day mortar cube (50mm) compressive strength was determined as 13.1 MPa; individual cube strengths were 13.3, 12.9 and 13.2 MPa. The average strength of 13.1 MPa compares well with the averages of 12.1 MPa and 15.4 MPa obtained during Phase I and Phase II testing.

3.2 Joist Hanger Test Results

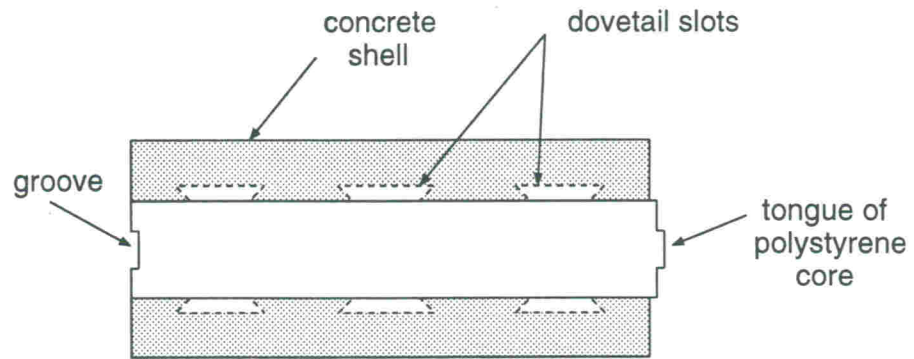
The following results were obtained for the six joist hangers tested in three assemblage setups as shown in Fig. 12:

1. The ultimate failure loads of the three setups were 4300, 4800 and 4900 lbs for an average total assemblage load of 4,667 lbs. On a per hanger basis this translates to 2,333 lbs or 10.38 kN. Note that the average failure capacity of 10.38 kN/hanger is 2.8 times higher than the 3.67 kN/hanger maximum load achieved during Phase II testing.
2. The typical failure mode consisted of screw pullout/wood splitting failures at the connection between the joist and the hanger. None of the failures involved a premature rotational bending failure of the joist hanger material as observed during Phase II testing prior to tying down the hanger by means of two screws. The only cracking of the mortar joint containing the embedded hanger occurred on one side of assemblage setup 3; the cracking took place at 3500 lbs corresponding to 71% of ultimate load.
3. The waferboard joint below the tested mortar joint would typically open up under progressive loading; this effect was similar to the crack opening observed in Phase II testing (see Phase II report, Fig. 19b).
4. The average steel stress in the joist hangers amounted to about 208 MPa at average ultimate load. None of the hangers failed in tension though one hanger displayed considerable yielding at the bend extending into the mortar joint.

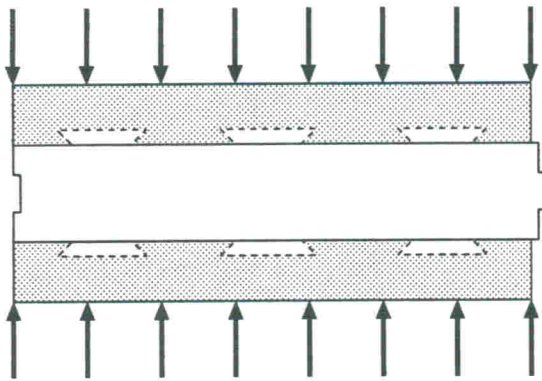
In summary, the joist hanger assemblage tests indicate that the mortar joint containing a joist hanger provides satisfactory tie-down capacity to prevent a premature rotational bending failure of the hanger. This means that the tie-down screws of the Phase II work are not required as long as there is continuity of Isobloc wall construction for at least one course above the level of the joist hangers.


Dr. G.T. Suter, P.Eng.

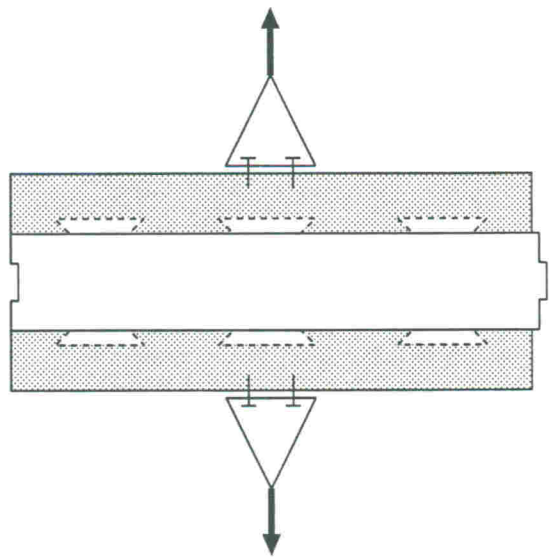




a) Flatwise section of Isobloc unit



b) Flatwise compression test



c) Flatwise tension test

Fig. 1 Specimens for polystyrene strength and stiffness tests

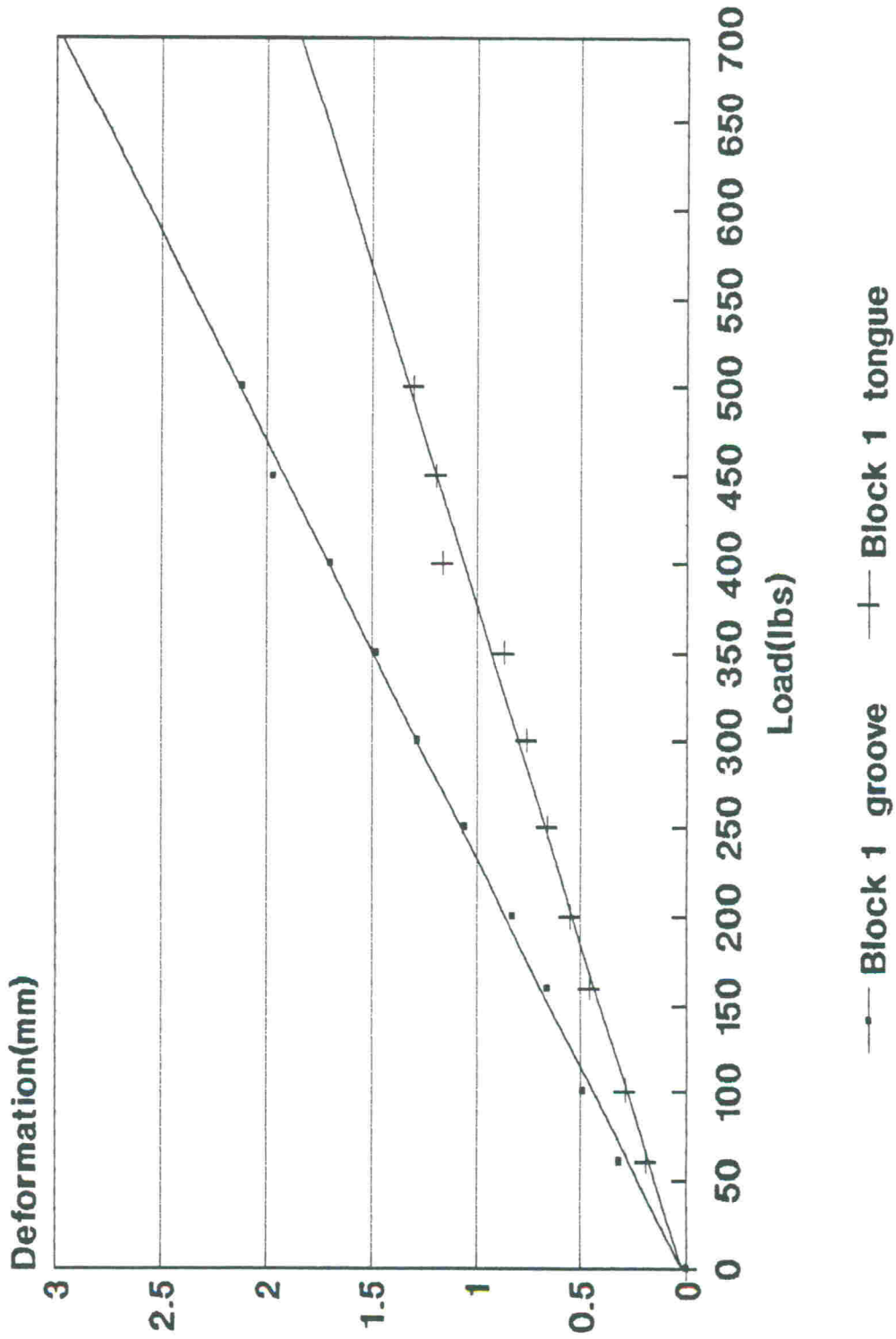


Fig. 2 Isobloc flatwise compression test: comparison of tongue to groove deformation

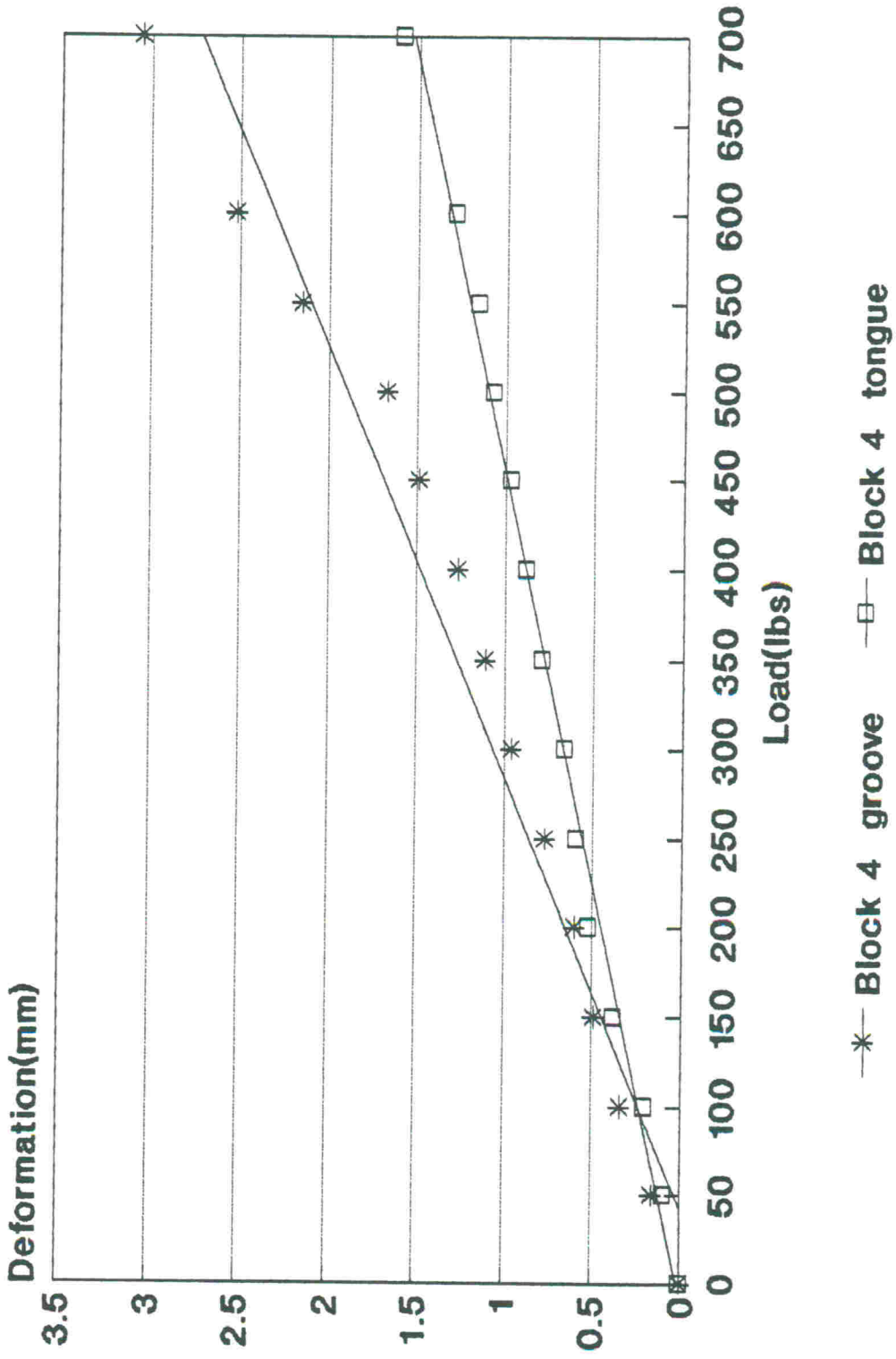


Fig. 3 Isobloc flatwise compression test: comparison of tongue to groove deformation

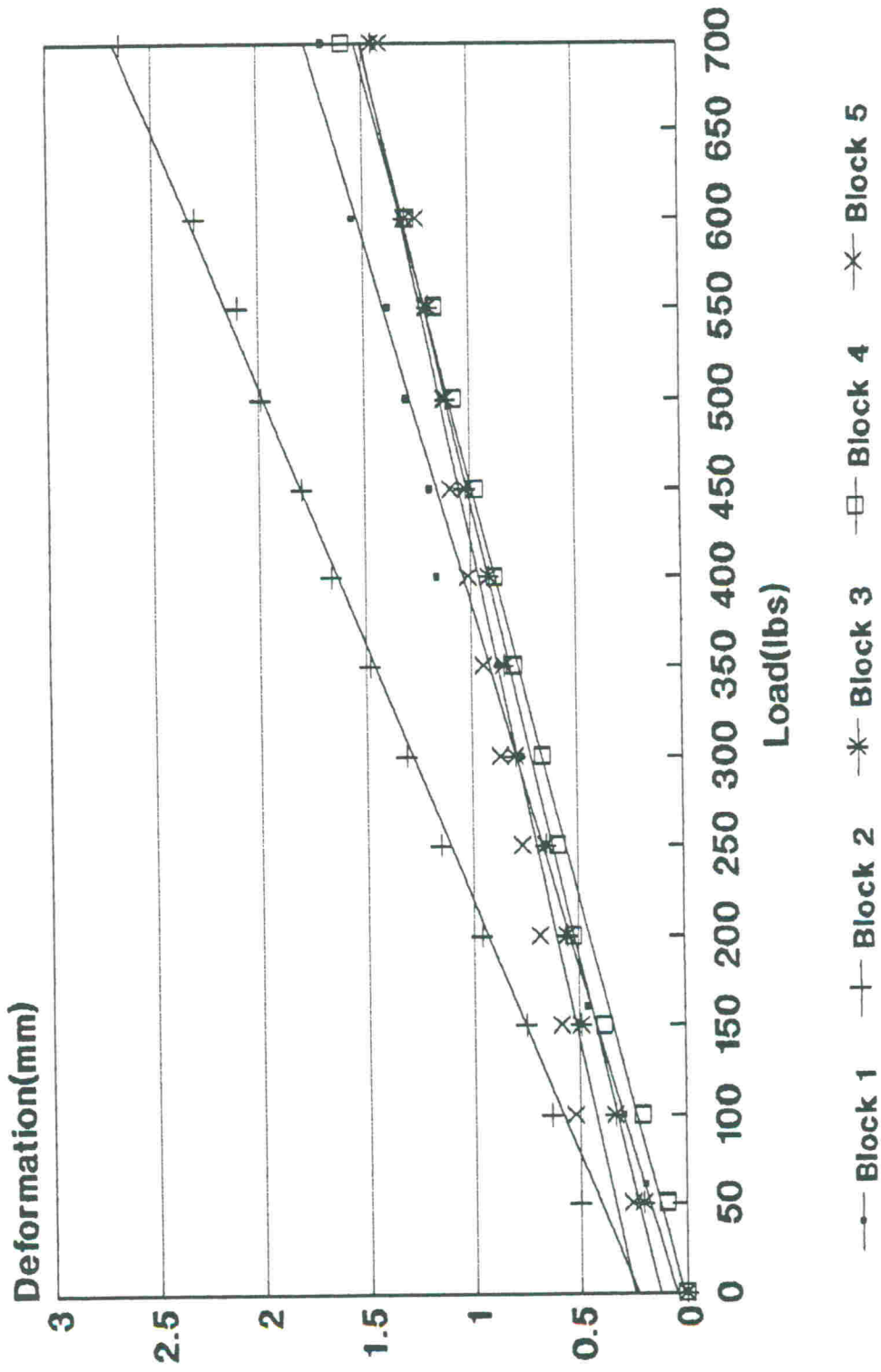


Fig. 4 Isobloc flatwise compression test: deformation of tongue side of insulation core

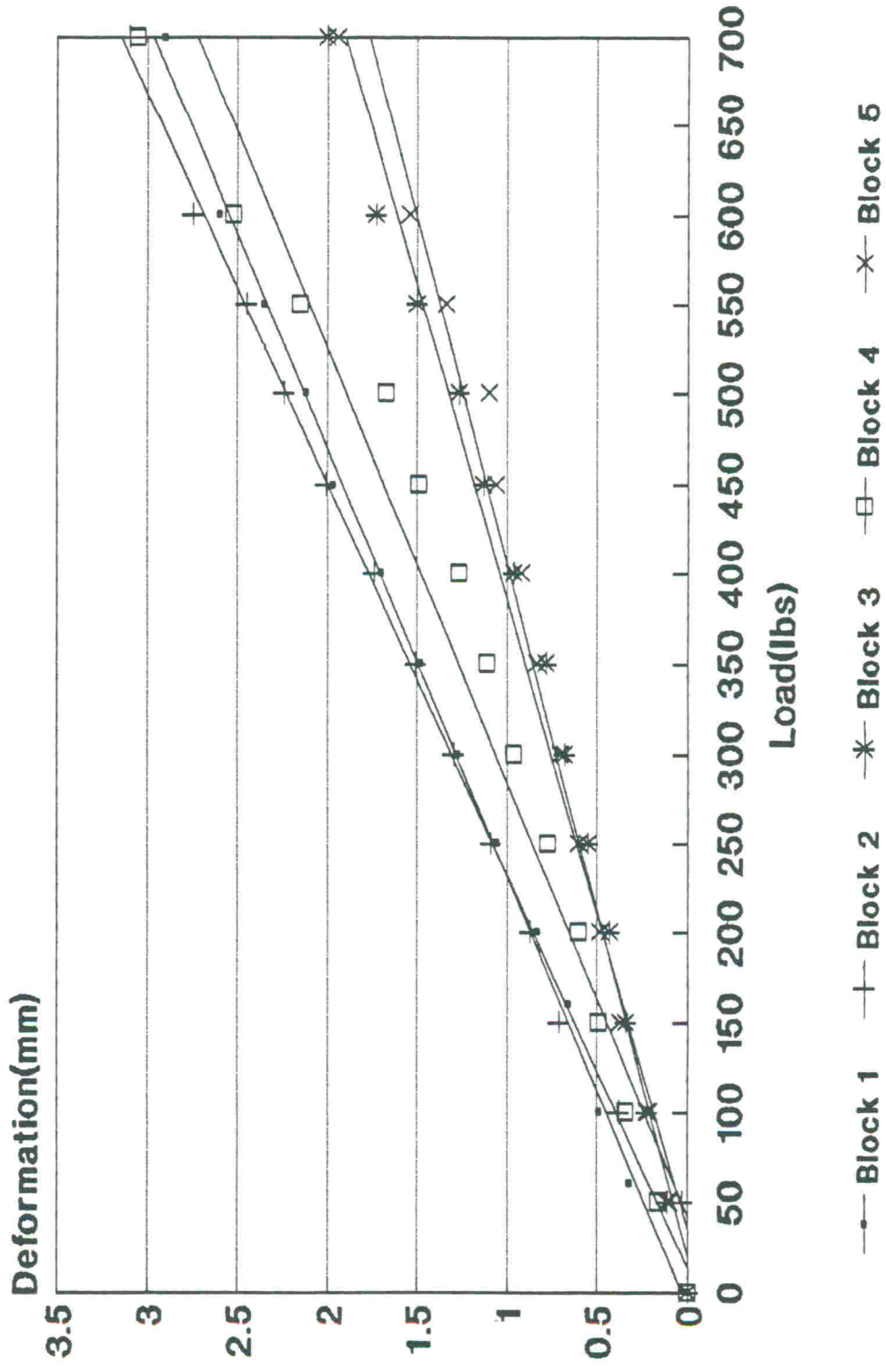


Fig. 5 Isobloc flatwise compression test: deformation of groove side of insulation core

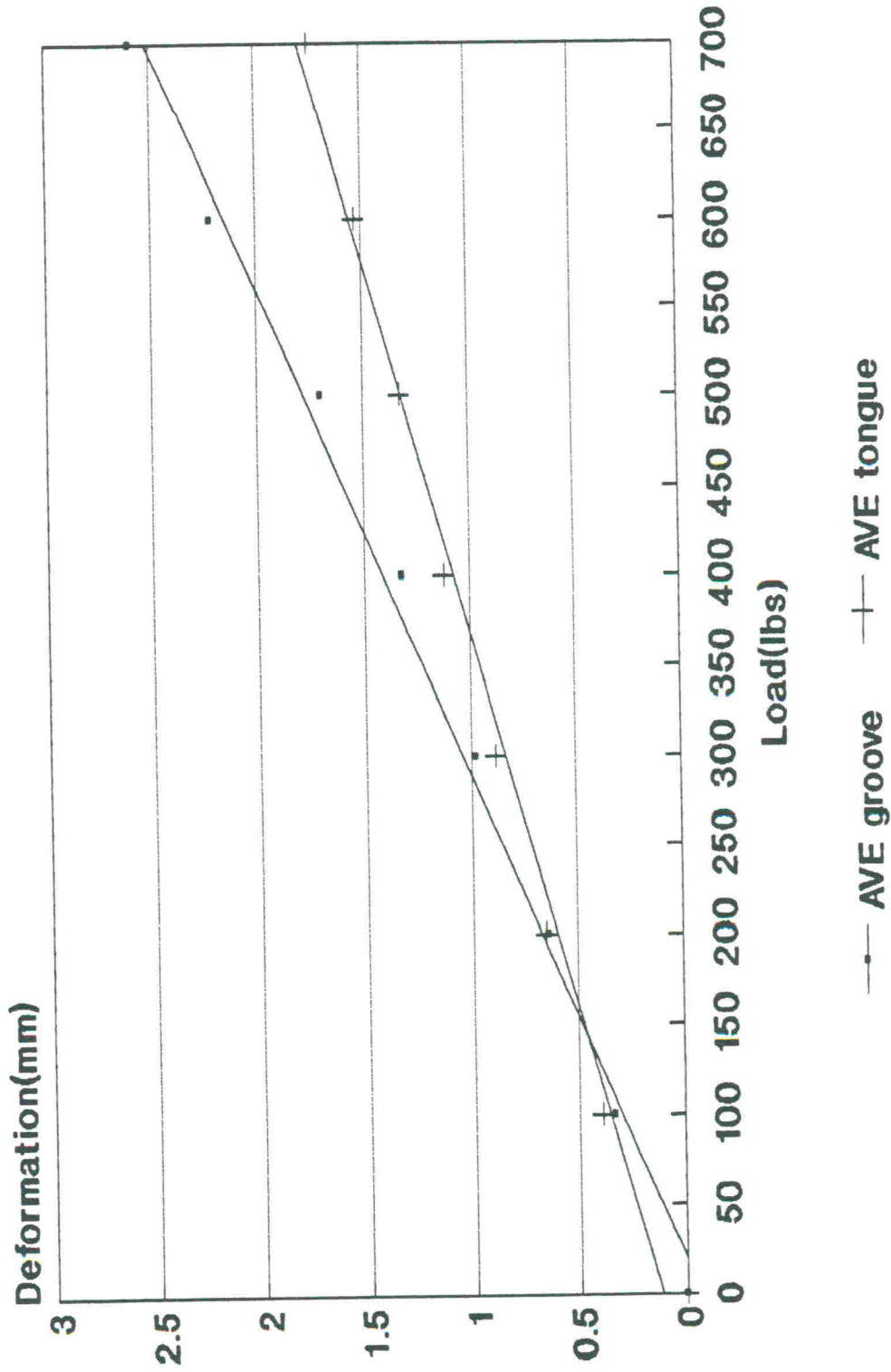


Fig. 6 Isobloc flatwise compression test: average of tongue and groove deformations

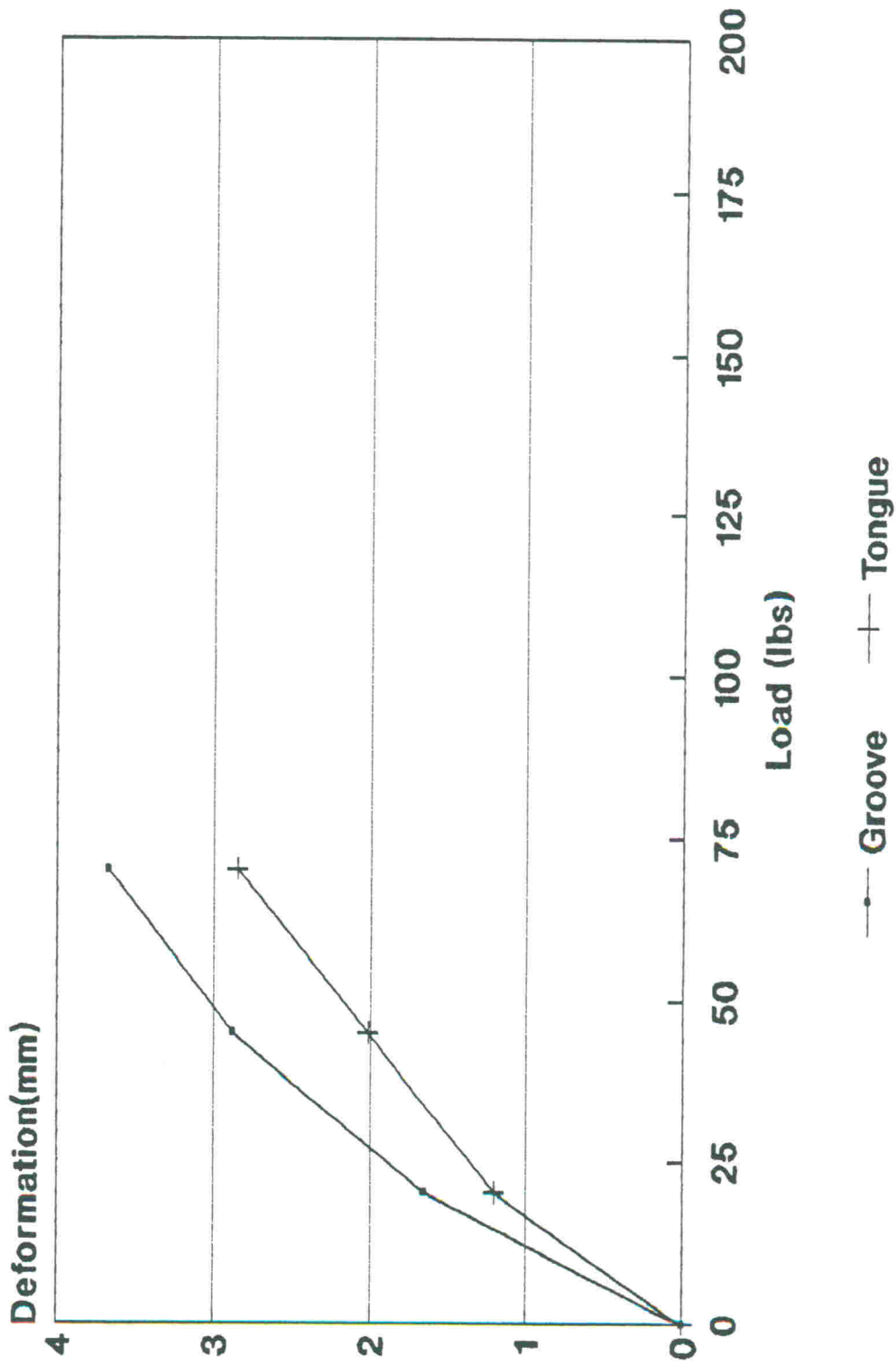


Fig. 7 Isobloc flatwise tension test: Block 1

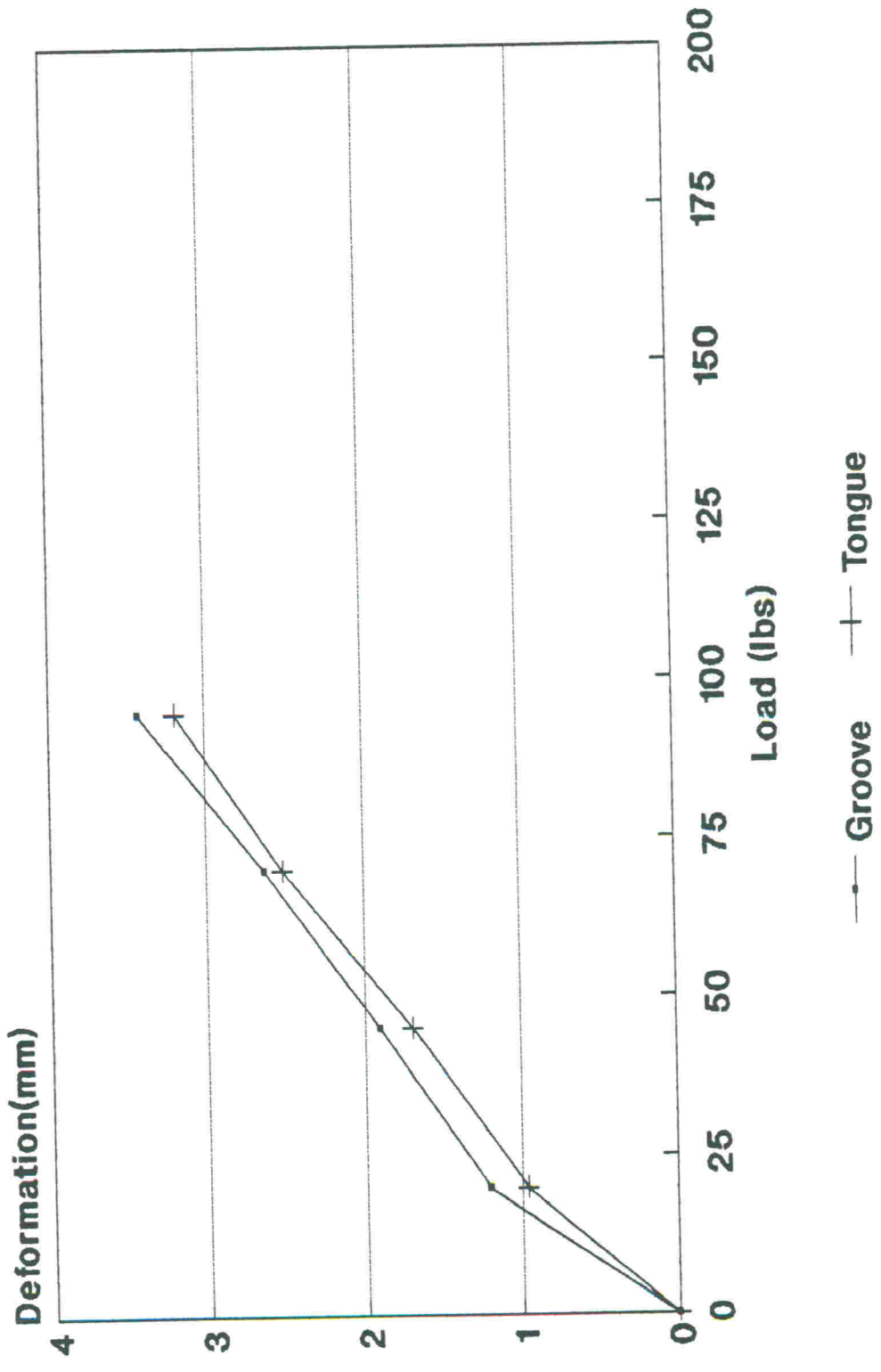


Fig. 8 Isobloc flatwise tension test: Block 2

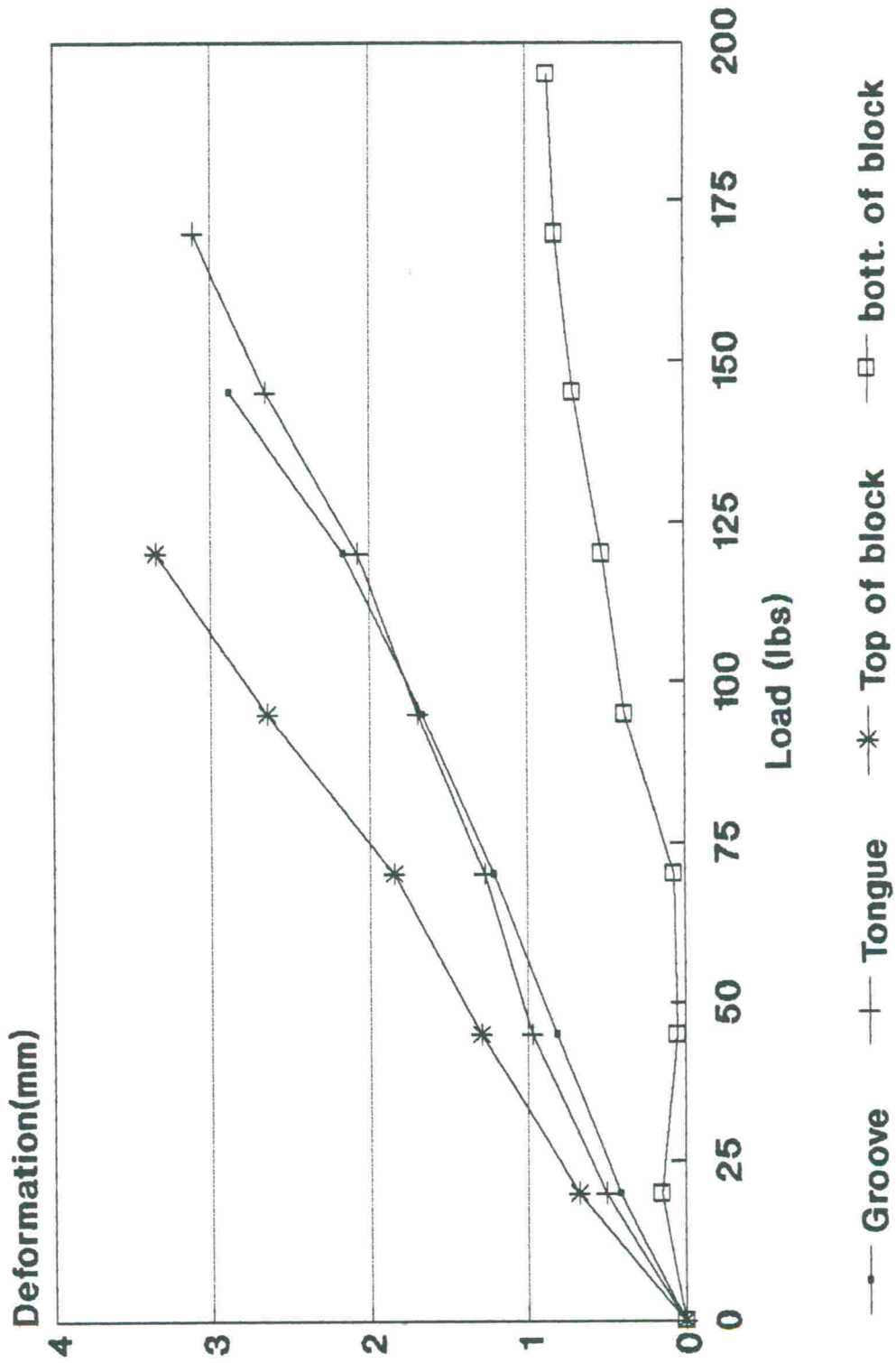


Fig. 9 Isobloc flatwise tension test: Block 3

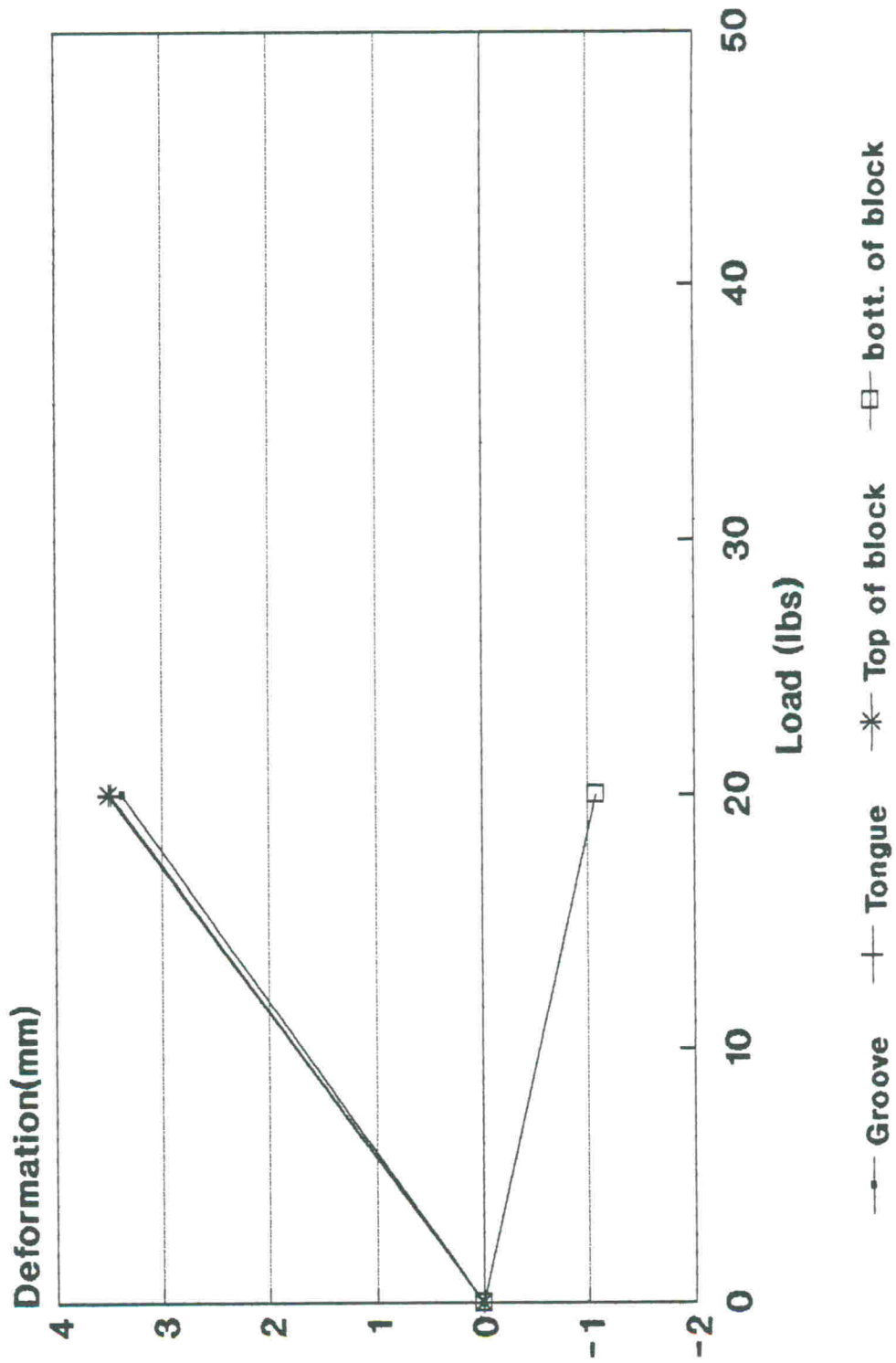


Fig. 10 Isobloc flatwise tension test: Block 4

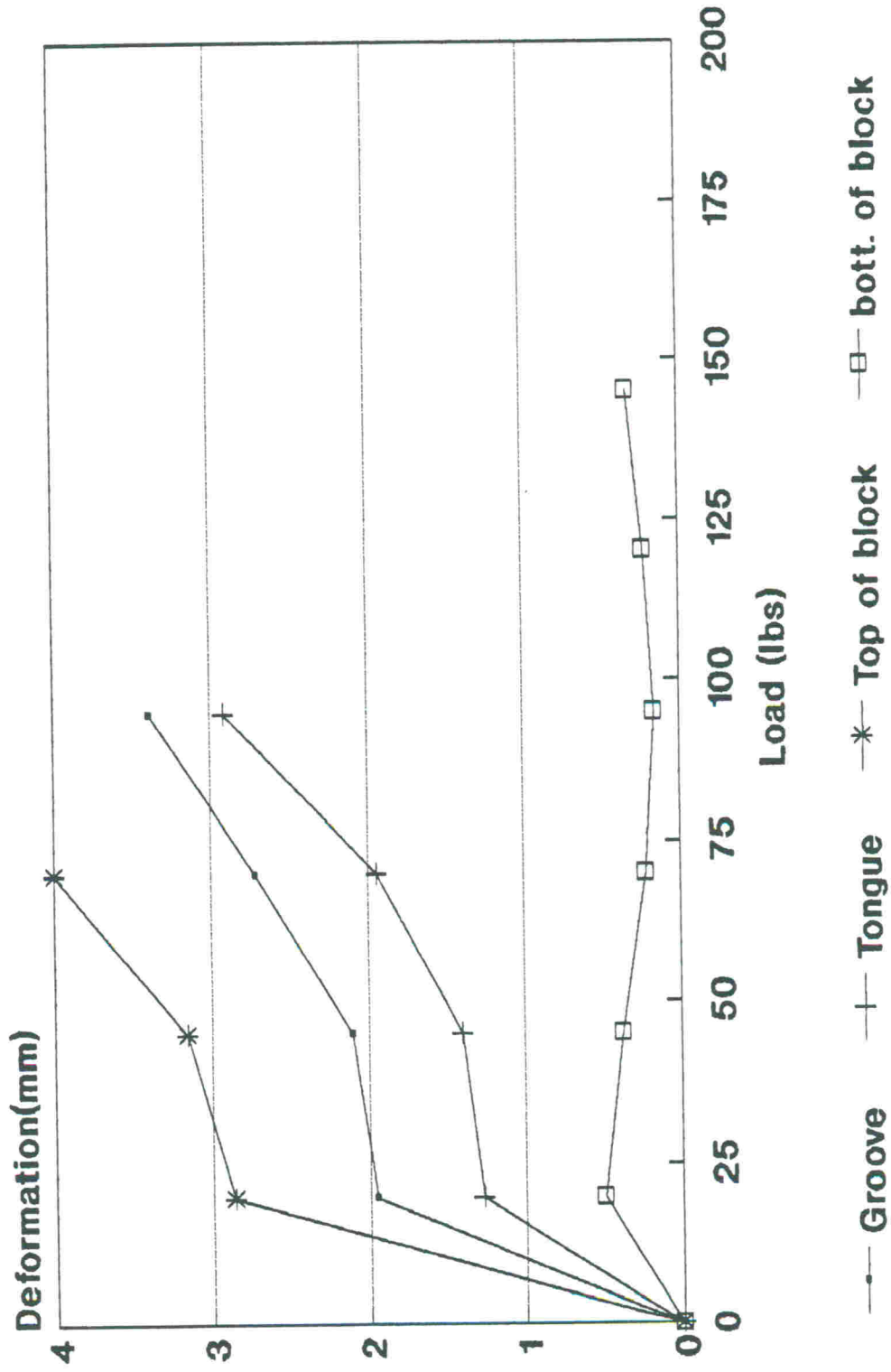
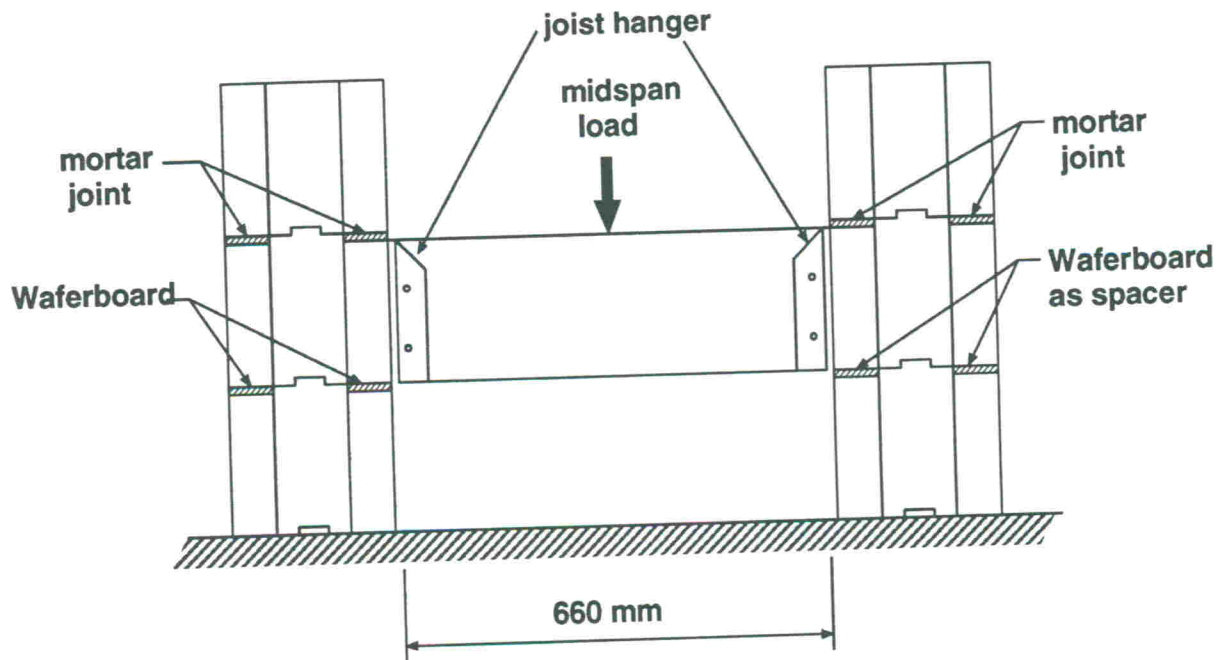


Fig. 11 Isobloc flatwise tension test: Block 5



**Fig. 12 Joist hanger assemblage test setup
(same joist hanger as in
Phase II work)**

APPENDIX D

SPECIAL TESTS ON EXPANDED POLYSTYRENE INSULATED CONCRETE MASONRY WALLS TYPE ISOBLOC